Zur Erlangung des Doktorgrades

An der Fakultät für Biologie

Der Ludwig-Maximilians-Universität

"Roquin binds to *ICOS* mRNA for P body-dependent and miRNA-independent posttranscriptional gene silencing"

Von Elke Glasmacher

Hiermit erkläre ich, Elke Glasmacher, dass die vorliegende Arbeit mit dem Titel: "Roquin binds to ICOS mRNA for P body-dependent and miRNA-independent posttranscriptional gene silencing" von mir selbstständig und ohne unerlaubte Hilfsmittel angefertigt wurde und ich mich dabei nur der ausdrücklich bezeichneten Quellen und Hilfsmittel bedient habe. Diese Arbeit wurde weder in der jetzigen noch in einer abgewandelten Form einer anderen Prüfungskomission vorgelegt.

Elke Glasmacher   München, der 23.08.09

Erster Gutachter: Prof. Dr. Dirk Eick
Zweiter Gutachter: Prof. Dr. Elisabeth Weiß

Tag der mündlichen Prüfung: 04.03.2010

1   Abstract

Roquin is an important factor in the prevention of autoimmune diseases. It limits the expression of the inducible T cell co-stimulator (ICOS) in T cells. This function is essential for the repression of self-antigen-triggered immune responses.

This thesis reveals a new mechanism by which Roquin exerts posttranscriptional gene silencing of ICOS. The findings uncover that Roquin has specialized in efficient translational repression of ICOS, unlike its paralog MNAB. Two parts within the Roquin protein provide essential functions for this repression. First, the carboxy-terminus localizes Roquin to P bodies, which are cytoplasmic loci enriched in translationally inactive mRNAs and proteins that are involved in translational inhibition. Second, the amino-terminus of Roquin can bind *ICOS* mRNA, for which a recently defined ROQ domain is critical. The amino-terminus can be functionally replaced by conserved sequences from Roquin's paralog MNAB, indicating a possible role of MNAB as a translational repressor.

A recent study suggested that microRNAs are involved in Roquin-mediated ICOS repression. These small non-coding RNAs can inhibit translation of mRNAs through the binding of partially complementary sites in the 3'UTR of the target gene. However, the biochemical analysis presented here disproves this concept and reveals an alternative pathway for Roquin-mediated ICOS repression.

The contribution of microRNAs for Roquin-mediated ICOS silencing was analyzed in two independent approaches: first in cells deficient in Dicer, which are incapable of microRNA biogenesis, and second in cells deficient in Argonaute 1-4 proteins, which are impaired in microRNA induced silencing complex (miRISC) formation. The data show that Roquin can silence ICOS even in the absence of microRNAs and miRISC formation, thereby excluding their requirement.

Instead, Roquin activity is inhibited by experimentally induced miRISC formation, but requires intact function of the P body components GW182, Lsm1 and Rck. Taken together, the data presented place Roquin-mediated translational repression parallel to the miRNA pathway.

2   Zusammenfassung

Roquin ist ein wichtiger Faktor in der Prävention von Autoimmunerkrankungen. Roquin reprimiert die Expression des induzierbaren co-stimulatorischen Rezeptors (ICOS) auf T-Zellen und gewährleistet somit, dass keine Immunantwort gegen Selbst-Antigene stattfinden kann.

Diese Doktorarbeit präsentiert den Mechanismus, durch welchen Roquin ICOS posttranscriptional reguliert. Die Ergebnisse zeigen, dass Roquin, im Gegensatz zu seinem Paralog MNAB, effectiv die Translation von ICOS reprimieren kann. Die carboxy-, sowie die aminoterminale Regionen des Roquin-Proteins besitzen die dafür notwendigen Funktionen. Die carboxyterminale Region lokalisiert Roquin zu sogenannten P bodies, in denen translational reprimierte mRNAs und Proteine, die an translationaler Repression beteiligt sind, ebenfalls lokalisieren. Die aminoterminale Region von Roquin, insbesondere die neu definierte ROQ-Domäne, kann an *ICOS*-mRNA binden und ermöglicht dadurch eine Repression von ICOS. Die aminoterminale Region von Roquin kann durch die stark konservierte aminoterminale Sequenz von MNAB funktionell ersetzt werden. Dies weist darauf hin, dass MNAB ebenso ein regulatorisches Protein sein könnte, jedoch von zur Zeit nicht identifizierten Ziel-Genen.

In einer vorausgegangenen Veröffentlichung wurde vorgeschlagen, dass Roquin mit miRNAs kooperiert, um ICOS zu reprimieren. MiRNAs sind kleine, nicht-kodierende RNAs, die die Translation von kodierenden mRNAs inhibieren können, indem sie an 3'UTR der Ziel-Gene binden. Diese Arbeit widerlegt das aktuelle Konzept und zeigt einen neuen alternativen molekularen Mechanismus für Roquin auf. Die mögliche Beteiligung von miRNAs für Roquin-vermittelte ICOS Repression wurde in zwei unabhängigen Ansätzen überprüft: zum Einem in Dicer-defizienten Zellen, in denen keine miRNA-Biogenese stattfinden kann, und zum Anderen in Argonaute 1-4-defizienten Zellen, in denen keine "miRNA induced silencing complex" (miRISC)-Formation stattfinden kann. Die Daten zeigen eindeutig, dass Roquin-vermittelte ICOS-Repression, auch in der Abwesenheit von miRNAs oder miRISC-Formation, unverändert stattfinden kann. Damit wird eine Beteiligung von miRNAs für Roquin-Aktivität ausgeschlossen.

Stattdessen wurde entdeckt, dass Roquin-Aktivität sogar durch experimentell induzierte miRISC-Formation inhibiert wurde und dass Roquin die intakte Funktion der P body-

Faktoren GW182, Lsm1 und Rck benötigt. Zusammenfassend zeigen die hier präsentierten Daten, dass die Roquin-vermittelte Repression parallel zur miRNA-vermittelten Repression verläuft.

3 Abbreviations and scientific notation

The following format was used when writing genes, mRNAs or proteins:

Gene	*Mrna*	Protein

Table 3-1 Abbreviations:

%	percent
°C	degree Celsius
5'CAP	modified nucleotide on the 5'end of the mRNA
aa	amino acid
Ago	Argonaute (protein)
ARE	AU-rich sequences
BCR	B cell receptor
BSA	bovine serum albumin
cDNA	complementary DNA
CDS	coding sequence
CpG	DNA regions with cysteine nucleotides occur next to guanine nucleotides in a stretch of bases
DNA	deoxyribonucleic acid
ELISA	enzyme-linked immunosorbent assay
ER	endoplasmatic reticulum
ES cell	Embryonic stem cell
FL	full length
ICOS	inducible T cell co-stimulatory molecule
IRE	iron-response element
IRES	internal ribosome entry site
kDa	kilo Dalton
LB media	Luria-Bertani media
min	minute
miR	microRNA
miRNA	microRNA
MNAB	Membrane nucleic acid binding protein
MOI	multiplicity of infection
mRNA	messenger ribonucleic acid
NMD	nonsense mediated mRNA decay
NMD	number
ORF	open reading frame
P body	processing bodies
PAGE	polyacrylamide gel electrophoresis
PBS	phosphate-buffered saline
PCR	polymerase chain reaction
pH	potentio hydrogeni

poly(A) tail	polyadenylated 3'end of mRNA
RING	really interesting new gene
RISC	RNA-induced silencing complex
RNAse	ribonuclease
rpm	revolutions per minute
san	sanroque gene that encodes for Roquin
SDS	sodium dodecyl sulfate
sh RNA	small hairpin RNA
SLE	systematic lupus erythematosus
TCR	T-cell receptor
T_{FH}	follicular helper T cells
TIA-1	T cell internal antigen-1
TTP	Tristetraprolin
UTR	untranslated region
v/v	volume per volume
w/v	weight per volume

4　　Table of contents

5 Introduction

5.1 Motivation of the research work

The primary aim was to investigate the mechanism of posttranscriptional regulation using Roquin and its repression of ICOS as a molecular model system. Although mRNA regulation is an important topic in scientific research, only some mechanisms have been discovered so far (section 5.3). It was recently proposed that microRNAs, a novel class of translational repressors, are required for Roquin's activity [1], but the molecular mechanism remained unclear. Understanding how Roquin exerts its repressive activity on ICOS could elucidate a new concept of mRNA regulation.

Roquin plays a critical role in the prevention of autoimmune diseases and was only recently discovered (section 5.2). Autoimmune diseases arise in most cases due to complex genetic predispositions and/or environmental triggers. There are only few reports showing that mutations in individual genes can disable central control mechanisms of the immune system against self-reactivity leading to autoimmunity (section 5.2). However, mutations in the *Roquin* as well as in the *ICOS* gene have been reported to cause autoimmune diseases in mouse and man [2-6]. Roquin limits ICOS expression in T cells [1]. Consequently, the discovery of the mechanism by which Roquin represses ICOS has potential for the development of therapeutics against autoimmune diseases, in which deregulation of ICOS is causal.

5.2   *Autoimmunity*

Autoimmunity is defined as an immune response of an organism against its own cells and tissues. The immune system fails to discriminate the body's own from foreign constituents. In autoimmune diseases, self-antigens, in addition to foreign antigens, trigger an immune response. Autoimmunity can lead to organ-specific or systemic symptoms. In the case of an organ-specific autoimmune disease, only one or few organs are targeted, e.g. the islets of Langerhans in the pancreas in the case of type 1 diabetes mellitus. In the case of systemic autoimmune disease, e.g. systemic lupus erythematosus (SLE), multiple organs are targeted [7].

Every individual in the animal kingdom is constantly exposed to an enormous diversity of pathogens. Components of the innate immune system can recognize common evolutionary conserved features of pathogens, e.g. unmethylated CpG DNA, and trigger the innate response to effectively diminish the invading pathogen [7]. Owing to short generation intervals, microorganisms can evolve more rapidly than the host they infect and therefore may escape this defense system. Therefore, a second line of defense, the so-called "adaptive immune system", has evolved in vertebrates to overcome main constraints of the innate immune system [7]. The adaptive immune response contains an enormous repertoire of receptors, which allows recognition of an almost infinite diversity of antigens [7]. Lymphocytes, also referred to as T and B cells, ensure a specific immune response after exposure to a pathogen, resulting in lifelong immunity [7]. However, the adaptive immune system is not only beneficial for the host. The huge diversity of receptors also bears a high risk in recognizing self-antigens by mistake, leading to autoimmune diseases. B and T cells can potentially recognize any antigen through surface-expressed B cell receptors (BCRs) or T cell receptors (TCRs), respectively [7]. The diversity is provided by two processes of somatic recombination and mutation of antigen receptor genes. First, the recombination of the variable (V), diversity (D) and joining (J) genes assembles unique BCR and TCR genes from three different gene segments. Second, somatic hypermutation substitutes single nucleotides of BCR genes in the late phase of an immune response. Millions of different receptors can be created by these two processes [7]. It is therefore rather surprising that only 3-8 % of the population develop an autoimmune disease during their life [8], especially since a significant fraction of T and B cell receptors can recognize self-antigen [9]. However, the immune system has not only developed ways to fight pathogens. Simultaneously, numerous and efficient mechanisms co-evolved to prevent harmful responses against self.

During immune reactions, the body produces effector T cells and B cells, which secrete antibodies that neutralize and diminish intruding pathogens. T or B cells develop in the central lymphoid tissues, the thymus or the bone marrow, respectively. Here, somatic gene recombination takes place allowing the production of surface bound TCRs and BCRs [7]. Mature T and B cells enter the periphery where they can be activated by receiving two signals from so-called antigen-presenting cells (APCs). Dendritic cells are the most abundant APCs and become activated upon receptor-independent uptake (macropinocytosis) of pathogens or infected tissue debris [7]. APCs degrade pathogen-derived proteins, subsequent to macropinocytosis, and present the generated peptides as antigens on the surface of major histocompatibility complexes (MHC) (signal 1) to the TCR of the T cell [7]. Signal 1 can only effectively activate T cells if provided along with co-stimulatory signals, for example through the co-receptor CD28 (signal 2) [7]. CD28 signaling is enhanced after upregulation of the CD28 ligand, also called B7, which occurs during pathogen-induced inflammation [10]. Thereby, effective T cell activation and T cell-induced immune responses are in most cases restricted to foreign antigen [10]. There are two main T cell-mediated immune responses. First, CD8 killer T cells themselves act by inducing apoptosis in infected cells of the body. Second, CD4 helper T cells upregulate co-stimulatory molecules and secrete cytokines to activate other cells of the immune system, such as macrophages, granulocytes and B cells. B cells can also be activated independently of T cell help by some microbial antigens, resulting in low-affinity antibodies produced in a rapid immune response [11]. However, for the generation of high-affinity antibodies, B cells differentiate in peripheral lymphoid tissues and undergo somatic hypermutation of their (V) gene region [7]. To avoid loss of affinity or gain of self-reactivity in this process, B cells require T cell help, executed in the so-called germinal center reaction [11]. This help is provided by follicular T helper (T_{FH}) cells, to which the B cells present the recognized antigen. T_{FH} cells highly express the inducible co-receptor ICOS as well as the co-stimulatory molecule CD40L and secrete interleukin-21, an important cytokine for the stimulation of the germinal center B cells. A positive interaction results in the selection of high-affinity memory B cells and long-lived plasma cells, which produce high-affinity antibodies [11].

During development, maturation and activation of lymphocytes, several mechanisms act together to prevent an immune response against self-antigens [9]. First, the lymphocytes that rearrange receptors with self-reactivity are triggered to undergo apoptosis, a process termed "clonal deletion" [7]. Second, B cells employ receptor editing to diminish self-reactivity of the BCR [12]. Third, self-reactive T and B cells that have escaped early control mechanisms

can be extrinsically suppressed [9], either by limiting essential factors for activation and survival (e.g. co-stimuli, essential growth factors or pro-inflammatory mediators) or by active suppression (e.g. through regulatory T cells or the secretion of anti-inflammatory cytokines) [9, 13-15]. Finally, a mechanism termed 'anergy' can cell-intrinsically reduce the ability of T and B cells to be activated through self-antigens [16-18]. A variety of proteins involved in such control mechanisms ensure the discrimination between self and foreign antigens, and the expression levels of these proteins are tightly controlled. For example, aberrant high expression of the inducible T cell co-stimulatory molecule (ICOS) was correlated with T cell activation and germinal center responses triggered by self-antigen [19]. In agreement with this, the newly discovered protein Roquin has been reported to play a crucial role in the prevention of autoimmune diseases by limiting ICOS expression in T cells [1]. Roquin was discovered in an ethylnitrosourea (ENU) screen in mice testing for the generation of auto-antibodies. ENU generates single base pair substitutions at an estimated rate of ~2 per megabase in the germline [2].

The so-called *sanroque* mouse carries one point-mutation in the *Rc3h1* gene, which causes an amino acid exchange in the Roquin protein at position 199 from methionine to arginine (M199R) [2]. The homozygous *san/san* mouse develops a severe autoimmune disease that resembles SLE in humans [2]. Patients with SLE suffer from periods of illness, including fever, malaise, joint pain, fatigue, myalgias and loss of cognitive abilities. SLE can be fatal, however due to improved diagnostic tests and subsequent treatment with immunosuppressive agents, fatalities are becoming rare [20]. For the diagnosis of SLE the presence of anti-nuclear antibodies, directed against nucleic components of the cell, is strongly indicative [21, 22]. Similar to the human disease, *san/san* mice develop auto-antibodies and, more specifically, antibodies directed against nuclear components. Further phenotypes include spontaneous germinal center formation and increased numbers of T_{FH} cells [1, 2, 23]. The most conspicuous molecular phenotype of *san/san* mice is the aberrant high expression of ICOS on all kind of T cells. The increased ICOS expression contributes most significantly to the pathology of *san/san* mice [1]. Therefore, the M199R mutation interferes with Roquin's function to repress ICOS, leading to T cell activation, T_{FH} cell development, germinal center formation and antibody production against self-antigens (Figure 5-1, page 14).

1. Foreign antigen:

Signal 1 and signal 2 (co-stimulatory signal) ⟶ T cell activation, ICOS upregulation

⟶ Follicular T helper differentiation, germinal center formation, plasma cell differentiation and high affinity antibody production

2. Self-antigen in wildtype mice:

Signal 1 alone ⟶ T cell anergy, Roquin suppresses ICOS upregulation

⟶ Follicular T helper differentiation, germinal center formation, plasma cell differentiation and high affinity antibody production

3. Self-antigen in *san/san* mice:

Signal 1 alone ⟶ Roquin M199R cannot suppress ICOS upregulation T cell activation, high ICOS levels

⟶ Follicular T helper differentiation, germinal center formation, plasma cell differentiation and high affinity auto-antibody production

Figure 5-1: Scheme of immune responses against foreign or self-antigen in wildtype mice and against self-antigen in *san/san* mice. (1) T cells are activated by foreign antigens through signal 1 and 2, ICOS becomes upregulated and CD4 T cells differentiate into follicular T helper (T_{FH}) cells. This allows the formation of germinal centers, in which plasma cells differentiate to produce high affinity antibodies. (2) If only signal 1 is provided during recognition of self-antigens, T cells become anergic and Roquin suppresses ICOS (in wildtype mice). T and B cells will not differentiate and no antibodies are produced. (3) After stimulation of T cells in *san/san* mice through signal 1 alone, Roquin M199R cannot suppress ICOS. T cells become activated, promote an immune response and initiate the production of antibodies against self.

The published data show that Roquin prevents autoimmunity by limiting the inducible co-stimulatory molecule ICOS on T cells and indicate that control of ICOS expression is one way to ensure that T cell activation and germinal center responses only occur against foreign antigens (Figure 5-1).

It has been reported that Roquin downregulates ICOS posttranscriptionally and that miRNAs are involved in this process [1]. Therefore, the next sections will focus on known mechanisms of posttranscriptional gene silencing and will include a description of miRNA biogenesis and function.

5.3   Posttranscriptional gene regulation

The individual amounts of proteins within a cell have to be regulated. This is essential for homeostasis and many intra- and inter-cellular processes. The quantity of a protein can be regulated at the level of transcription or posttranscriptionally at the level of translation or protein stability (Figure 5-2).
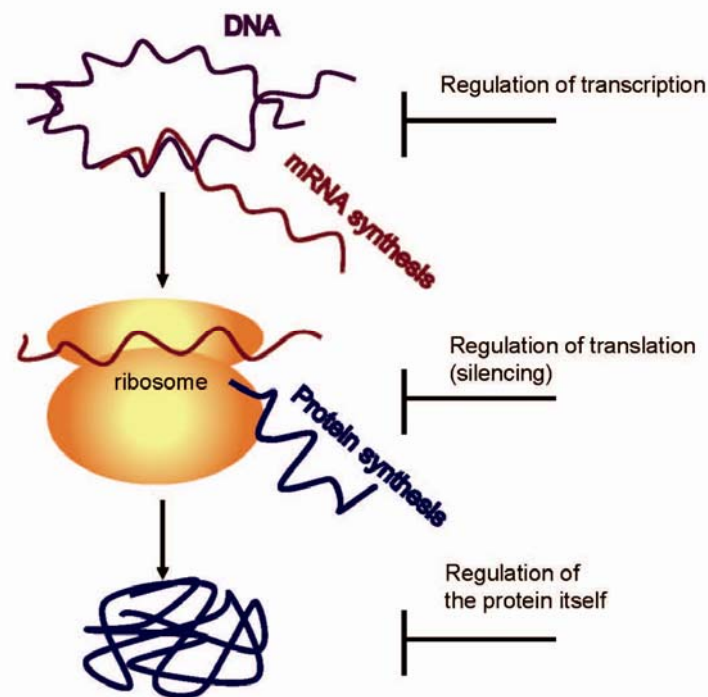
Figure 5-2: Schematic representation of levels of regulation at which protein expression is affected. Regulation can occur at the step of mRNA transcription, protein translation (silencing) or the protein itself.

The expression of genes is generally regulated by transcriptional activation or repression. In a lengthy procedure the generated mRNA transcripts need to be translated, the polypeptides folded and often modified posttranscriptionally before a functional enzyme/protein is produced. Cells need to be able to quickly adjust protein levels in response to endogenous or exogenous triggers (e.g. Ca^{2+} levels, starvation, etc). This can be achieved in several ways without going through the whole process of transcription and/or translation, e.g. by phosphorylation/dephosporylation of proteins or posttranscriptional repression/de-repression by miRNAs. These mechanisms are extremely important for a wide range of physiological

processes, including development, differentiation, reproduction and immune responses. Changing the level of a protein can further be achieved by specific targeting of the protein for degradation. Such a mechanism is for example exerted by E3-ubiquitin ligases that conjugate ubiquitin to target proteins (in form of poly-ubiquitinylation), which will trigger degradation by the proteasom, [24]. Interestingly, E3-ubiqutin ligases are not only very important in many basic cellular functions [24], but seem to play a critical role in the prevention of autoimmune diseases [25, 26].

Apart from regulation of protein stability, the amount of a protein is also determined by the half-life of its mRNA and by the extent to which its mRNA is available for translation. Deregulated translational repression and mRNA turnover can result in various diseases, e.g. cancer, inflammatory disease and Alzheimer's disease [27-31]. Consequently, substantial efforts are being invested to improve our understanding of the mechanisms that regulate mRNA turnover and efficiency of translation.

Obviously, translational control involves several posttranscriptional procedures that share mRNA as a substrate [32-34]. During mRNA biogenesis, the primary transcript is processed by removal of introns and modified by addition of a poly(A) tail and a 5'CAP that consists of a modified guanine nucleotide [35]. Subsequently, the mRNA is exported from the nucleus into the cytoplasm for translation. The mRNA is subject to quality control and can be degraded in a process known as nonsense mediated decay (NMD) [35]. NMD is a translation-dependent process that recognizes and degrades mRNAs that contain a premature translation termination codon, and thereby prevents the accumulation of carboxy-terminally truncated proteins [36].

The mRNAs that pass the criteria of NMD are still subject to regulation of translation and decay (Figure 5-2, page 15). Many proteins are involved in the regulation of translation and mRNA decay. Roquin has been proposed as a factor that promotes ICOS mRNA decay [1]. Therefore, the next section will focus on intrinsic (*cis*) elements and extrinsic (*trans*) factors that control the half-life of mRNAs.

5.3.1 mRNA turnover is regulated by *cis*-elements and *trans*-acting factors

The stability of mRNAs in eukaryotes varies tremendously, with half-lifes of mRNAs ranging from approximately 15 minutes to more than 24 hours [37]. These differences arise on the one hand from *cis*-elements within the mRNA itself and on the other hand from *trans*-acting factors in the cytoplasm (Figure 5-3, page 17).
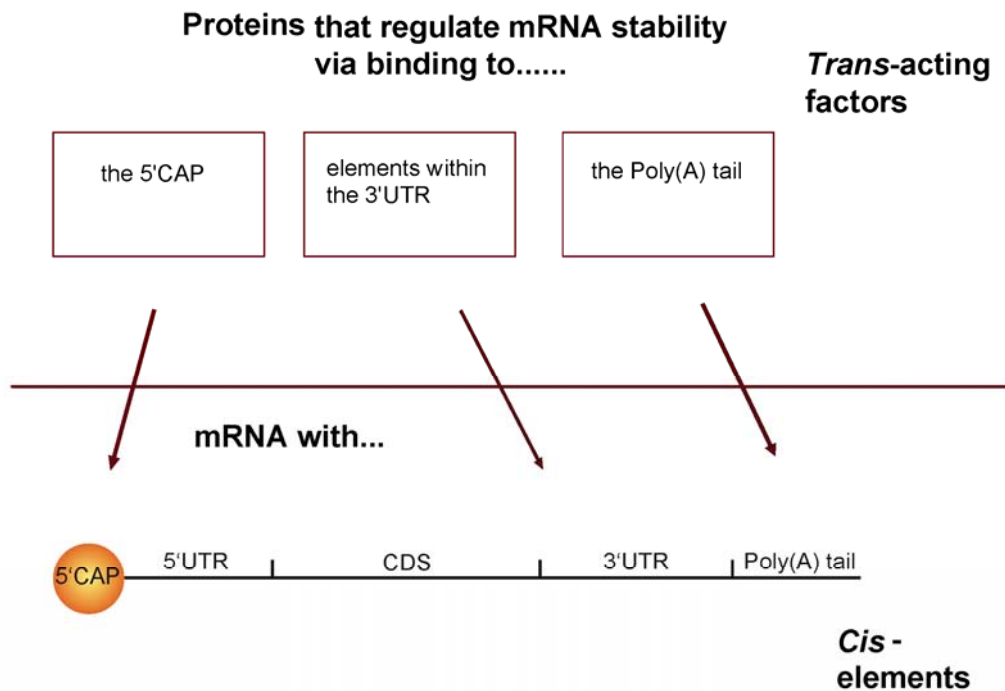
Figure 5-3: <u>Simplified schematic representation of regulatory elements for mRNA stability.</u> Eukaryotic mRNAs contain a 5'CAP, a 5' untranslated region (5'UTR), a coding sequence (CDS), a 3'UTR and a poly(A) tail. Elements (*cis*-elements) within the mRNA are the 5'CAP, elements within UTRs and the poly(A) tail. Proteins in the cytoplasm (*trans*-acting factors) can influence mRNA turnover by regulating the 5'CAP, the Poly(A) tail or by recognizing elements in 3'UTRs.

The regulation of mRNA stability is crucial for T cell responses (section 5.3); and at least 100 mRNAs with a short half-life show differential regulation between resting and activated T cells [38]. Not only cytokine mRNAs, but also transcripts encoding cell surface receptors, proteins involved in signal transduction, transcription factors, regulators of the cell cycle and factors that are pro- or anti-apoptotic show extreme regulation at the level of mRNA stability in the process of T cell activation [38].

Typically, mRNAs are stabilized through their poly(A) tail and the 5'CAP [39, 40]. In fact, deadenylation is the first step in the decay of many mRNAs [41-43], which is then followed by decapping [44, 45]. mRNAs without 5'CAP and without poly(A) tail are rapidly degraded by 5' to 3' and 3' to 5' exonucleases as well as by endonucleases [35, 46]. Generally, the poly(A) tail of mRNAs is gradually shortened by exonucleases as soon as mRNAs reach the cytoplasm [35]. Therefore, mRNA half-life depends on the length of the poly(A) tail, except for replication-dependent histone mRNAs. These mRNAs have a 3' stem-loop instead of a

poly(A) tail that affects the rate at which the mRNA is translated and degraded [47, 48]. Still, regulation of half-life for most mRNAs is achieved by controlling the 5'CAP or the poly(A) tail (Figure 5-3). Examples of *trans*-acting factors effecting the 5'CAP or poly(A) tail will be mentioned later in the section. Beforehand, some *cis*-elements within mRNAs that can regulate mRNA stability will be described here.

Typically, gene-specific regulation via mRNA stability occurs through *cis*-elements in the 3' untranslated region (3'UTR). For example, the 3'UTR of *ICOS* mRNA renders the mRNA sensitive for Roquin-dependent repression [1]. Regulation through the 3'UTR can even work independently of the remainder of the mRNA [46]. Some *cis*-elements in the 3'UTR of a number of mRNAs have been discovered in recent years. For example, the 3'UTRs from mRNAs encoding ferritin and the transferrin receptor contain so-called iron response elements (IREs). These mRNAs are regulated posttranscriptionally in response to changes in intracellular iron concentrations. The IRE is a 23-27 base pair (bp) stem-loop that can be recognized by an iron regulatory protein (IRP), a *trans*-acting factor [46]. Another example for a *cis*-element is the U-rich region of approximately 20 nucleotides within the 3'UTR of the two oncogenes *c-fos* and *v-fos*. This region promotes deadenylation and thereby mRNA decay [49, 50]. Additionally, the 3'UTRs of c-*fos* and v-*fos* also contain AU-rich elements (AREs). In combination both *cis*-regulatory elements have been shown to be extremely potent for RNA destabilization [51, 52].

AREs are encoded in 3'UTRs of many mRNAs, for example in the 3'UTR of a lot of cytokines, such as *IL-1, IFN-γ, TNF-α* and *IL-2,* as well as immediate early genes, such as c-myc [37, 46]. These mRNAs are among the shortest-lived mRNAs in eukaryotes [53]. The 3'UTR of *ICOS* mRNA also contains three AUUUA pentamers. However, it is not clear whether these AUUUA pentamers can cause destabilization of the *ICOS* mRNA. The reason is that different AU-rich RNA sequences can function as destabilizing mRNA signals and that it has not been functionally tested for *ICOS* mRNA whether the three AUUUA pentamers can lead to destabilization of the mRNA. Although it remains elusive what configuration makes AREs effective [46, 54, 55], AU-rich elements have been shown to be essential *cis*-acting elements for the destabilization of many mRNAs [56].

As mentioned above, mRNA regulation not only depends on *cis*-elements within the mRNA, but also on the presence of *trans*-acting factors in the cytoplasm that influence mRNA decay (Figure 5-3). The next section will therefore describe some of the best known *trans*-acting factors.

Some *trans*-acting factors can destabilize mRNAs, while others function as stabilizers [46]. The best known mRNA stabilizing proteins are the poly(A)-binding protein (PABP) and the 5' CAP-binding protein eIF4E [57], both being required for active translation. Consequently, translation itself prevents the mRNA from degradation. Also extensively studied were the RNA-binding proteins '*c-fos*- and *c-myc*- coding region determinant-binding protein' that have been identified for the regulation of *c-fos* and *c-myc*, respectively [41, 46, 58]. Another example is the iron regulatory protein (IRP) that can bind to IREs encoded in the mRNAs of *transferrin* and *ferritin* and subsequently causes mRNA stabilization.

However, reports are accumulating about *trans*-acting factors that can function as mRNA destabilizers. *Trans*-acting factors can destabilize mRNAs without possessing intrinsic mRNase activity, like RNases [46]. Instead, they promote mRNA decay as regulatory proteins [46]. One important protein family of *trans*-acting factors are the ATP-dependent RNA helicases that participate in almost all pathways of RNA processing and degradation [59]. RNA helicases unwind secondary structures or displace bound proteins and/or RNA [59]. For example, it has been shown that the ATP-dependent helicase DDX6 (also referred to as Rck) has a key role in translation repression [60], mRNA decay [61], and general mRNA protein complex (mRNP) remodeling [60, 62]. Another important protein family of *trans*-acting factors are the Lsm2-8 and Lsm1-7 complexes that can act as chaperones for RNA-RNA and RNA-protein interactions [59]. The Lsm1-7-Pat1 complexes can function as decapping activators of the mRNA and thereby promote the degradation of mRNAs via 5'-3' exonucleases [63]. Similarly, the DCP1:DCP2 complex functions as a decapping activator and therefore promotes mRNA decay [64]. However, mRNA decay is not only promoted by decapping mechanisms. Instead, deadenylation is thought to be the first step for the decay of most mRNAs. The deadenylation complex CCR4-Not is therefore a central *trans*-acting factor [59, 65]. Another family of proteins, the AU-rich binding proteins (AUBPs), can also be considered as *trans*-acting factors [46]. They recognize AREs in the 3'UTR of a variety of mRNAs. Examples are AUF1, HuR, KSRP and TTP [37]. AUF1, KSRP and TTP contain zinc finger domains that can bind nucleic acids and cause destabilization of the target mRNA [66, 67]. HuR is an exception that can also recognize AREs in 3'UTRs but with an RNA-recognition motif (RRM) that leads to stabilization of the mRNA [68]. Thereby, HuR is an important antagonizing factor for mRNA decay pathways. Nevertheless, Tristetraprolin (TTP) is the most prominent example of AUBPs, which contains CCCH-type zinc finger domains [69-73], similar to Roquin. For Roquin the mechanism of translational repression was unclear until now, but the mechanism of TTP has been studied quite extensively. The

combination of two CCCH-type zinc fingers allows TTP to bind directly to the *TNF-α* mRNA [70, 74]. TTP promotes mRNA decay by interaction with other *trans*-acting factors, for example CCR4, a component of the CCR4-Not deadenylation complex, and DCP2, a component of the DCP1:DCP2 decapping complex, or the 5'-3' exonuclease XrnI [75]. Many mRNA decay processes are functionally linked through the use of common factors or by being physically connected [45]. Indeed, *trans*-acting factors, together with their mRNA targets, co-localize within discrete cytoplasmic domains, known as processing bodies (P bodies) [45]. In support of that notion, *ICOS* mRNA, the target of Roquin, was reported to localize to P bodies [1]. However, Roquin itself has been described to localize to different cytoplasmic domains, known as stress granules [2], to which some other proteins involved in mRNA regulation can also localize [76]. Therefore, the next section will introduce P bodies and stress granules, and describe their function in mRNA decay.

5.3.2 P bodies and stress granules are cytoplasmic loci involved in mRNA silencing

Processing bodies (also called P or GW bodies) are compartments without membrane in the cytoplasm of eukaryotic cells. They contain translationally inactive mRNAs as well as enzymes that are involved in mRNA turnover.

P bodies were first described in 1997, showing that XRN1, the main cellular 5'-3' exoribonuclease, localized in discrete, prominent loci in the cytoplasm [45, 77]. This discovery remained unappreciated until 2002, when an autoimmune serum recognized a novel protein of unknown function, GW182, that stained the same compartments [78, 79].

The decapping activators DCP1:DCP2 [80] and Lsm1-7, Rck or the deadenylase complex CCR4-Not [81], all introduced in the section 5.3.1 and 5.3.3, also localize to P bodies. The fact that all proteins involved in mRNA destabilization and translational repression could all be detected in P bodies, raised the question whether these loci are exclusively used for storage of translationally inactive RNAs or whether these are places at which mRNA decay actually occurs. There are three strong indications that mRNA degradation takes place in P bodies [45]. First, P body assembly depends on the presence of RNA in the cell [82, 83]. Second, P bodies disappear when mRNA decay is blocked at an early stage in cells, e.g. by preventing deadenylation in cells [84, 85]. Third, P bodies enlarge if the progression of mRNA decay is blocked and intermediates accumulate [79, 80]. In spite of this, it may also be the case that

the P body structure itself is not required for mRNA decay [45], since P body components can dynamically exchange with the cytoplasmic pool [76].

In addition to P bodies, stress granules constitute another compartment in the cytoplasm, in which translational repression takes place. Many proteins involved in translational repression do not only localize to P bodies, but also to stress granules [76]. For example, TTP can be detected in P bodies, as well as in stress granules, if stress was previously induced [75, 76, 86]. When cells are exposed to adverse conditions, such as heat shock, oxidative stress or energy deprivation, they initiate a stress response that involves the assembly of stress granules and bulk shutdown of mRNA translation [75]. Such a stress response is mediated by phosphorylation of the eukaryotic initiation factor (eIF) 2α [87]. The activation of one or more of the eIF2α kinases leads to stress granule assembly by decreasing the levels of eIF2-GTP-tRNA^{MET}, the ternary complex that is required for loading the initiator methionine onto the 48S preinitiation complex to start translation [87]. This allows binding of the RNA-binding protein TIA-1 (T cell internal antigen-1) to the 48S complex instead of the ternary complex and promotes polysome disassembly and aggregation of TIA-1. The latter leads to the formation of stress granules [87]. Stress response is not only a basic mechanism for cell survival, but is also activated during T cell differentiation to control cytokine levels, for example [88]. As compared to P bodies, stress granules are bigger in size. Despite this obvious difference, both can be physically linked for the regulation of some RNAs [89]. However, to which extent these two cell compartments cooperate in function or exchange components is not clear.

Interestingly, components of the microRNA (miRNA) pathway, for example Argonaute 2 (Ago2), also localize to P bodies as well as stress granules [90-92], and it has been suggested that miRNAs themselves are involved in the mechanism by which Roquin represses ICOS [1]. Therefore, the biogenesis and function of miRNAs is introduced/described in the next section.

5.3.3 MicroRNAs, a unique class of *trans*-acting factors

MicroRNAs (miRNAs) are small (~22 nucleotide) non-coding single-stranded RNAs that represent a novel class of *trans*-acting factors that were first discovered in 1993 [93]. miRNAs bind to partially complementary sequences in 3'UTRs of mRNAs, which causes translational inhibition and mRNA decay. They repress the translation of a big part of all mRNAs, including critical factors for cell growth, proliferation, development and differentiation [94]. Consequently, deregulation of miRNAs was found to be implicated in

the development of diseases, such as cancer and autoimmunity. For example, mice overexpressing the miR-17-92 cluster suffer from a lymphoproliferative and autoimmune disease that was associated with auto-antibody production [95]. Overexpression of miR-155 in mice caused pre-B cell leukemia and B cell lymphoma [96]. miR-155 can also be found overexpressed in different human lymphoma, including B cell lymphoma, such as Hodgkin or diffuse large B cell lymphoma [94, 97]. miRNAs are transcribed as several hundred bp long primary miRNAs (pri-miRNAs) and are processed in the nucleus by an enzyme complex of Drosha/DGCR8 (Figure 5-4 step 1-2, page 23). The resulting ~90 bp pre-miRNAs are then exported by Exportin-5 into the cytoplasm, where they are recognized by Dicer (Figure 5-4 step 3-4, page 23). Dicer processes pre-miRNAs into double-stranded miRNAs, from which one strand, the mature miRNA, is selectively loaded into the RNA-induced silencing complex (RISC) by one of the Argonaute 1-4 (Ago1-4) proteins (Figure 5-4 step 5, page 23). This process is also known as miRISC formation. Binding of RISC loaded miRNAs to sequences in the 3'UTR of mRNAs induces translational inhibition, followed by destabilization of the mRNA [98-101]. Several findings argue that P body formation itself as well as P body components are essential for miRNA-mediated translational inhibition (Figure 5-4 step 6, page 23). First, Ago proteins and mRNAs that are targets of miRNAs accumulate in P bodies in a miRNA-dependent manner [92, 102, 103]. Second, GW182, a major P body component, interacts with Argonaute proteins and is required for miRNA-mediated repression [104, 105]. Knockdown of GW182 or introduction of a dominant-negative mutant of GW182, interferes with miRNA-mediated repression and P body formation [102, 103]. And third, a helicase essential for general translational repression, Rck, (section 5.3.1) that also localizes to P bodies (section 5.3.2), has been identified to be crucial for miRNA-mediated silencing and P body formation [106]. In contrast to these results, there have also been reports that miRNA-mediated silencing does not require P bodies as such. For example, the knockdown of Lsm1, an enzyme involved in many mRNA decay processes (section 5.3.1) disrupts P body formation, but does not affect Ago2-mediated miRNA function [106]. However, another publication reported that Lsm1 is actually required for the repression of about 5% of miRNA-targeted mRNAs [107].
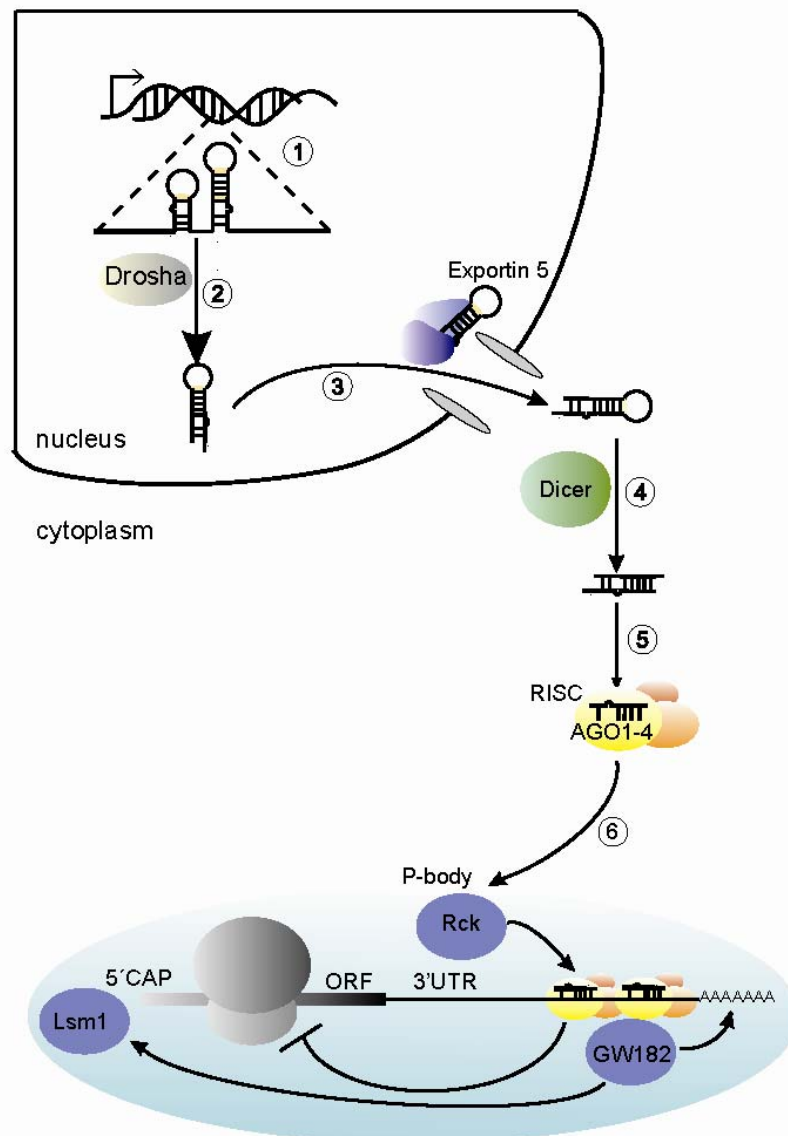
Figure 5-4: <u>miRNA biogenesis and translational inhibition by miRNAs.</u> Numbers indicate steps involved in miRNA biogenesis, translational inhibition and mRNA decay: (1) Primary miRNAs (pri-miRNAs) are transcribed, (2) Drosha processes pri-miRNAs into precursor miRNAs (pre-miRNAs). (3) Pre-miRNAs are exported into the cytoplasm by Exportin 5. (4) Dicer processes pre-miRNAs into mature miRNAs. (5) The mature miRNA strand gets loaded onto the RISC complex. (6) Inhibition of translation by miRNAs requires the P body components Rck and GW182 and about 5% of all miRNAs also depend on Lsm1.

Still, this report, and a report by Izaurralde and colleagues [45] suggest that P body formation is rather a consequence of translational inhibition than the cause. Although it remains controversial whether P body formation is required for miRNA-mediated repression, it is now generally accepted that proteins located in P bodies and promoting general mRNA decay (section 5.3.1 and 5.3.2), such as the decapping activator complex DCP1:DCP2 and

deadenylation activator complex CCR4-Not, are required for miRNA-mediated silencing [107-110]. Actually, many translational repression or mRNA decay pathways overlap [111] and are poorly separated from each other in current publications. For example, TTP does not seem to require the miRNA pathway, judged by most publications about TTP, but it has once been reported that Dicer and Argonaute proteins, as well as miR-16, are involved in the mechanism of TTP [112]. Similarly, Roquin-dependent ICOS repression has recently been proposed to critically depend on specific sequences in the *ICOS* 3'UTR that could be recognized by miR-101 [1]. However, it has not been clarified in these reports how and at which state TTP or Roquin actually cooperate with the miRNA pathway. To understand these mechanisms and their cooperation, it seems necessary to discriminate and dissect these pathways genetically. Such an attempt has not been reported so far.

5.3.4 Posttranscriptional gene silencing by Roquin

At the beginning of this research project in 2006, Roquin was portrayed as an essential factor in T cells for the prevention of autoimmune diseases (section 5.2). At that point in time, the molecular function was completely unknown. The RING finger domain and CCCH-type zinc finger of Roquin implied that Roquin could be a regulator of protein stability or mRNA translation. RING finger domains can exert E3 ubiquitin ligase activity and therefore regulate protein levels posttranscriptionally (section 5.3). Interestingly, other E3 ubiquitin ligases, such as Cbl-b and Itch also play a role in the prevention of autoimmune diseases [25, 26]. In fact, Rle-1, the homolog of Roquin in *C.elegans,* exhibits E3 ubiquitin ligase activity towards DAF-16, the worm homolog of Foxo3a [113]. However, it was unclear whether mammalian Roquin can posttranscriptionally regulate proteins and if it requires its RING finger domain for its activity. The CCCH-type zinc finger domain suggests interaction with nucleic acids. MNAB, the paralog of Roquin, has been shown to interact with DNA *in vitro,* an interaction that partly depends on the CCCH-type zinc finger [114]. Other nucleic-acid binding proteins, such as TTP and Zc3h12a, also contain CCCH-type zinc fingers and can regulate mRNA levels posttranscriptionally [70, 115]. TTP and Zc3h12a can bind and destabilize mRNA with either two zinc fingers or an additional amino-terminal domain, respectively [70, 115]. It was unclear whether Roquin or MNAB, both containing only one CCCH-type zinc finger, can also regulate or bind to mRNAs. Interestingly, Roquin and MNAB share a conserved N-terminal domain upstream of the CCCH-type zinc finger with so far unknown function. It was known that this so-called ROQ domain bears an essential function for the prevention of autoimmune

diseases, because the M199R mutation in the ROQ domain of Roquin causes the disease in *san/san* mice (section 5.2).

In 2007 it was published that Roquin regulates ICOS posttranscriptionally by promoting *ICOS* mRNA decay [1]. In agreement with this, Roquin was shown to localize to stress granules, further indicating that Roquin could regulate mRNA levels (section 5.3.2). In addition, the publication in 2007 suggested that miRNAs are required for the repression of ICOS by Roquin [1]. This implied a novel mode of mRNA regulation. However, it remained unclear how Roquin could exert this function and how it would cooperate with the miRNA pathway.

To address these open questions in this project, a structure-function analysis of Roquin-mediated ICOS repression was performed. To do so, a panel of point- or deletion-mutants as well as chimeras (combining sequences of Roquin and MNAB) were generated. Mutant and wildtype proteins were analyzed in their subcellular localization and tested for their ability to bind to *ICOS* mRNA and to repress ICOS expression. Finally, a genetic dissection was performed using cell systems of knockdown or knockout of key molecules in translational repression or/and mRNA decay. This dissection aimed to investigate a functional requirement or contribution of miRNAs and miRISC formation and to discriminate a functional involvement of the stress granule or P body pathway in Roquin-mediated ICOS repression.

6   Materials

6.1   Antibodies
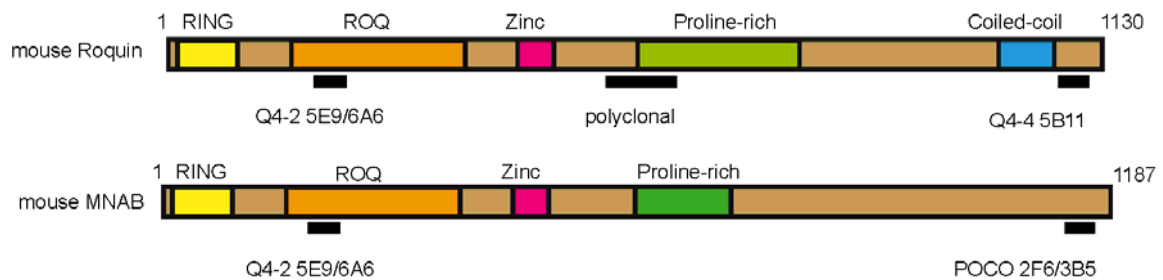
Figure 6-1: <u>Illustration of the structure of mouse Roquin and mouse MNAB.</u> This illustration shows individual RING and zinc fingers, ROQ and coiled-coil domain, as well as proline-rich regions of Roquin and MNAB. Black bars indicate the regions from which peptides were synthesized and used to generate rat monoclonal antibodies, or the region that includes epitopes recognized by commercial polyclonal antibodies.

Antibodies against mouse Roquin and MNAB were generated in collaboration with Elisabeth Kremmer's group (section 11). Antibodies were produced by injection of BSA-conjugated peptides into rats:

Q4-2 (Roquin or MNAB RSLGERTVTELILQHQNPQQLS),

Q4-4 (Roquin NKTSSLNLSEDSEGGGDNNDSQR),

POCO (MNAB VMSEDKNDFLKPIANGKMVNS).

Hybridoma cells lines 5E9, 6A6, 5B11, 2F6 and 3B5 were repeatedly subcloned and effective antigen recognition was evaluated by ELISA and immunoblots (section 8.1.1).

Monoclonal anti-CD3, anti-CD28, anti-IL4, anti-IFN-gamma and anti-IL-12 were purified on protein G sepharose columns using supernatants from 145-2C11, 37N, IIB11, Xmg-1.2 and C17.8 hybridomas, respectively.

Table 6-1 Purchased antibodies:

Antibody	Company
Anti-mouse ICOS-PE, anti-mouse CD44-APC; anti-human ICOS-biotin (ISA-3), Streptavidin-APC, Streptavidin-PE, anti-mouse Thy1.1-PerCP or -APC and anti-mouse CD4-APC.	eBioscience
Cy5-conjugated anti-mouse or anti-rabbit and HRP-conjugates	Jackson Immuno Research
primary antibodies against Roquin (514A) and DDX6 (461A)	Bethyl
Anti-GFP (A11122)	Invitrogen
Anti-Flag-tag (M2)	Sigma
Anti-Argonaute-2 (C34C6)	Cell Signaling Technology
Anti-Tubulin (B-5-1-2) or TIA-1 (C-20)	Santa Cruz Biotechnology

6.2   Oligonucleotides

Oligonucleotides were synthesized by the company METABION.

Table 6-2 Primers:

Primer name	Sequence from 5' end	Purpose
Roquin Pos 900 Forw	GACCAGTGGTCCTCTTTGC	Primer used for sequencing within the Roquin open reading frame.
Roquin Pos 2300 rev	GCTGCCACAACATCTTTGGG	Primer used for sequencing within the Roquin open reading frame.
Roquin mut1 forw	GTAGTGCATGGATTGGTTGATTATATCCAGAACCACAGC	Primer used to correct a mutation in the original cDNA clone of Roquin obtained from Dr. Carola Vinuesa.
Roquin mut1 rev	GCTGTGGTTCTGGATATAATCAACCAATCCATGCACTAC	Primer used to correct a mutation in the original cDNA clone of Roquin obtained from Dr. Carola Vinuesa.
Roquin depletion away for	GGGTACAAGCAAGCAAGCAGAAAATGGCCAGCCCGAGCCCCC	Primer used to correct a mutation in the original cDNA clone of Roquin obtained from Dr. Carola Vinuesa.
Roquin depletion Away rev	GGGGCTCGGGCTGGCCATTTTCTGCTTGCTTGCTGCTTGTACCC	Primer used to correct a mutation in the original cDNA clone of Roquin obtained from Dr. Carola Vinuesa.
Roquin mut2 forw	GGGAGGTGAACACCCTGGCAAGCCAGCCACAGCCCCCTTC	Primer used to correct a mutation in the original cDNA clone of Roquin obtained from Dr. Carola Vinuesa.
Roquin mut2 rev	GAGGGGGCTGTGGCTGGCTTGCCAGGGTGTTCACCTCCC	Primer used to correct a mutation in the original cDNA clone of

		Roquin obtained from Dr. Carola Vinuesa.
ICOS human forw BamHI	GAGAATCCGGACCATGAAGTCAGGCCTCTGGTATTTC	Forward primer to clone human ICOS cDNA.
ICOS humanFL rev XhoI	GAGCTCGAGGGTTACTACTGTTAAAATCTCTTTG	Reverse primer to clone human ICOS cDNA including its 3'UTR.
ICOS human rev CDS XhoI	GAGACTCGAGGGTTATAGGGTCACATCTGTGAG	Reverse primer to clone human ICOS containing only the open reading frame.
Roq SalI ATG weg forw	GAGAGTCGACCCCTGTACAAGCTCCACAATGG	Primer to clone the Roquin open reading frame without start codon and 3' to the GFP open reading frame.
Roq NotI rev	GAGAGCGGCCGCCTAGGGAGCAGAATTGGAAAC	Primer to clone the Roquin open reading frame.
Roquin 2880 STOP no coil rev	GGGAGAAAATGTCCATGGCAGAAGTGGCCAGTTAAGGAAAACCCC	Primer to insert a STOP codon in the Roquin open reading frame at position 2880 (bp) for deletion of the coiled-coil domain.
Roquin 2880 STOP no coil forw	GGGGTTTTCCTTAACTGGCCACTTCTGCCATGGACATTTTCTCCC	Primer to insert a STOP codon in the Roquin open reading frame at position 2880 (bp) for deletion of the coiled-coil domain.
RING RoquinTG-GC	TCTGAGTGCAAATTGGGGCGGAAAGGAAATCCGTCC	Primer to mutate cysteine at position 14 (aa) to alanine in Roquin.
RING RoquinTG-GC	GGACGGATTTCCTTTCCGCCCCAATTTGCACTCAGA	Primer to mutate cysteine at position 14 (aa) to alanine in Roquin.
Roquin 1550 STOP no ProlR	GGGAGCACAGTGACACAACTGATTCCATGAGGGACAGACCCCAGC	Primer to insert a STOP codon at position 1550 (bp) in the Roquin open reading frame for deletion of the carboxy-terminus including the proline-rich region.
Roquin 1550 STOP no ProlF	GCTGGGGTCTGTCCCTCATGGAATCAGTTGTGTCACTGTGCTCCC	Primer to insert a STOP codon at position 1550 (bp) in the Roquin open reading frame for deletion of the carboxy-terminus including the proline-rich region.
Zinc Roq forw new	GCAAATACAAAACATACATGGCTCGAGATATGAAGCAAAGGG	Primer to mutate cysteine at position 418 (aa) to arginine.
Zinc Roq rev neu	CCCTTTGCTTCATATCTCGACCGATGTATGTTTTGTATTTGC	Primer to mutate cysteine at position 418 (aa) to arginine.
ICOSFL POS 896 correct rev	GGAGACAGGGATTCCACTCCCAGTGAGCACACAGGAGCTGGGC	Primer to correct a mutation in full length ICOS at position 896 (bp).
ICOSFL POS 896 correct for	GCCCAGCTCCTGTGTGCTCACTGGGAGTGGAATCCCTGTCTCC	Primer to correct a mutation in full length ICOS at position 896 (bp).
GFP NotI forw	CACCGCGGCCGCACCATGGTGAGCAAGGGCGAGGA	Primer to clone GFP into PETOPO.
GFP BglII XbaI rev	AGATCTAGATTACTTGTACAGCTCGTCCATGCCGA	Primer to clone GFP into PETOPO.
Roq RINGC34A forwn	CCCATCAGTTTGGGCGCTGGCCATACTGTCTGCAAA	Primer to mutate cysteine at position 34 (aa) to alanine, when cysteine at position 14 (aa) is already mutated to alanine.
Roq RINGC34A revn	TTTGCAGACAGTATGGCCAGCGCCCAAACTGATGGG	Primer to mutate cysteine at position 34 (aa) to alanine, when cysteine at position 14 (aa) is

		already mutated to alanine.
Roquin M199R rev	CAGAGCTTCCTCCTGCCTCGCTGGTCCAAGGAACTGGC	Primer to mutate methionine at position 199 (aa) to arginine.
Roquin M199R forw	TGCCAGTTCCTTGGACCAGCGAGGCAGGAGGAAGCTCTG	Primer to mutate methionine at position 199 (aa) to arginine.
humanCD4NotIforw	GAGCGGCCGCACCATGAACCGGGGAGTCCC	Primer to clone the human CD4 open reading frame.
Human CD4 BglII rev	GAGATCTTCAAATGGGGCTACATG	Primer to clone the human CD4 open reading frame.
ICOSFL POS 1636 rev	GAGAATGCTGCTGGCCCATTAAAGATG	Primer for sequencing of human ICOS.
hICOS BglII AgeI forw	CACCAGATCTTAGTAATAGACCTGGTAT	Primer to clone the human ICOS cDNA into PETOPO.
hICOS CDS AvrII BamHI rev	CCTAGGTAGTAATAGGGATCCTTATAGGGTCACATCTGTGA	Primer to clone only the open reading frame of human ICOS.
hICOSFL AvrIIBamHI rev	CCTAGGTAGTAATAGGGATCCCTTTGCCTTCTTACTACTGTTA	Primer to clone the human ICOS cDNA with its 3'UTR.
hICOSFL XhoI till20 bp before	GAGACTCGAGGGTTAAGATAATATAAGTATGC	Primer to clone human ICOS cDNA with its 3'UTR deleting the putative miR101 binding site.
Roquin no RING SalI f	GAGAGTCGACCATGGAGACCACTATCAATACGGAC	Primer to clone the Roquin open reading frame without its RING domain.
Roquin no ROQ forw new	GAGAGTCGACCATGACAATTGCTCTCCAGCGGACTGG	Primer to clone the Roquin open reading frame without its RING domain.
ICOSUTR only BglII forw	CACCAGATCTTTGGCCAGTTTTCCTCAACT	Primer to clone only the human ICOS 3'UTR into PETOPO with a BglII restriction site.
ICOSUTR only XbaI rev	TCTAGAGTGGCTCCTCTTAAAACTGGATT	Reverse primer to clone the human ICOS 3'UTR into PETOPO with a XbaI restriction site
Roquin no Nterm for	GAGAGTCGACCATGGAAGAACTGGAAAAGTTTC	Primer to clone Roquin without RING, ROQ and Zinc finger
Roquin Zinc Cys2 Ala forw	GAAGCAAAGGGGAGGACGCCCTCGTGGTGCCAGCTGTACGTTTGC	Primer to mutate the 2nd cysteine (aa) 34 in the zinc finger domain.
Roquin Zinc Cys2 Ala rev	GCAAACGTACAGCTGGCACCACGAGGGCGTCCTCCCCTTTGCTTC	Primer to mutate the 2nd cysteine (aa) 34 in the zinc finger domain.
Roquin Pos1280 BssSI MNAB comp:	CAAAGGGGAGGATGCCCACGAGGTGCCAGCTGTACGTTTGC	Primer to generate Roquin/MNAB chimeras with a BssSI restriction site introduced into the Roquin cDNA.
Roquin Pos 1280 BssSI MNAB comp:	GCAAACGTACAGCTGGCACCTCGTGGGCATCCTCCCCTTTG	Primer to generate Roquin/MNAB chimeras with a BssSI restriction site introduced into the Roquin cDNA.
AGO2 Pos 470 F-V forw	CG GAA GTC CAT CTG AAG TCC GTC ACA GAG CAG CTC AGA AAG	Primer to mutate position 470 (aa) phenyl-alanine to valine together with position 505 (aa) in the GW182 binding site.
AGO2 Rev 470 F-V	CTT TCT GAG CTG CTC TGT GAC GGA CTT CAG ATG GAC TTC CG	Primer to mutate position 470 (aa) phenyl-alanine to valine together with position 505 (aa) in the GW182 binding site.
AGO2 Pos 505 F-V forw	CG GAC AGC GTG GAG CCC ATG GTC CGG CAC CTG AAG AAC ACG	Primer to mutate position 505 (aa) phenyl-alanine to valine together

		with position 470 (aa) to mutate the GW182 binding site.
AGO2 Pos 505 rev	CGT GTT CTT CAG GTG CCG GAC CAT GGG CTC CAC GCT GTC CG	Primer to mutate position 505 (aa) phenyl-alanine to valine together with position 470 (aa) to mutate the GW182 binding site.
Roquin forw PCR	GAGAGCGGCCGCCTAGGGAGCAGAATTG GAAAC	Primer to clone Roquin open reading frame.
Roquin rev PCR	GAGATGATCACTAGGGAGCAGAATTGGA AAC	Primer to clone Roquin open reading frame.

6.3   Expression constructs

Expression constructs were generated by the following principle:

First, primary constructs were generated. For that, the open reading frame of the gene of interest was PCR amplified and cloned into so-called entry vectors (Invitrogen), which contain a gateway cloning cassette (see below). Then secondary expression constructs, also containing the gateway cloning cassette, were generated by a lambda recombination reaction (section 7.3.5), which leads to an insertion of the open reading frame into the expression construct.

6.3.1   Generation of primary constructs

The open reading frames of mouse **Rc3h1 (Roquin) (AY948287)**, human **RC3H2 (MNAB) (NM_001100588)**, human **ICOS including the 3'UTR (NM_012092)** or human **Argonaute 2 (NM_012154)** were PCR-amplified, ligated into cloning vectors (pENTR11, pCR8-GW or pENTR-D Topo) and sequenced (primary vectors). Mutations originating from provided vectors or introduced by PCR-amplification were corrected by site-directed mutagenesis using the XL Quickchange kit (section 7.3.3). All intentionally inserted point-mutations were generated in the same way (section 7.3.3).

The following Roquin constructs were generated and verified by sequencing:

For orientation purposes see Figure 6-2.

Deletion-mutants of Roquin constructs with and without GFP-tag:
-Roquin aa 1-951
-Roquin aa 1-509
-Roquin aa 55-1130
-Roquin aa 338-1130
-Roquin aa 441-1130
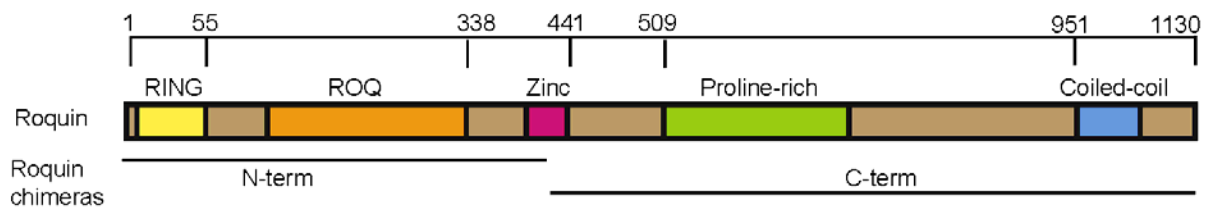
Figure 6-2: <u>Schematic depiction of the structure of Roquin.</u> It shows individual domains, as well as the proline-rich region. Lines indicate the regions, which were fused to generate chimeras. Numbers refer to amino acid end points of the generated deletion-mutants.

Point-mutants of Roquin without tag:
-Roquin C14AC34A
-Roquin M199R
-Roquin C419RC428R

Additional constructs:

-Roquin-WT and

-Roquin/MNAB chimeras

(The conserved amino-termini of Roquin and MNAB were exchanged. To clone these constructs in frame, I made use of a conserved BssSI restriction site, which -for cloning purposes- was present in the wrong orientation. Therefore, I first changed this BssSI site by point-mutagenesis in Roquin without modifying the reading frame (Figure 6-3).
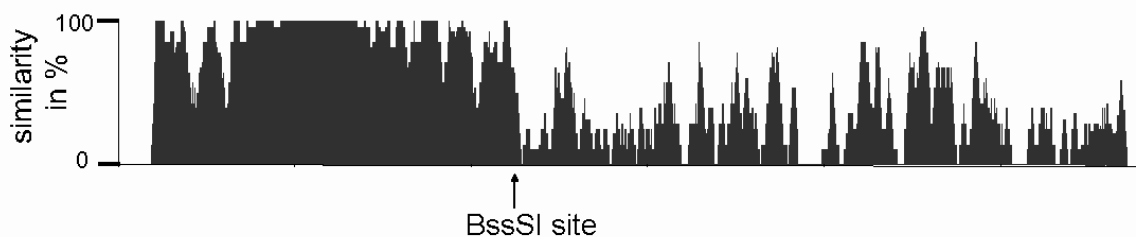

Figure 6-3: <u>Alignment of human MNAB and mouse Roquin open reading frames.</u> Black bars indicate regions of identity. The BssSI site used for fusion of open reading frames and generation of chimeras is indicated.

The following ICOS constructs were generated and sequence-verified:

-ICOS cDNA including the 3'UTR (1-2539) and without the 3'UTR (1-600)

-ICOS cDNA including the 3'UTR, but deleted in the putative miR-101 binding site (1-2211)

-the 3'UTR of ICOS (601-2539) fused 3' to the coding region of GFP or human CD4

The following Argonaute 2 constructs were generated and sequence-verified:

-the open reading frame of human Argonaute 2

-the open reading frame of human Argonaute 2 F470V/F505V

6.3.2 Generation of secondary constructs

Secondary expression constructs were produced via lambda recombination (LR) (Invitrogen) (section 4.3.5) using pLNCX2, pKMV-IRES-GFP or pMSCV-IRES-Thy1.1 retroviral vectors or the adenoviral expression vector pCAGAdDu. The map of the KMV vector is shown below to illustrate the backbone of a retroviral vector (Figure 6-4).
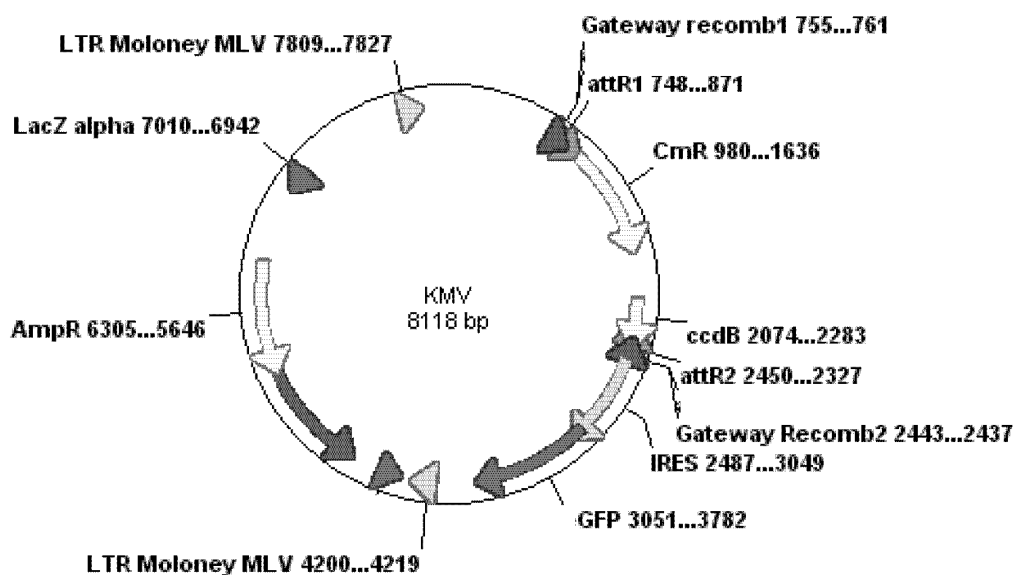

Figure 6-4: <u>Schematic depiction of the destination vector KMV.</u> LTR: long terminal repeats. These are retroviral promoters that encode all sequences for gene regulation including enhancer, promoter, transcription initiation, transcription termination and polyadenylation signals. Moloney MLV: Moloney murine leukemia virus. LacZ alpha: the first gene of the lac operon for colony selection. AmpR: ampicillin resistance. IRES: Internal ribosome entry site, the ribosome binds CAP-independently on the same RNA and translates a second protein (e.g. GFP or Thy1.1 (in the case of the MSCV-IRES-Thy1.1 vector) which is a glycosylphosphatidylinositol (GPI) anchored protein that is rapidly expressed on cell surfaces). CmR: chloramphenicol-resistance. ccdB: potent- death gene for cells that do not contain a ccdB gene. Gateway recombination sites(attR1 and attR2): lambda recombinase recognition sites for LR reaction (section 4.3.5) to insert the gene of interest.

6.3.3 Constructs generated for dual luciferase activity measurements

Adenoviral plasmids for dual luciferase activity assays were cloned based on the psiCHECK2 dual luciferase construct (Promega), in the context of an adenoviral backbone of pAd-Pl (Invitrogen). A gateway cassette was placed between the renilla luciferase open reading frame and the polyadenylation signal. Hoxc8 or ICOS 3'UTRs were inserted by LR reaction (section 7.3.5). The adenoviral pCAGAdDu vector was constructed by insertion of a gateway cassette, an internal ribosome entry site (IRES), the open reading frame of green fluorescent protein (GFP) and the bovine growth hormone polyadenylation sequences in the context of a CMV early enhancer and chicken beta-actin (CAG) promoter.

6.4   Knockdown sequences

The double-stranded oligonucleotide used to knockdown the mouse CD4 protein was inserted into a modified pSuper-retroviral vector that co-expresses the H1 promoter-transcribed hairpins independently from the human CD25 mRNA, which is driven by a mouse PGK promoter.

Adenoviral knockdown vectors expressed hairpins from a U6 promoter and co-expressed GFP independently from a mouse PGK promoter (purchased from Sirion GmbH).

The selected sequences were:

Sh-mCD4:	ACAAAGAGGTGTCCGTACA
Sh-mLsm1:	CCTCACACATTGACCAGAGTA
Sh-mRck:	GCCAAGAACTATGTCTTTATA
Sh-Rc3h1:	CGCACAGTTACAGAGCTCATT
Sh-a stop cassette	TTTTTGGCCTTTTTTAGCTG
Sh-scrambled sequence:	ACAAGATGAAGAGCACCAA
Sh-GFP:	CAACAGCCACAACGTCTAT

6.5   Cell lines

HEK293A, HEK293T cells and NIH3T3 cells were purchased from ATCC. Dicer wildtype and knockout mouse embryonic fibroblast (MEF) clones were selected after immortalization in culture (section 8.1.3). MEF cells deficient in *Argonaute 2* or *TIA-1* and ES cells deficient in Argonaute 1-4 were obtained from research groups mentioned in section 11

6.6 Mice

Mice were housed in a specific pathogen-free barrier facility and used in accordance with institutional, state and federal guidelines. BALB/c and DO11.10 mice were obtained from Taconic farms and sacrificed at 6-12 weeks of age. DO11.10 CarΔ1 mice are transgenic for the DO11.10 T cell receptor that is specific for a chicken ovalbumin (OVA) peptide -amino acids 323-339- presented by the MHC class II molecule I-Ad. CD4 T cells from these mice express this TCR at high frequency (≥96%) and are therefore naive, but can be activated through the peptide *in vitro* or *in vivo*. Additionally, they express a signaling-inactive version of the human coxsackie adenovirus receptor and are therefore permissive for adenoviral infection [116]. C57BL/6 Dicer fl/fl mice were bred with BALB/c CarΔ1 and C57BL/6 CD4 Cre mice to obtain T cells deficient in Dicer that can be manipulated with adenoviral infection.

6.7 Chemicals, enzymes, devices and cits.

Table 6-3 Devices:

Device	Official name and Company
Agarose gel chambers	Peqlab Biotechnologie GmbH
Bacterial incubator	Brutschrank BINDER BF 53 (Binder Labortechnik) Innova 4400 incubator shaker (New Brunswick Scientific GmbH)
CO2 incubator	Forma Direct Heat CO2 Incubator HEPA Class 100 (Thermo Electron Corporation)
FACS machine	BD FACS Calibur Flow Cytometer (BD Biosciences)
Ice machine	Scotsman AF 200 (Scotsman Icesystem)
Accuracy weighing machine	KERN ABJ-220-4M (Kern und Söhne GmbH) KERN EW 220-3NM (Kern und Söhne GmbH)
Confocal microscope	Type: 301-185.104-000 Order-No: 500277 (Leica)
Fluorescence microscope	Axiovert 200M (Zeiss)
Gel documentation	(Peqlab Biotechnologie GmbH)
Magnet stirrer	RCT basic safety control (IKA)
Microscope	Axiovert 40C (Zeiss)
Microwave	Bosch
pH meter	pH-Meter inoLab® pH 720 (Wissenschaftlich Technische Werkstätten)
Coasting mixer	Tube Roller-Mixers, SRT1 (Stuart) (ScienceLab)
Energy supplier	Stromgeber EC105 (Thermo Electron Corporation) BioRad energy supplier (BioRad)
Spectro photometer	Eppendorf BioPhotometers (Eppendorf)

	Thermo Scientific NanoDropTM 1000 Spectrophotometer (Thermo Fisher Scientific Inc.)
Sterile-working bench	BDK, Luft und Reinraumtechnik
Thermo cycler	Biometra TGradient Thermal Cycler 96 (Biometra) DNA Engine 48/48 Dual Alpha Unit With Two Heated Lids (BioRad) Light Cycler 480II (Roche)
Thermo mixer	Thermomixer compact (Eppendorf) Thermomixer comfort (Eppendorf)
Table centrifuge	Centrifuge 5415D (Eppendorf) Centrifuge 5417R (Eppendorf)
UV-lamp	Transilluminator model. TS-40 (Ultra-Violet Products Ltd.)
Vortexer	Vortex Genius 3 (IKA)
Protein gel chamber	BioRad
Blotting chamber	BioRad
Water-bath	WB7 (Memmert)
Centrifuges und Rotors	Beckman Coulter Avanti-J-26XP (Beckman Coulter) JS-7.5 Swinging-Bucket Rotor (Beckman Coulter) JA-10 Rotor, Fixed Angle (Beckman Coulter) Allegra®X-12R Centrifuge (Beckman Coulter) Rotor FX 6100 (Beckman Coulter) Rotor SX 4750 (Beckman Coulter)

Table 6-4 Chemicals:

Chemical	Company
β-Mercaptoethanol 99%	Sigma-Aldrich
0,05% Trypsin/ 0,02% EDTA in PBS	Pan biotech GmbH
1 kb Plus DNA Ladder	Invitrogen
Ampicillin	Roche
Biozym DNA Agarose	Biozym Scientific GmbH
Brefeldin A	Sigma-Aldrich
BSA (Albumin Fraktion V)	Roth
Chloroform min. 99%	Sigma-Aldrich
dATP (100 mM)	Fermentas
dCTP (100 mM)	Fermentas
dGTP (100 mM)	Fermentas
Dimethyl Sulphoxide (DMSO)Hybri-Max	Sigma-Aldrich
dTTP (100 mM)	Fermentas
Ethidium bromide 1% (w/v)	Serva
FuGene® HD Transfection Reagent	Roche
Glycogen blue	Ambion
Kanamycin sulfate	Roth
Paraformaldehyde	Sigma-Aldrich
Saponin	VWR International GmbH

Tri®Reagent	Invitrogen
Trypton	Merck
Milk powder	Roth
Yeast Extract	Serva

Table 6-5 Enzymes:

Enzyme	Company
Gateway LR Clonase II Enzyme Mix	Invitrogen
Herculase® II Fusion DNA Polymerase (40 reactions)	Stratagene
iProof^{TM} High Fidelity DNA Polymerase (2U/µl)	Bio-Rad
Proteinase K	Invitrogen
T4 DNA Ligase (10.000 U/ml)	New England Biolabs
Taq Polymerase (5.000 U /ml)	New England Biolabs
Topoisomerase I (*E.coli*) (5.000 U/ml)	New England Biolabs
Restriction enzymes	New England Biolabs

Table 6-6 General buffers (otherwise mentioned in the corresponding method-section):

Buffer	Contents
5x TBE	45 mM Tris-HCl, 1 mM EDTA pH 8.0
10x TE	100 mM Tris/HCl pH 8.0, 10 mM EDTA pH 8.0
6x DNA dye	0.25 % bromophenol blue, 0.25 % xylene xyanol, 30% glycerol
TAC	13 mM Tris, 140 mM NH_4Cl, pH 7.2
PBS	137 mM NaCl, 10 mM phosphate, 2.7 mM KCl

Table 6-7 Kits:

Kit	Company
peqGOLD Plasmid Miniprep Kit I	PeqLab Biotechnologie GmbH
Nucleobond®Xtra Maxi Kit	Macherey-Nagel GmbH & Co. KG
QIA®PCR purification Kit	Qiagen
QIA®quick gel extraction Kit	Qiagen
pENTR/D-TOPO Cloning Kit	Invitrogen
GW8/-TOPO Cloning Kit	Invitrogen
Dynabeads®Mouse CD4 (L3T34) Kit	Dynal Biotec.
CD4+ T cell Isolation Kit (mouse)	Miltenyi Biotec.
XL QuickChange	Stratagene
TaqManMicroRNA Assay	Applied Biosystems

7   Methods

7.1   *Bacterial culture*

7.1.1   Amplification and storage of bacteria

LB media and LB agar were prepared with 'ready to mix' powder (SERVA), supplemented with ampicillin (100 µg/ml), spectinomycin (50 µg/ml) or kanamycin (30 µg/ml) for the selection of bacterial resistance. Single colonies were scraped off LB agar plates and a fresh overnight bacterial culture was used for storage at -80°C, mixed at an 1:1 ratio with glycerol.

7.1.2   Transformation of bacteria

Chemical competent DH5alpha (Invitrogen) were thawed on ice. 0.5 µg plasmid were added followed by 15 min of incubation on ice. A heat shock was performed at 42°C in a water-bath for 30 s. Thereafter cells were placed on ice for two minutes. After shaking the cells at 400 rpm and 37°C for one hour in 300 µl LB media, the cell suspension was spread out onto an LB agar plate and incubated at 37°C over night. Single colonies were selected for downstream applications.

7.2   *Cell-culture and viral infection of mammalian cells*

7.2.1   Preparation and expansion of primary T cells

Peripheral CD4 T cells were isolated from spleen and lymph nodes using anti-mouse CD4 Dynabeads (Invitrogen). Isolated CD4 T cells were kept in T cell medium (below). T cells were stimulated for 36-48 hours on goat anti-hamster IgG-coated plates with anti-CD3 (0.1 µg/ml) and anti-CD28 (1.0 µg/ml), supplemented with anti-IL-4 (10 µg/ml) to induce Th1 differentiation. For Th2 differentiation conditions, anti-IL-12 (3 µg/ml), anti-IFN-gamma antibodies (5 µg /ml) and murine IL-4 containing supernatants from I3L6 cells (equals 1000 U/ml recombinant IL-4) were added. After stimulation for 48 hours, cells were expanded in T cell media containing 10 U/ml recombinant human IL-2 (provided by the WHO, NIBSC).

Primary cells can be kept in cell culture for about five days after stimulation or even another
week, if a second stimulation has been carried out.

T cell medium:

RPMI media
10% fetal calf serum (FCS)
0.1 mM beta-mercapto-ethanol
100 U/ml penicillin-streptomycin
10 mM HEPES

(Suppliers are listed in section 7.2.2)

7.2.2   Cell-culture conditions

HEK293 cells and MEF cells were grown in DMEM medium (see below). Embryonic stem
(ES) cells were grown in ES cell DMEM medium on feeder cells and passaged twice on 0.1%
gelatine prior to infection.

DMEM medium (suppliers listed below):
DMEM
10% FCS
1000 U/ml penicillin-streptomycin
10 mM HEPES

ES cell DMEM medium (suppliers listed below):
DMEM
20% FCS
2 mM L-glutamine
100 U/ml penicillin-streptomycin
1 mM sodium pyruvate
0.1 mM non-essential amino acids (NEAA)
0.1 mM ß-mercapto-ethanol
2000 U/ml leukemia inhibitory factor (LI)F

Table 7-1: Medium and suppliers:

Medium	Company
Dulbecco's Modified Eagle Medium (DMEM)	Gibco, Invitrogen
RPMI 1640, without L-glutamin	BioWhittaker, Lonza

Table 7-2: Additional ingredients:

Additive for medium	Company
100x NEEA	BioWhittaker, Cambrex
fetal calf serum (FCS)	BioWhittaker, Lonza
fetal calf serum (FCS)	Gibco, Invitrogen
GIBCO™ L-Glutamine-200 mM (100x), flüssig	Gibco, Invitrogen
GIBCO™ MEM Vitamin Solution (100x), flüssig	Gibco, Invitrogen
HEPES (1M)	Gibco, Invitrogen
Sodium pyruvate (100 mM)	BioWhittaker
LIF	Provided by Marc-Schmidt-Supprian
PenStrep (10 000 U/ml)	Gibco, Invitrogen

7.2.3 Storage of cells

Stocks from cell lines can be stored in liquid nitrogen in a mixture of 90% fetal calf serum (FCS) and 10% DMSO. 10^7 cells were taken up in 1.2 ml of 90% FCS and 10% DMSO, transferred into 2 ml freezing tubes (NUNC) and placed into a -80°C freezer over night. The special isopropanol isolation of the freezing box allows a slow adjustment of the cells to the temperature in order to minimize the generation of ice crystals, which are detrimental to the cells. Next day, the cells were transferred into a liquid nitrogen container for long-time storage. Reculturing of the cells is done by thawing in a water-bath at 37°C and transfer into pre-warmed fresh cell-culture medium.

7.2.4 Transfection of cells with FuGene HD or the calcium phosphate method

Transfection of cells with FuGene HD:

HEK293A cells were transfected with FuGene HD according to the manufacturer's protocol. Cells were counted one day prior to transfection and plated with 6×10^5 cells in the volume of 1 ml into one well of a six well plate. The following day transfection was performed using a mixture of 2 µg total DNA, 6 µl FuGene HD and 100 µl OPTI-MEM medium (Gibco). The cells were used for analysis after ~24 hours.

Transfection of HEK293T cells by the calcium phosphate method:

Cells were counted one day prior to transfection and plated out using a concentration of 3×10^5 cells/ml in a volume of 17 ml in a 15 cm-diameter cell culture dish. The next day cells were

transfected with co-precipitates of DNA and calcium phosphate. To produce co-precipitates a mixture of 25 µg total DNA, 1.1 ml sterile water and 125 µl cold 2 M CaCl$_2$ (stored at -20°C) was slowly vortexed in a 50 ml falcon tube. 1.25 ml of 2xHBS (freshly thawn) was added drop-wise. The solution was incubated for 15 minutes at room temperature and thereafter added drop-wise to the HEK293T cells. Transfected cells were analyzed one day later or kept in culture for two additional days if used for retroviral amplification (section 7.2.6).

2x HBS-stock solution:

8.0 g NaCl
6.5 g HEPES (260.29 MW)
10 ml Na$_2$HPO$_4$ stock solution
(Na$_2$HPO$_4$ stock solution: 5.25 g Na$_2$HPO$_4$ in 500 ml of water)
adjusted pH to 7.0 at room temperature; aliquoted and stored at -20°C

7.2.5 Confocal microscopy

For confocal microscopy HEK293A cells were counted 24 hours prior to transfection, adjusted to 5×10^4 cells in 100 µl medium and grown on sterile glass slides in a 12 well dish for one hour. Then 1 ml medium was added. The next day, transfection with FuGene HD followed (section 7.2.4). Another day later, the cells were fixed with 4% (w/v) paraformaldehyde and washed three times with IF-wash-buffer (below). Staining was carried out using primary antibodies (1:100 for hybridoma supernatants, and 1:1000 for anti-Roquin and to 1:2000 for anti-Rck purchased antibodies) and secondary Cy5-coupled anti-mouse or anti-rabbit antibodies (1:200) all of which were diluted in IF-wash-buffer. DAPI staining followed for 1 min in DAPI solution (below). Microscopy was performed in self-made mounting medium (below).

CD4 Th2 cells were infected with an adenovirus encoding GFP-tagged Roquin. The cells were immobilized by using poly-L-lysine (2 ug/ml Sigma) coated glass slides and fixed with 4% paraformaldehyde, stained with DAPI and analyzed as previously described.

IF-wash-buffer:
Phosphate buffered saline (PBS)
0.5 % (v/v) NP-40
0.01% (w/v) sodium-azide
10% (v/v) FCS

DAPI solution:
15 µg DAPI (Sigma D8417)/ 100 ml 2X SSC buffer

20X SSC for DAPI solution:
0.3 M $Na_3C_3H_5O(CO_2)_3$ H_2O
3 M NaCl
ad to 100 ml with H_2O
adjust to pH 7

Mounting medium:

Glycerol was mixed with equal parts w/v of 2x PBS and was adjusted to 0.1% n-propyl gallate (Sigma) final concentration.

7.2.6 Production of and infection with retro- and adenovirus

Type 5 replication-deficient adenoviruses were produced by calcium phosphate transfection of *Pac*I-digested adenoviral vectors into HEK293A cells. The viruses were amplified in HEK293A cells and viral stocks were purified using mini columns according to the manufacturer's instructions (Cell Biolabs). Titers were determined in A549 cells by FACS approximately 40 hours after transduction. ES or MEF cells (1×10^6) were transduced with recombinant viruses at an multiplicity of infection (MOI) of 100.

Retroviral supernatants were produced by calcium phosphate transfection of amphotropic packaging vectors and retroviral expression vectors into HEK293T cells. Supernatants were collected 72 hours post transfection, passed through 0.45 µm filters, mixed with polybrene at a final concentration of 5µg/ ml and added to MEF cells, which were spin-infected at 900*g* for 1 hour at room temperature. The medium was replaced after 24 hours and transduced cells were analyzed three days post infection.

7.2.7 FACS-analysis

For flow cytometry analysis of adherent cells, cells were scraped off the plates using a mixture of 30% cell-dissociation solution and 70% PBS and thereafter stained in FACS buffer (below) for 20 min on ice. For the analysis of ICOS surface expression on CD4 cells, cells were stained two days after stimulation (section 4.2.1) in FACS buffer for 20 min on ice.

Flow cytometry was performed on a FACS Calibur device (Becton Dickinson) and raw data were analyzed with Flow Jo (Treestar) software. Antibodies used for FACS analysis are listed in section 6.1.

FACS buffer:

PBS, pH 7.4
1% FCS
0.01% of sodium azide

Saponin-buffer:

PBS, pH 7.4
0.5% saponin
1% BSA

7.3 Techniques for handling nucleic acids

7.3.1 PCR for genotyping and generation of constructs

PCR for genotyping Dicer alleles was performed with Taq Polymerase (Biolabs) according to the manufacturer's protocol:

Primers that recognize wildtype and floxed alleles:

F1:   ATTGTTACCAGCGCTTAGAATTCC

R1:   GTACGTCTACAATTGTCTATG

Primers that recognize Cre deleted Dicer alleles:

F1:   TCGGAATAGGAACTTCGTTTAAAC

R2:   GTACGTCTACAATTGTCTATG

The PCR program for genotyping Dicer alleles:

Segment	Cycles	Temperature	Time
1	1	94°C	3 min
2	30	94°C	0.5 min
		58°C	0.5 min
		72°C	0.75 min
3	1	72°C	10 min

PCR procedure to produce new constructs:

For the generation of new constructs, a combination of 1 µl Taq Polymerase (Invitrogen), for the generation of A-overhangs, and 0.3 µl Vent proofreading polymerase (Biolabs), to increase proofreading, was used. PCR was performed according to the manufacturer's protocol of the Taq polymerase from Invitrogen. Most primers were designed to match an annealing temperature of 58°C (section 6.2). PCR products were loaded onto an agarose gel, the desired bands were dissected and subsequently extracted from the gel (Qiagen). The pure PCR products were then ligated into TOPO cloning vectors (Invitrogen) according to the manufacturer's protocol.

7.3.2 Preparative plasmid purification

Cost-saving plasmid purification from 3-5 ml bacterial culture:

Resuspension, lysis and neutralization buffers for this technique were taken from the MAXI kit of Macherey-Nagel. Bacteria of a 3 ml overnight culture were pelleted by centrifugation at 14 000 g for five min. Cells were resuspendend in 100 µl resuspension buffer and lyzed in 200 µl lysisbuffer for five min. Neutralization was carried out by adding 150 µl neutralization buffer. After centrifugation at 14 000 g for 5 min at room temperature the supernatant was transferred into a new tube. DNA was then precipitated using 100% ethanol. Centrifugation took place at 14 000 g for 10 min at room temperature. After disposal of the supernatant, the DNA pellet was washed with 75% ethanol with subsequent centrifugation at 14 000 g for 5 min at room temperature. The DNA pellet was air-dried for 5 min and taken up in 30 µl TE buffer (see below). The quality of DNA allows to perform restriction digests and lambda recombination reactions.

Plasmids used for sequencing and further cloning techniques were purified with the peqGOLD Plasmid Miniprep.

TE buffer:

10 mM Tris-HCl, pH 7.5
1 mM EDTA

7.3.3 Site-directed mutagenesis

All point-mutations were introduced by site-directed mutagenesis using the XL Quick Change kit (Stratagene). Primers (section 6.2) were chosen and the reaction mix was prepared according to the manufacturer's protocol. The protocol for the PCR reaction was slightly altered to increase the number of colonies:

Table 7-3 Program for QuickChange thermocycler:

Segment	Cycles	Temperature	Time
1	1	95°C	1.2 min
2	18	95°C	1 min
		60°C	1 min
		68°C	1.1 min
3	1	68°C	7 min

The PCR product was DpnI digested for one hour and then 5 µl of the PCR product were transformed into competent DH5α cells. Some of the resulting colonies were selected for sequencing

7.3.4 Ligation of DNA fragments

First, restriction digests of 10 µg plasmid and 10 µg insert were performed at 37°C, over night (total volume 45 µl), using the required enzymes (New England Biolabs) and buffers, according to the manufacturer's protocol. Second, gel extraction (Qiagen) and ligation of the fragments with T4 DNA ligase (New England Biolabs) took place overnight at 16°C and according to the manufacturer's protocol.

7.3.5 Lambda recombination reaction

The lambda recombination (LR) reaction allows to transfer DNA fragments of interest between different vectors while maintaining the reading frame. This system, also known as gateway cloning system, is a technique developed by Invitrogen. Entry clones contain the gene of interest, which is flanked by attL1 and attL2 sites. Destination vectors contain a death gene (ccdB), which is also flanked by attR1 and attR2 sites. The LR recombinase recognizes the attL and attR sites and performs a recombinant reaction. Different destination vectors are available for different purposes. The destination vectors used in this thesis are mentioned in section 3.3. During the LR reaction, the entry clone is mixed with the destination vector of

interest and the LR recombinase. Only destination vectors that have recombined are selected. This is ensured by differences in antibiotic resistance between the destination and entry vector and the expression of a death gene (ccdB) in clones that have not recombined. LR reactions carried out for the purposes of this thesis were performed according to the manufacturer's protocol.

7.3.6 RNA-immunoprecipitation (RNA-IP)

HEK293T cells (5 x 10^6 cells) were transfected with expression vectors and harvested for the RNA-IP two days later. The cells were washed twice with PBS and crosslinked in 10 ml crosslinking-buffer (below) on a roller mixer for 10 min at room temperature. Crosslinking reactions were quenched with glycine (pH 7.0) at a final concentration of 0.25 M for 5 min. The cells were centrifuged at 300 g for 5 min, followed by a PBS wash and resuspension in 1 ml RIP-lysis-buffer (below). Three rounds of sonication at 15% amplitude (Branson Digital Sonifier) in an ice-water bath for 30 s followed. Insoluble material was removed by centrifugation at 16 000 g for 10 min at 4°C. Unspecific binding of RNA to magnetic Protein G Dynabeads (Invitrogen) was reduced by pre-clearance of the cell lysates by mixing it with 15 µl Protein G Dynabeads for 1 h at 4°C. 100 µl of the precleared lysate was used as an input control and the remainder was incubated together with 25 µl GFP antibody-coated Protein G Dynabeads and 20 units of RNasin (Promega) for two hours at room temperature. The beads were washed five times with 1 ml of high-stringency-buffer (below) and incubated on a roller mixer for 10 min at room temperature. The beads containing the immunoprecipitated samples were collected and resuspendend in 100 µl of resuspension buffer (below). Resuspended beads were incubated at 70°C for 45 min to reverse crosslinking. The RNA present in the immunoprecipitations and inputs was extracted with Trizol reagent (section 7.3.7) and cDNA synthesis was performed with the QuantiTect Reverse Transcription kit (Qiagen) according to the manufacturer's protocol.

PCR amplification (28 cycles) was carried out at an annealing temperature of 56 °C and using the following primers:

ICOS-3'UTR F1: GTCAAAATGGTCCCCATCAG, R1: TTTCCAGGCTGTGTGGTTTT;

5S-rRNA F1: GTCTACGGCCATACCACCCTG , R1: GCCTACAGCACCCGGTATTCC.

Crosslinking-buffer:

PBS, pH 7.4

1% (v/v) formaldehyde (Sigma)

RIP-lysis-buffer:

50 mM Tris-HCl, pH 7.5
1% (w/v) NP-40
0.1% (w/v) sodium deoxycholate
0.05% (w/v) SDS
1 mM EDTA
150 mM NaCl
Complete protease inhibitors mix (Roche)
1 mM DTT

High-stringency-buffer:

50 mM Tris-HCl, pH 7.5
1% (v/v) NP-40
0.1% (w/v) sodium deoxycholate
0.05% (w/v) sodium dodecyl sulfate
1 mM EDTA
0.5 M NaCl
1 M urea
1 mM DTT
0.2 mM PMSF

Resuspension-buffer:

50 mM Tris pH 7.0
5 mM EDTA
10 mM DTT
1% (w/v) SDS.

7.3.7 Extraction of genomic DNA and cellular total RNA from eukaryotic cells

Proteinase K digest of mouse tails or eukaryotic cells for genotyping:

10^7 cells or 0.5 cm of each mouse tail were lyzed in 200 µl proteinase K-containing genotyping-buffer (below) and shaken overnight at 800 rpm and 55°C. Proteinase K was heat-inactivated at 95°C for 15 min the next day. 300 µl water was added and 0.5 µl were then used as template for PCR.

Genotyping-buffer:

100 mM Tris-HCl, pH 8.5

5 mM EDTA
0.2% SDS
200 mM NaCl
fresh 0.2 mg/ml proteinase K
fresh 0.2 mg/ml protease K

Extraction of cellular RNA:

For the isolation of total RNA from immunoprecipitation samples the MirVana kit (Ambion) was used according to the manufacturer's instructions. For other applications the Tri reagent (Sigma) was applied as follows: Harvested cells were lyzed in 1 ml of Trizol by pipetting up and down six times and incubated for 5 min at room temperature. 200 µl of chloroform were added and samples were first vigorously shaken and then incubated at room temperature for 2 min. The organic and aqueous phases were separated by centrifugation at 12 000 g for 15 min at 4°C. The aqueous phase was transferred into fresh 1.5 ml tubes and precipitated with 500 µl isopropanol in the presence of 1 µl Glycoblue-carrier (Ambion). Precipitated RNA was collected by centrifugation at 12 000 g for 10 min at 4 °C and removal of the supernatant. The resulting pellet was then washed with 1 ml 75% (v/v) ethanol, centrifuged at 7 600 g for 5 min at 4 °C, air-dried for 5 min, and resuspended in 20 µl of RNase-free water at 55 C for 5 min.

7.3.8 Reverse transcription PCR

After reverse transcription with the QuantiTect Reverse Transcription Kit (Qiagen) according to the manufacturer's protocol, gene-specific qPCR assays were performed with a LightCycler 480II using the following primers and universal probes (Roche, http://www.roche-applied-science.com/sis/rtpcr/upl/ezhome.html):

mICOS F1:   CGGCAGTCAACACAAACAA;   R1: TCAGGGGAACTAGTCCATGC; probe: #6;

hICOS F2:   GGATGCATACTTATTTGTTGGCTTA;   R2: TGTATTCACCGTTAGGGTCGT; probe #47;

Lsm1 F1:   TGGTCAGAGGAGAGAATGTGG;   R1: CTGAAGGGGCGTGTCACT; probe: #80.

For relative quantification hypoxanthine guanine phosphoribosyl transferase 1 (Hprt1) was used.

Hprt1 F1:   TCCTCCTCAGACCGCTTTT;   R1: CCTGGTTCATCATCGCTAATC; probe: #95.

All primer/probe sets were tested for efficiency and all results were analyzed by efficiency-corrected advanced relative quantification. For the quantification of miRNA expression

levels, miRNA species-specific first strand synthesis was carried out using the TaqMan microRNA Reverse Transcription kit and stem-loop primers specific for miR-101, miR-328, miR-196a and miR-214 (Applied Biosystems). Quantitative PCRs for miRNAs were performed with a LightCycler 480II with U6 as a reference for relative quantification and analyzed by efficiency-corrected advanced relative quantification.

7.4   Techniques for handling proteins

7.4.1   Immunoprecipitation and analysis of associated RNAs

For immunoprecipitation of protein-bound RNAs, $2x10^8$ CD4 T cells or $1x10^7$ transfected HEK293T cells were lyzed on ice in 2 ml IP-lysis-buffer (below). Lysates were passaged through a 26G needle, shock frozen and cleared by centrifugation for 10 min at 10 000 g. 30 µl Protein-G magnetic beads (Invitrogen) were coupled over night with 5 µg polyclonal anti-Roquin or anti-GFP antibodies at 4°C. Coupled beads were incubated with lysates (passed through a 0.45 µm filter) in the presence of 20 units RNasin at 4°C for 4 hours. Prior to the isolation of RNA, the beads were washed twice with IP-lysis-buffer and twice with IP-wash-buffer (below). RNA was isolated from beads with the miRVana kit (section 7.3.7).

IP-lysis-buffer:
20 mM Tris-HCl pH 7.5
150 mM NaCl
0.25% NP-40
1.5 mM $MgCl_2$
"complete" protease inhibitors without EDTA (Roche)
1mM DTT

IP-wash-buffer:
20 mM Tris-HCl pH 7.5
300 mM NaCl
0.5% NP-40
2.5 mM $MgCl_2$
"complete" protease inhibitors without EDTA (Roche)
1 mM DTT

7.4.2 Luciferase assay

For luciferase activity assays, MEF cells were plated onto 12-well plates at 1-2 x 10^5 cells per well and infected with adenoviruses. After two days the dual-luciferase reporter assay (Promega) was performed. PBS-washed cells were lyzed in 150 µl lysis-buffer (included in the kit) for 30 min at room temperature and subjected to one freeze and thaw cycle. Lysates were cleared by centrifugation at 20 000 g for 5 min and 20 µl supernatant lights units were measured.

7.4.3 Western blot analysis

For Western blot analysis $5x10^6$ cells were washed twice in PBS and then lyzed in 20 µl freshly prepared RIPA-buffer (below). Lysates were incubated 15 min on ice and then centrifuged at 14 000 g and 4°C for 15 min. Supernatants were transferred directly into a new tube containing 4x SDS sample buffer (below) and heated at 95°C for 5 min.

RIPA stock solution:
20 mM Tris-HCl, pH 7.5
250 mM NaCl
10 mM $MgCl_2$
1% NP-40
0.1% SDS
0.5% Na-desoxycholate

RIPA-buffer (freshly added to RIPA stock solution):
1 mM DDT
1 mM PMSF
10 µg/ml leupeptin
10 µg/ml aprotinin
8 mM beta-glycerophosphate
0.1 mM sodium-orthovanadate
10 mM NaF

4x SDS sample buffer:
200 mM Tris/HCl, pH 6.8
8% SDS
0.1% bromophenol blue
4% glycerol
10% fresh beta-mercaptoethanol

Thereafter, protein lysates were loaded on 8%, 9% or 10% Lämmli gels, depending on the protein size, run at 100 Volt and blotted on PVDF membranes at 40 V over night in blotting-buffer (below). Membranes were blocked in 5% milk dissolved in TBS (below) for two hours at room temperature. A procedure of washing steps with TBS containing 0.05% Tween (3 times 7 min) and incubation of primary antibody (for two hours) and secondary horseradish peroxidase-coupled (for 1 hour) antibodies followed. Membranes were stained with ECL plus Western blotting reagent (GE healthcare).

Blotting-buffer:
15 g Tris
72.1 g glycine
1 l methanol
ad 5 l H_2O

TBS:
10 mM Tris/HCl pH 8.0
150 mM NaCl

Table 7-4 SDS-PAGE gels (for 2 gels):

Ingredient	Volume for 8% gel	Volume 9% gel	Volume for 10% gel
Acrylamide 30%	2.7 ml	3 ml	3.3 ml
1.5 M Tris/ HCl	2.5 ml	2.5 ml	2.5 ml
10 % SDS	100 μl	0.1 ml	100 μl
10% APS	100 μl	0.1 ml	100 μl
H_2O	4.6 ml	4.3 ml	4 ml
TEMED	6 μl	6 μl	4 μl

Table 7-5 Collecting gels: (for 2 gels):

Ingredient	Amount
Acrylamide 30%	830 μl
1.5 M Tris/ HCl	630 μl
10 % SDS	50 μl
10% APS	50 μl
H_2O	3.4 ml
TEMED	5 μl

8 Results

8.1 Evaluation of tools

8.1.1 Determination of antibody specificity

Antibodies against mouse Roquin and mouse MNAB were produced by immunizing rats with peptides from Roquin and MNAB proteins (section 6.1). The peptides were chosen to obtain antibodies that would bind to both proteins by recognizing an amino-terminal epitope that is shared by Roquin and MNAB (antibody Q4-2). In addition, peptides were selected to yield antibodies against carboxy-terminal epitopes that are unique in Roquin (antibody Q4-4) or MNAB (antibody POCO) proteins (Figure 8-1 a, page 54). Peptide-antigen recognition was evaluated by enzyme-lined immunosorbent assay (ELISA) and protein identification using Western blots. The hybridoma lines 5E9 (rat IgG2b), 6A6 (rat IgG2b), 5B11 (rat IgG2a), 2F6 (rat IgG2a) and 3B5 (rat IgG2a) were repeatedly subcloned and specific Roquin and MNAB recognition of the monoclonal antibodies was verified by Western blotting of overexpressed proteins (Figure 8-1 b-e, page 54). A549 cells were infected with recombinant adenoviruses generated from pCAGAdDu vectors that either encoded mouse Roquin or human MNAB using a multiplicity of infection (MOI) of 100. Cells were lyzed in RIPA buffer and extracts from equal cell numbers were analyzed by SDS-PAGE. Immunoblots were either probed with a mixture of the monoclonal antibodies Q4-2 6A6 and Q4-2 5E9 that recognized MNAB as well as Roquin (Figure 8-1 b, page 54). In addition, a mixture of the monoclonal antibodies POCO 3B5 and POCO 2F6, which exclusively recognized MNAB (Figure 8-1 d, page 54), or with the monoclonal antibodies Q4-4 5B11, which specifically recognize Roquin (Figure 8-1 c, page 54), was tested. The identity of the band that showed immunoreactivity with Roquin-recognizing antibodies was confirmed with commercial purified polyclonal antibodies (section 6.1), which exclusively recognize Roquin (Figure 8-1 e, page 54). In summary, the overexpressed MNAB and Roquin proteins were equally well recognized by Q4-2 monoclonal antibodies and migrated at the calculated size of 132 kDa and 121 kDa, respectively. As expected, MNAB was specifically detected by POCO antibodies. Roquin was exclusively stained with Q4-4 monoclonal antibodies. These results confirm the specificity of the generated monoclonal antibodies and demonstrate appropriate expression of

the full length Roquin and MNAB proteins from our adenoviral vectors. Interestingly, cDNA-based MNAB expression not only resulted in the full-length protein, but also in a shortened version, which was detected by antibodies binding to either the carboxy-terminus or the amino-terminus. Since POCO antibodies bind epitopes near the far end of the carboxy-terminus, the second MNAB isoform is more likely to lack the amino-terminal region, presumably the RING finger domain (Figure 8-1 b, d, page 54). The visualized difference between the two forms of MNAB indicates a difference of approximately 40 amino acids, further indicating that the second isoform might lack the RING finger domain. This variant of the MNAB protein may derive from an alternative start codon usage or from proteolytic cleavage. Although endogenous Roquin and MNAB protein levels can not be seen in these immunoblots, we could detect endogenous Roquin in different cell types and tissues with Q4-4 and polyclonal antibodies, e.g, Figure 8-27 and other data not shown, but it remained a technical challenge to detect endogenous MNAB and was therefore analyzed via immunoprecipitation (Figure 8-11).

8.1.2   Testing expression of Roquin and MNAB proteins

Chimeras of mouse Roquin and human MNAB were generated through reciprocal exchange of their carboxy- and amino-termini, using a conserved fusion site in the zinc finger of Roquin and MNAB (section 6.3). To test whether these fusion proteins are correctly expressed and recognized by the corresponding antibodies, HEK293T cells were transfected using the calcium phosphate method (section 7.2.4) with retroviral expression vectors that encode wildtype Roquin or the Roquin/MNAB chimeras. Equal cell numbers were lyzed in RIPA buffer and extracts from equal cell numbers were analyzed by SDS-PAGE. Western blots were probed with a mixture of the monoclonal antibodies Q4-2 clone 6A6 and Q4-2 clone 5E9 that recognized Roquin and both chimeras (Figure 8-2 b, page 55), or with a mixture of the monoclonal antibodies POCO clone 3B5 and POCO clone 2F6, which only recognized the chimera with the carboxy-terminus of MNAB (Roquin/MNAB) (Figure 8-2 c, page 55), or with the monoclonal antibody Q4-4 clone 5B11, which recognized Roquin and the chimera encoding the carboxy-terminus of Roquin (MNAB/Roquin) (Figure 8-2 a, page 55). The polyclonal antibodies (section 6.1) recognized Roquin and the MNAB/Roquin chimera (Figure 8-2 d, page 55). Of note, the MNAB/Roquin chimera was also detectable in an amino-terminally shortened version showing a similar pattern as wildtype MNAB (Figure 8-1 b, d, page 54). This indicates that the alternative start codon or proteolytic cleavage is specified only through amino-terminal sequences of MNAB. To verify that Roquin and its

mutant Roquin M199R are expressed at similar levels, A549 cells were infected with recombinant adenoviruses coding for either Roquin or Roquin M199R at a multiplicity of infection (MOI) of 100. Extracts from equal cell numbers were analyzed by SDS-PAGE. Western blots were probed with specific antibodies for Roquin. Immunoblot detection revealed comparable expression levels for both proteins (Figure 8-3, page 55). To verify the expression of different deletion- and point-mutants of Roquin (section 6.3), HEK293T cells were transfected using the calcium phosphate method (section 7.2.4) with retroviral expression vectors encoding wildtype or deletion- and point-mutants of Roquin. Equal cell numbers of transfected cells were analyzed by SDS-PAGE. Western blots were either probed with a mixture of monoclonal antibodies Q4-2 clone 5E9 and clone 6A6, which recognizes an epitope within the ROQ domain, or with the polyclonal antibodies (Figure 8-1, page 54). As expected, all deletion-mutants were recognized by the antibody mixture Q4-2, except for the one mutant lacking the RING finger and ROQ domain (Roquin aa 338-1130) (Figure 8-4 a, page 56). All amino-terminal deletion- and point-mutants were recognized by the polyclonal antibodies (Figure 8-4 b, page 56). The mutants lacking either the RING finger (Roquin aa 55-1130) or the coiled-coil domain (Roquin aa 1-951) were expressed at lower levels as compared to wildtype Roquin or compared to the mutant lacking the carboxy-terminal regions, including the proline-rich region (Roquin aa 1-509) (Figure 8-4 a, page 56). The latter was expressed at even higher levels than wildtype Roquin. Importantly, point-mutants of Roquin (Roquin C14A/C34A, Roquin C419R/C428R) and the deletion-mutant lacking the RING finger and ROQ domain (Roquin aa 338-1130) were expressed similarly strong as wildtype protein (Figure 8-4 a, b, page 56).
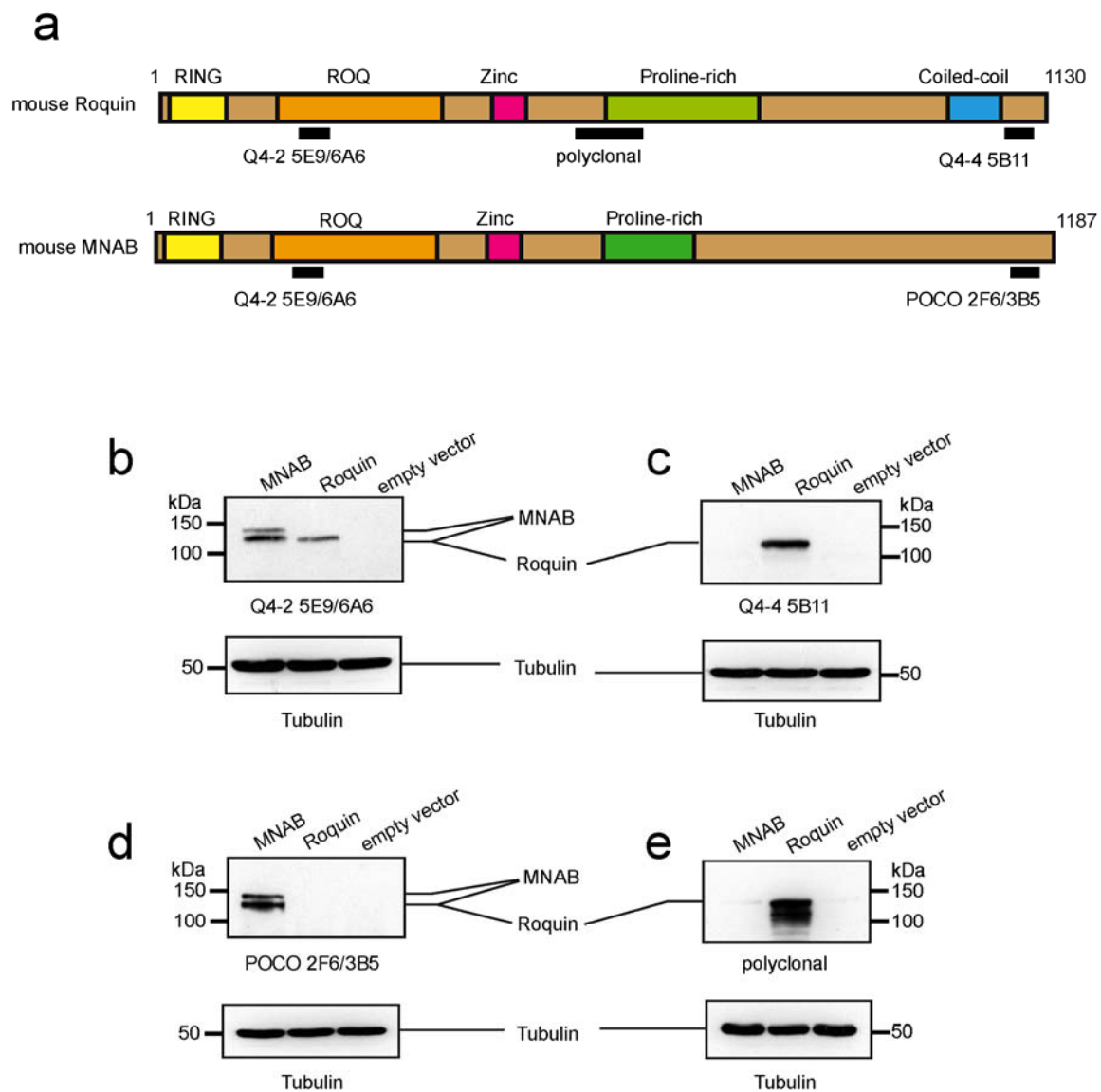
Figure 8-1: <u>**Analysis of mouse Roquin and human MNAB overexpression.**</u> **(a) Schematic depiction of the structure of mouse Roquin and MNAB with their individual RING and zinc fingers, ROQ and coiled-coil domains as well as proline-rich regions. Black bars indicate the regions from which sequences were chosen to synthesize peptides and to generate rat monoclonal antibodies. One additional black bar points to the region that includes epitopes recognized by commercial polyclonal antibodies. (b-e) A549 cells were infected with recombinant adenoviruses to express either mouse Roquin or human MNAB. Extracts derived from equal cell numbers were analyzed. Immunoblots were probed with the antibodies indicated in (a), specifically recognizing mouse Roquin (c, e), mouse MNAB (d), or both proteins (b).**
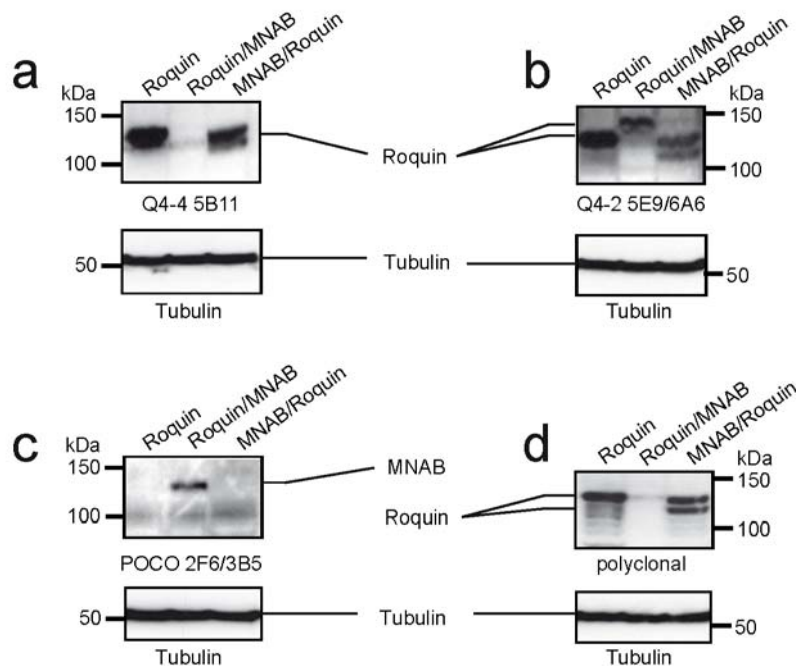
Figure 8-2: <u>Expression test of Roquin/MNAB chimeras.</u> **(a-d) HEK293T cells were transfected using the calcium phosphate method with retroviral constructs encoding wildtype mouse Roquin, human MNAB or chimeras of both proteins (section 6.3). Western blots of overexpressed wildtype and chimeric proteins were probed with antibodies specifically recognizing Roquin (a, d), MNAB (c) or both proteins (b).**
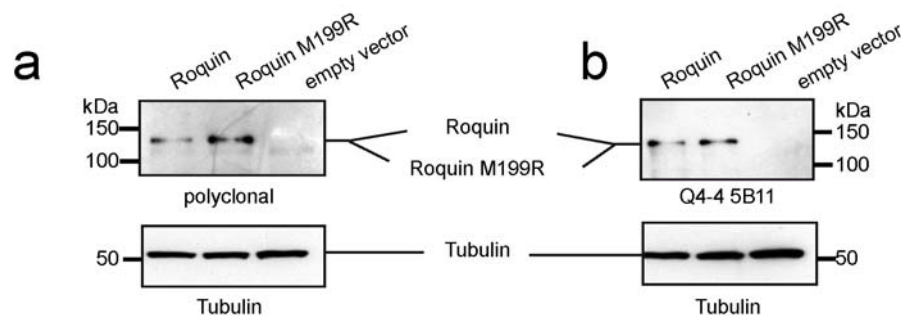
Figure 8-3: <u>Expression test of Roquin M199R compared to Roquin wildtype.</u> **(a, b) A549 cells were infected with recombinant adenoviruses at an MOI of 100 generated from adenoviral pCAGAdDu vectors that encoded inserts of Roquin wildtype or the Roquin M199R mutant. Cells were lyzed in RIPA buffer and extracts from equal cell numbers were analyzed by SDS-PAGE. Immunoblots were probed with the indicated antibodies.**
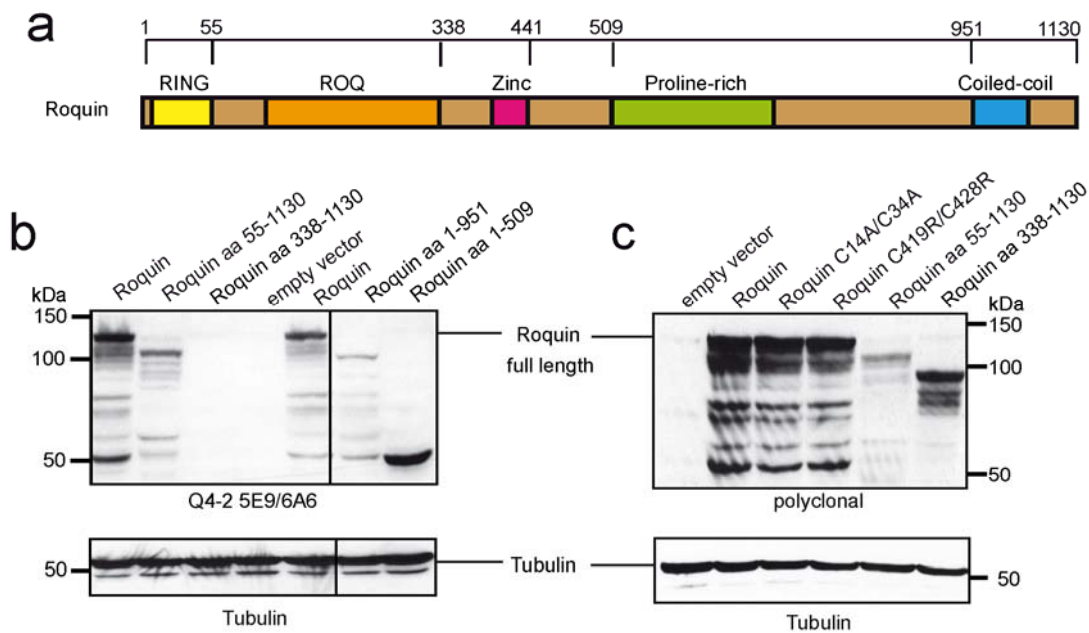
Figure 8-4: <u>Expression test of deletion- and point-mutants of Roquin.</u> **(a) Schematic depiction of domains and proline-rich regions within Roquin. Numbers refer to amino acid end points of the generated deletion-mutants. (b, c) HEK293T cells were transfected using the calcium phosphate method with retroviral constructs encoding Roquin in its wildtype form or as deletion- or point-mutants. Cell lysates were separated by SDS-gels and immunoblots were probed with the indicated monoclonal (a) or polyclonal antibodies (b).**

8.1.3 Creating Dicer-deficient MEF clones

Wildtype and Dicer fl/fl mouse embryonic fibroblasts (MEFs) were generated and immortalized through infection with a retrovirus that expressed SV40 large T as previously described [117]. Cells were then superinfected with a retrovirus to express Cre recombinase as well as a puromycin resistance gene and then treated with puromycin for five days. miRNA expression was decreased by ~90% ten days after infection, but regained wildtype levels after 26 days. We suspected that cells in which the Cre recombinase did not effectively delete Dicer alleles had a growth advantage over knockout cells and could therefore outgrow the latter (Figure 8-5 a, page 57). Subsequently, clones were selected by limiting dilution. One Dicer fl/fl clone with deleted Dicer alleles and a Dicer wt clone were identified after Cre selection and kept in culture (Figure 8-5 b, page 57). Even though Dicer knockout MEFs grew slower, they could be expanded in cell-culture and be infected with retroviruses and adenoviruses (section 8.2.7).
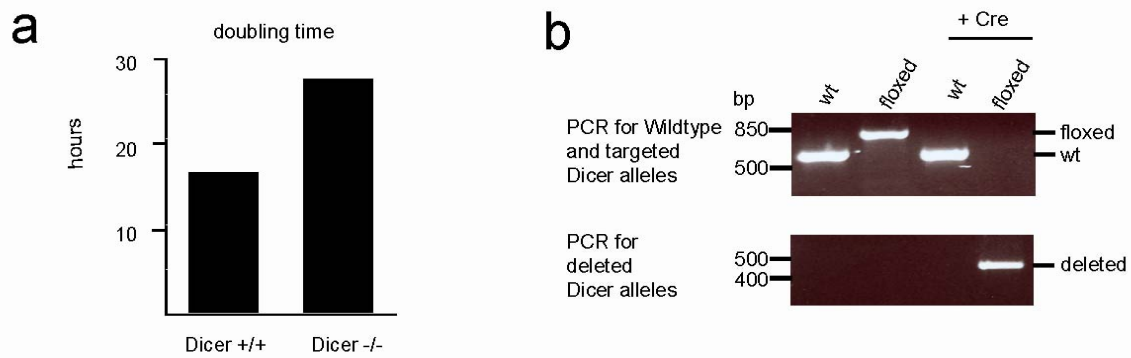
Figure 8-5: <u>Cell growth of Dicer wildtype and knockout cells (a) and genomic PCR for Dicer alleles (b)</u>. (a) Dicer wildtype and knockout cells were compared in their cell growth. (b) Genomic PCR was performed on bulk populations of wildtype and Dicer fl/fl mouse embryonic fibroblasts, as well as on individual clones after Cre infection. Primers that can recognize the wildtype and floxed Dicer alleles (section 7.3.1) were used for genomic PCR.

8.2   Analytical data

8.2.1   Roquin is a repressor of translation

A previous report suggested that Roquin regulates ICOS via the *ICOS* 3'UTR and that Roquin can promote *ICOS* mRNA decay [1]. Before we asked how Roquin regulates *ICOS* mRNA levels, we wanted repeated key experiments of that publication [1]. To do so a number of reporter constructs were generated. First, a construct that only contains the ICOS coding region (ICOS CDS) or a construct containing the ICOS coding region and the 3'UTR (ICOS FL) (section 6.3) were generated and tested for repression by Roquin (Figure 8-6, page 58).

Our experiments agree with the finding that Roquin can repress ICOS protein expression only when ICOS is expressed in the context of its 3'UTR (Figure 8-6 a, page 58). This observed repression was lost upon removal of the carboxy-terminus of Roquin (aa 1-509), creating an inactive mutant of Roquin, which will be described in detail in section 8.2.3. *ICOS* mRNA levels were lower in cells that overexpress ICOS FL and Roquin wildtype, compared to cells that overexpress ICOS FL and the inactive mutant, as determined by quantitative PCR (Figure 8-6 b, page 58). This confirms that Roquin can promote *ICOS* mRNA decay, as proposed earlier [1].
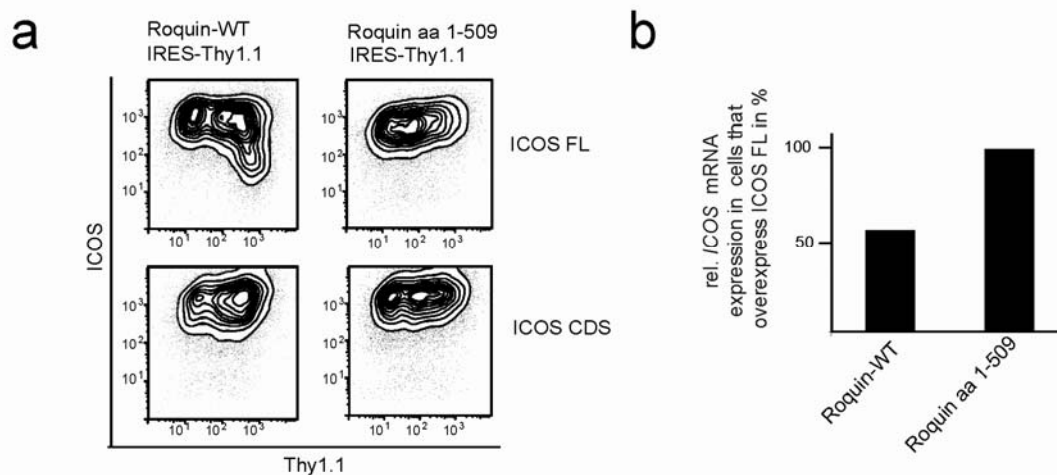
Figure 8-6: <u>Roquin represses *ICOS* mRNA through the 3'UTR.</u> MEF cells were transduced with retroviruses that encode either the ICOS coding sequence (ICOS CDS) or the ICOS coding sequence and the 3'UTR (ICOS FL). They were superinfected with retroviruses encoding Roquin-WT or its inactive mutant (Roquin aa 1-509) (section 8.2.3) in the context of bicistronic Thy1.1 expression. Flow cytometric analysis showing (a) contour plots of antibody-stained ICOS and Thy1.1 surface expression. (b) *ICOS* mRNA levels were quantified from cells that were transduced with ICOS FL and Roquin or ICOS FL and Roquin 1-509, as shown in the upper panel of (a).

Second, constructs were generated to test whether Roquin activity solely depends on the 3'UTR, but is independent from the coding region. For that, the coding regions of human CD4, another membrane protein that is translated at the endoplasmatic reticulum, or of GFP, an intracellular protein that is translated in the cytoplasm, were fused to the 3'UTR of *ICOS*. 3T3 cells were retrovirally infected with either one of these constructs and superinfected with retroviruses encoding wildtype Roquin or the inactive mutant of Roquin (Figure 8-7, page 59). To compare Roquin-dependent downregulation of these proteins, human CD4 and GFP levels were quantified on cells with low, intermediate or high surface expression of Thy1.1. The Thy1.1 marker is translated by an IRES sequence and therefore co-expressed with either Roquin or its inactive mutant.

Overexpression of wildtype Roquin effectively reduced the levels of human CD4 or GFP proteins and occurred in a dose-dependent manner, but was not observed for Roquin's inactive mutant (Figure 8-7, page 59). However, Roquin-mediated repression was stronger in cells that were transduced with a construct that encoded the coding region of ICOS together with its 3'UTR (Figure 8-7, page 59).
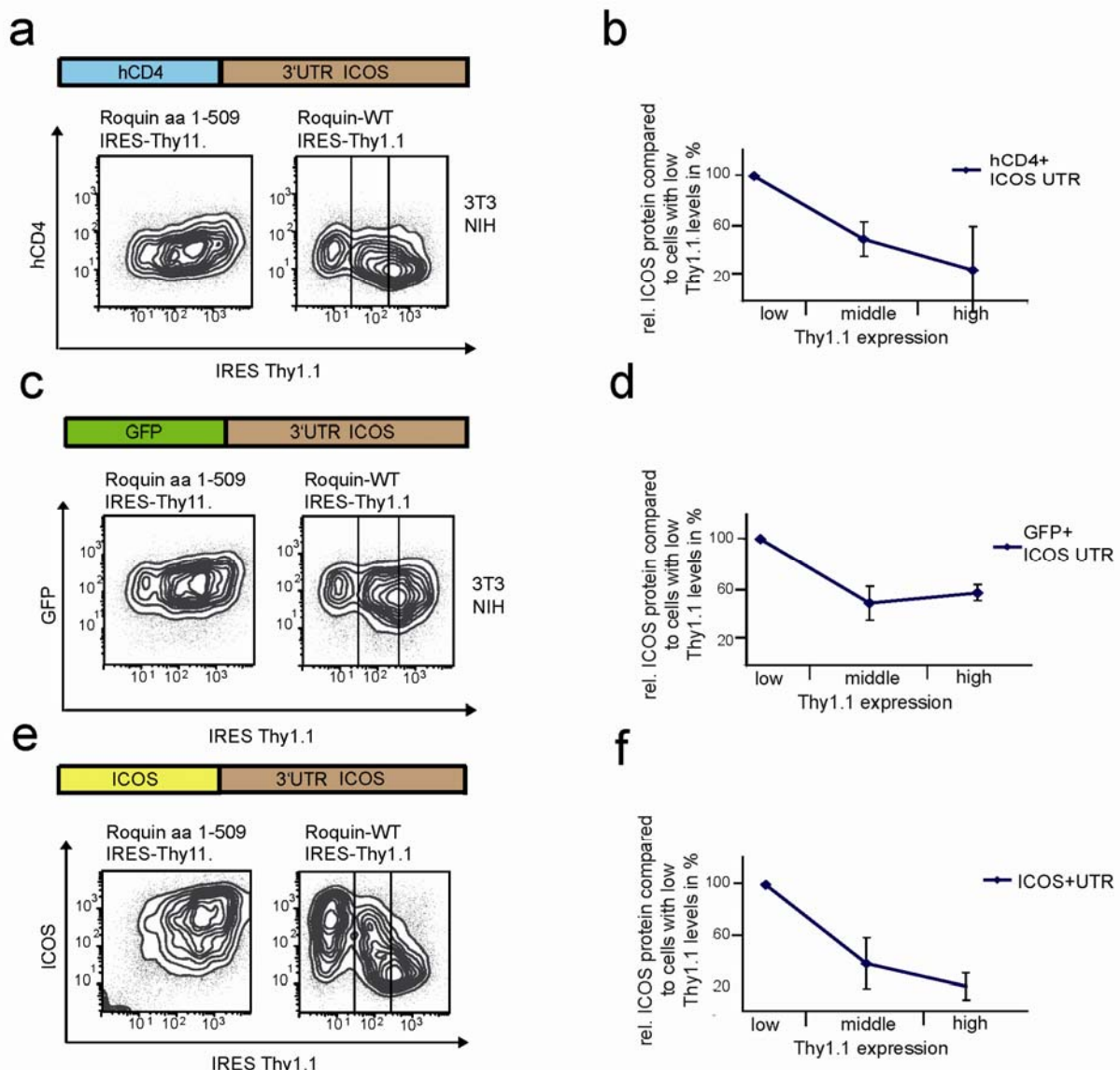
Figure 8-7: Roquin-mediated repression of ICOS does not depend on sequences in the coding region of ICOS. 3T3 cells were transduced with retroviruses that encode the coding regions of either human CD4 (a, b), GFP (c, d) or ICOS (e, f) upstream of the 3'UTR of ICOS. Cells were superinfected with Roquin-WT or its inactive mutant (Roquin aa 1-509) co-expressed with Thy1.1 from bicistronic retroviruses. Flow cytometric analysis (a, c, e) shows contour plots of CD4/GFP/ICOS and Thy1.1 expression. The boxes indicate cells with low, intermediate and high Thy1.1 expression that were used for the quantification shown in (b, d, f) of mean fluorescence intensities of antibody-stained human CD4 or ICOS or the mean fluorescence intensity emitted from GFP.

To unambiguously demonstrate Roquin's strong dependence on the ICOS 3'UTR for the downregulation of ICOS, a luciferase assay with an adenoviral luciferase reporter construct was performed (Figure 8-8, page 60). This construct contained the renilla luciferase open

reading frame in conjunction with the 3'UTR of ICOS as well as an independently co-expressed firefly luciferase open reading frame.
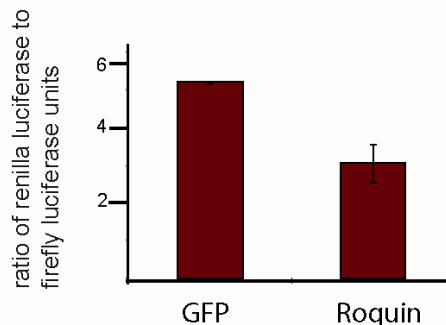
Figure 8-8: <u>Roquin represses the renilla luciferase open reading frame placed in the context of the ICOS 3'UTR.</u> MEFs were co-transduced with GFP or Roquin IRES-GFP and the ICOS 3'UTR luciferase reporter adenoviruses. The ratio of measured renilla and firefly luciferase light units is shown.

Co-infection of Roquin IRES-GFP or GFP with the ICOS 3'UTR reporter construct revealed that Roquin was able to repress the renilla luciferase open reading frame in the context of the ICOS 3'UTR (Figure 8-8). Finally, a construct was generated to test whether Roquin represses ICOS in a cap-dependent manner. This construct contained the ICOS coding region and its 3'UTR (ICOS full length) downstream of an IRES sequence. Translational repression by Roquin was compared to a construct encoding the full length open reading frame of ICOS that was translated in a 5'CAP-dependent manner (Figure 8-9).
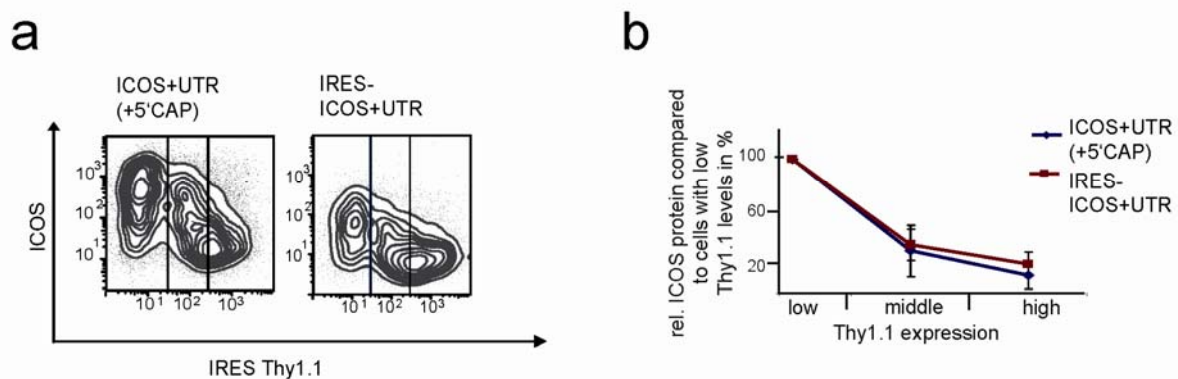
Figure 8-9: <u>Roquin decreases ICOS levels in a 5'CAP-independent manner.</u> 3T3 cells were either transduced with retroviruses that encode an IRES sequence placed upstream of the ICOS coding region followed by the ICOS 3'UTR or transduced with a virus that translates ICOS and its 3'UTR 5'CAP-dependent. Additionally they were superinfected with Roquin-WT from a bicistronic Thy1.1 co-expressing retrovirus. Flow cytometric analysis shows contour plots of ICOS and Thy 1.1 expression (a). Boxes indicate cells with low, intermediate and high Thy1.1 expression used for quantification (b).

To visualize a possible partial contribution of the 5'CAP to Roquin-dependent downregulation of ICOS, the levels of ICOS surface protein were quantified on cells with low, intermediate or

high surface expression of Thy1.1 in both experiments. Roquin repressed ICOS levels in the context of an IRES sequence or with a 5'CAP structure without attenuation and in a similar dose response.

In section 8.1.1 it was observed that the paralog of Roquin, MNAB, when expressed from a cDNA, resulted in a full length as well as in a truncated form that possibly lacks the RING finger domain. This raised the question whether biologic activities of Roquin or MNAB depend on the RING finger. Since there were no previous reports about MNAB targets, Roquin-mediated ICOS repression was determined for a Roquin mutant that was deleted in the RING finger or contained two point-mutations in the RING finger that are homologous to mutations in RING fingers that had been shown to inactivate other E3 ligases [118, 119] (Figure 8-10).
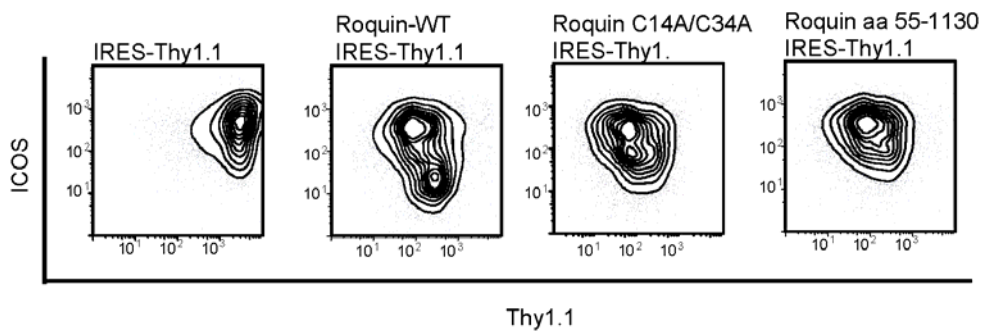
Figure 8-10: <u>The RING finger domain contributes, but is not essential, for Roquin activity.</u> Flow cytometric analysis showing MEF cells that were transduced with retroviruses encoding the human ICOS cDNA with 3'UTR and superinfected with Roquin or Roquin proteins with deletion- or point-mutantions in the RING finger from bicistronic Thy1.1 co-expressing retroviruses.

Interestingly, point-mutations or deletion of the RING finger in Roquin only cause a moderate decrease in activity, compared to Roquin wildtype (Figure 8-10). As compared to wildtype Roquin, the point-mutant was expressed at a similar level. However, the RING finger deletion-mutant (Roquin aa 55-1130) was expressed at lower levels (Figure 8-4, page 56). This may explain why the point-mutation imposed a stronger repressive effect on ICOS than the deletion-mutant. The results show that Roquin-mediated ICOS repression does not require the RING finger. Therefore, Roquin appears to be different from other E3 ubiquitin ligases that completely depend on their intact E3 ligase activity [25, 120, 121]. Hence, the

data suggest that Roquin regulates ICOS on the mRNA level and that the RING finger domain only contributes to its full activity.

8.2.2   MNAB, a paralog of Roquin, is unable to downregulate ICOS

MNAB and Roquin are paralogs with a similar domain organization. Both proteins have amino acid identities ranging from 71.4% within the RING finger, 92.4% in the newly defined ROQ domain and only 18.9% in the zinc finger domain. However, this degree of similarity for the RING finger and ROQ domain indicates that both proteins could perform similar functions.

To address this question we compared protein levels of mouse Roquin and mouse MNAB. Since Roquin protein levels in mouse tissue are highest in the thymus (data not shown), we compared Roquin and MNAB protein levels in this organ. To be able to detect both proteins, an enrichment was performed by immunoprecipitation with an antibody (Q4-2) that recognizes an epitope from a peptide that is shared in both proteins. Endogenous MNAB migrates higher than Roquin, as expected (section 8.1.1). MNAB appears only in one band, whereas endogenous Roquin migrates in two isoforms. Interestingly, MNAB was much higher expressed than Roquin (Figure 8-11 a). Comparing mRNA expression levels of *Roquin* and *MNAB* in lymphoid organs, *Roquin* and *MNAB* mRNAs show a similar expression profile, with highest expression in the thymus, followed by slightly decreased expression in lymphnodes and a significant lower expression in spleen (Figure 8-11 b). It is not clear how *Roquin* and *MNAB* levels relate to each other on mRNA levels since the measurements were performed in different PCR runs. These cannot be compared reliably with each other due to technical variations. Summarizing, *Roquin* and *MNAB* show a similar expression profile, but MNAB might be higher expressed in general, at least on the protein level. It should be noted that the differential expression of *MNAB* and *Roquin* in thymus, lymhnodes and spleen can also be due to the different T and B cell-composition of these organs and that the data presented above probably reflect the differential expression of *Roquin* and *MNAB* mRNA in lymphocytic cells.
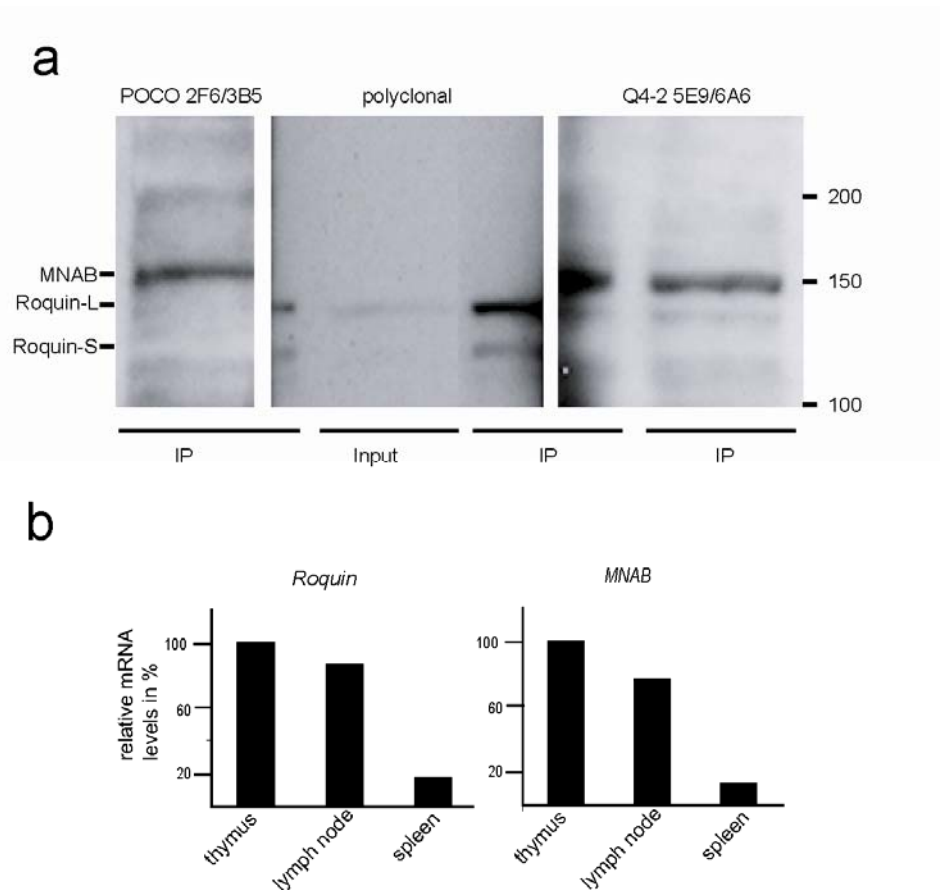
Figure 8-11: **MNAB and Roquin protein and mRNA expression in lymphoid organs.** **(a)** Immunoprecipitations of Roquin and MNAB from thymus were performed with an antibody recognizing MNAB and Roquin (Q4-2) (section 8.1.1). Extracts from equal cell numbers were used for immunoprecipitation and analysis by SDS-PAGE. Immunoblots were probed with the indicated antibodies. **(b)** Thymus, lymph nodes and spleen were isolated from BALB/c mice. Single cell suspensions were used for RNA isolation. *Roquin* and *MNAB* mRNA expression levels were determined by quantitative PCR.

To investigate whether MNAB can also downregulate ICOS, ICOS surface levels of *in vitro* differentiated Th2 cells that overexpressed Roquin or its paralog MNAB were compared. Primary CD4 T cells from DO11.10 CARΔ1 mice (section 6.6) were used to introduce adenoviral expression vectors (section 6.3.2). After *in vitro* differentiation of primary CD4 T cells into Th2 cells, the cells were infected with bicistronic adenoviruses that encode MNAB, Roquin or Roquin M199R and in each case GFP from an IRES sequence. Cells overexpressing MNAB, and consequently also GFP, did not significantly decrease ICOS expression (Figure 8-12 a, c, page 64). In the same approach Roquin effectively reduced ICOS surface levels (Figure 8-12 a). Furthermore, the effect was exclusively observed in GFP positive cells, in cells that actually overexpressed Roquin. The exchange of amino acid

199 from methionine to arginine created a functional hypomorph of Roquin that downregulated ICOS with an attenuated dose response, similar to previously reported findings [1, 2]. This effect of Roquin was specific for ICOS as there was no change in the surface expression of another activation-induced protein CD44 (Figure 8-12 b, d).
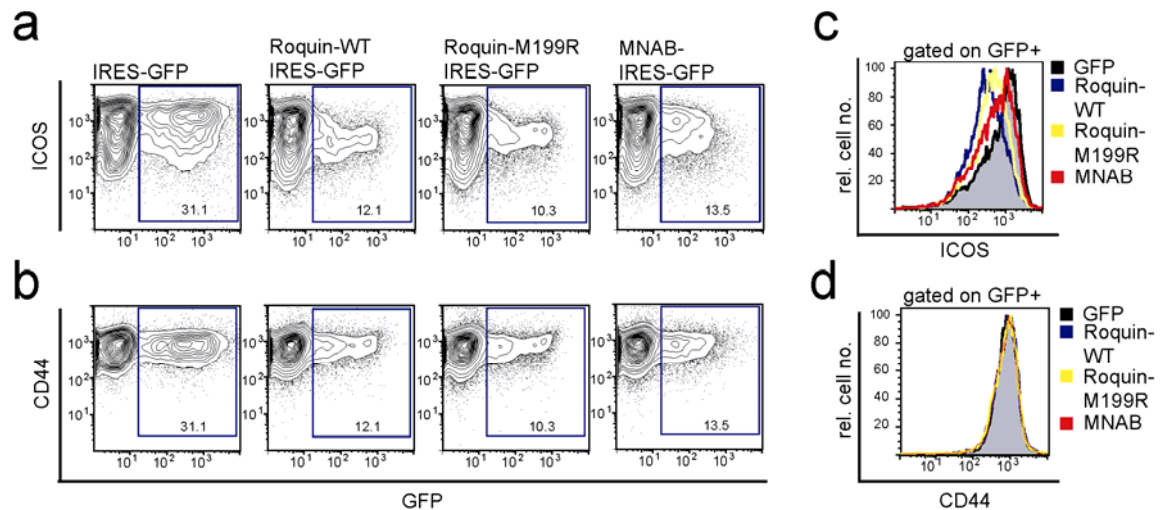

Figure 8-12: <u>Roquin has specialized to repress ICOS surface levels on T cells.</u> (a-d) *In vitro* **differentiated Th2 cells from DO11.10 CARΔ1 mice were infected with the indicated adenoviral vectors at an MOI of 50 on day 4 and analyzed two days later by flow cytometry for ICOS (a) or CD44 (b). The boxes (a, b) indicate GFP positive cells, for which ICOS (c) or CD44 expression levels (d) were quantified.**

To identify unique sequences in Roquin that are critical for ICOS downregulation chimeras of Roquin and MNAB were analyzed for ICOS repression. In these chimeras the conserved carboxy-termini of Roquin and MNAB were reciprocally exchanged (section 6.3). Expression of Roquin/MNAB chimeras in MEF cells revealed that sequences carboxy-terminal to the zinc finger in Roquin contribute to downregulate the co-expressed ICOS (Figure 8-13, page 65).

In fact, the amino-terminus of MNAB in the context of the carboxy-terminus of Roquin was able to support ICOS downregulation. In contrast, the carboxy-terminus of MNAB fused to the amino-terminus of Roquin produced a protein with strongly reduced activity (Figure 8-13, page 65).
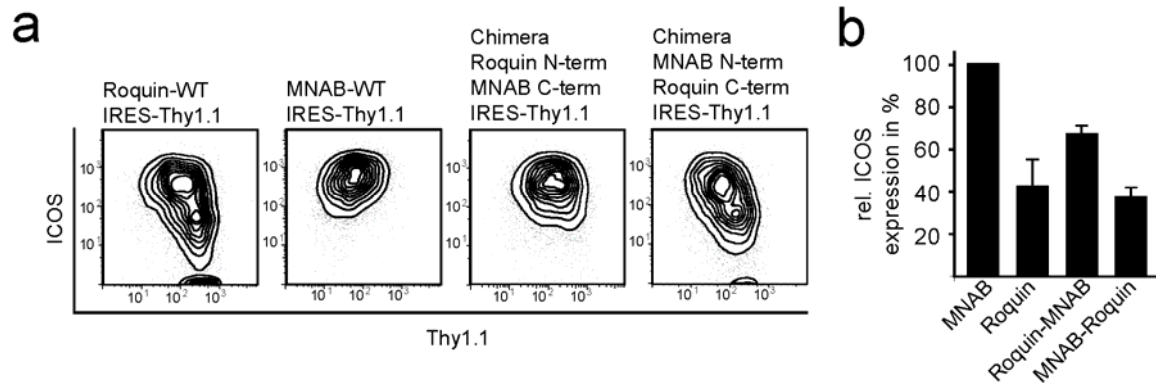
Figure 8-13: <u>The carboxy-terminus of Roquin has specialized for efficient ICOS repression.</u> **(a-b) MEF cells were transduced with retroviruses that encoded the human ICOS cDNA with 3'UTR and superinfected to co-express Roquin or MNAB or chimeras of both proteins from bicistronic Thy1.1 co-expressing retroviruses. Flow cytometric analysis showing contour plots of antibody-stained ICOS and Thy1.1 surface expression (a) or a bar diagram of the average ICOS expression from three independent experiments of the relative mean fluorescence intensity (MFI) of all cells normalized to the ICOS MFI in cells transduced with MNAB expressing constructs (b).**

These data show that the amino-terminal sequences of MNAB can exert a similar function as those of Roquin, whereas the carboxy-terminus cannot. Retroviruses encoding both chimeras showed comparable mRNA expression as judged from Thy1.1 levels. Transfection of the chimera-encoding vectors led to similar protein expression in HEK293 cells (Figure 8-2). However, quantification of ICOS downregulation revealed that even the amino-terminus of Roquin in the context of the carboxy-terminus of MNAB was more potent in repressing ICOS than the corresponding sequences in MNAB (Figure 8-13). These findings demonstrate that, in contrast to MNAB, the entire Roquin protein, but especially its carboxy-terminus, has evolved for efficient downregulation of ICOS.

8.2.3   The carboxy-terminus of Roquin determines the localization of Roquin to P bodies

To investigate whether Roquin protein is enriched in a specific subcellular localization, confocal microscopy studies of HEK293T cells, transfected with Roquin proteins fused to an amino-terminal or carboxy-terminal GFP, were performed. The images show that the green

fluorescent signal from wildtype Roquin co-localized with endogenous Rck (Figure 8-14 a), a marker of processing bodies (P bodies) [122].
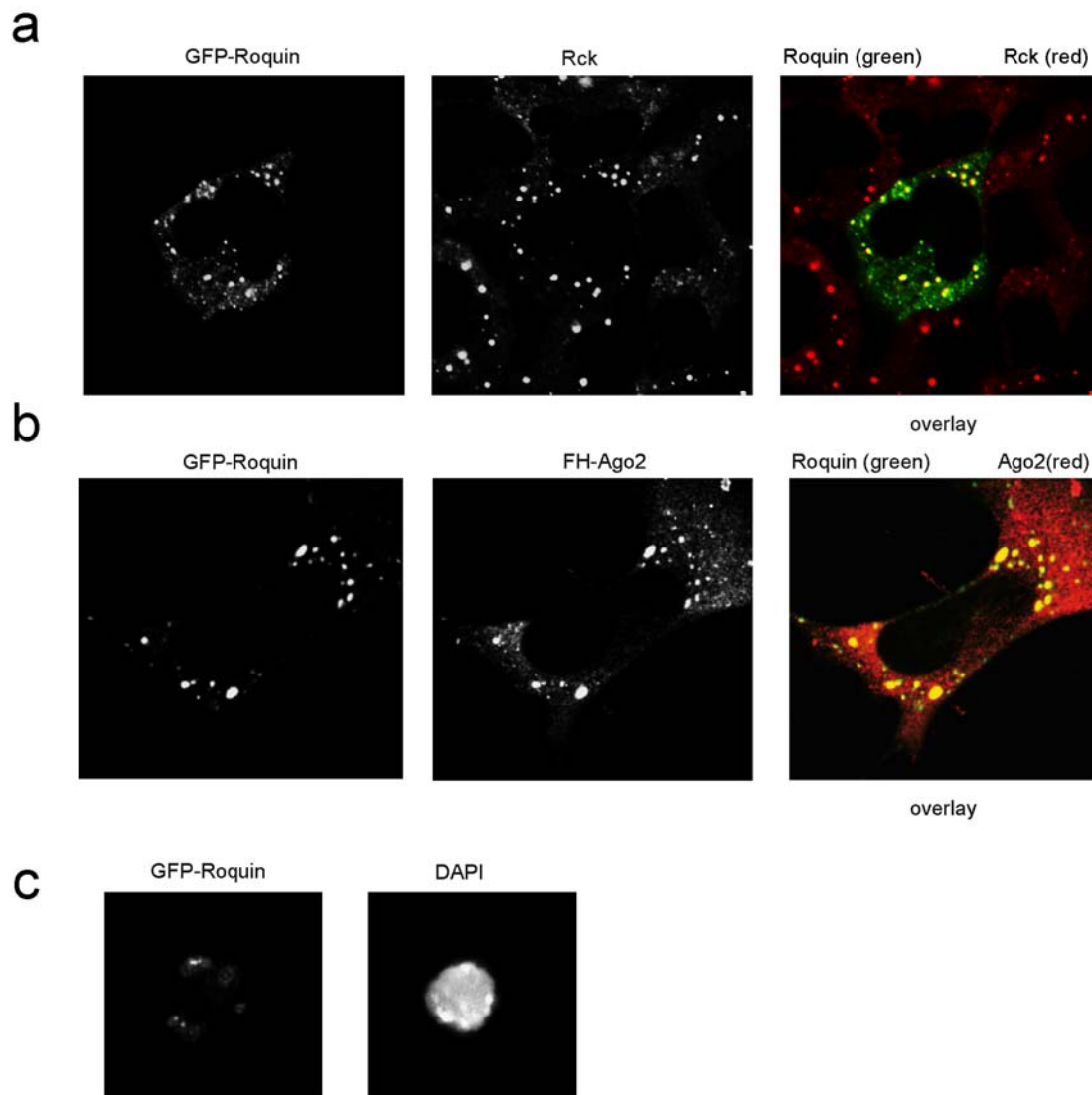

Figure 8-14: <u>**Roquin co-localizes with P body-markers.**</u> **(a-c) Confocal microscopy was performed to determine co-localization of endogenous Rck (stained with anti-Rck in red) with GFP tagged-Roquin (green) (a) as well as co-localization of Flag-HA tagged-Ago2 with GFP tagged-Roquin (green) in HEK293T cells (b) and localization pattern of GFP-tagged Roquin in T cells (c).**

We also observed co-localization with co-expressed Flag-HA tagged Ago2 protein (Figure 8-14 b), which had been shown to be predominantly cytoplasmic, but also localize to P bodies [92]. GFP-fused Roquin proteins were additionally compared to untagged Roquin proteins and all revealed the same subcellular localization (data not shown).

These findings demonstrate a co-localization of transfected Roquin with different P body markers. Interestingly, a comparable localization pattern was observed when GFP-Roquin was introduced into primary CD4 T cells (Figure 8-14 c).

Since the amino-terminal domains of Roquin and MNAB can be functionally exchanged, we tested if MNAB and Roquin localize in the same loci. Indeed, Roquin and MNAB partially co-localize in A549 cells (Figure 8-15), indicating that MNAB may also be enriched in P bodies.
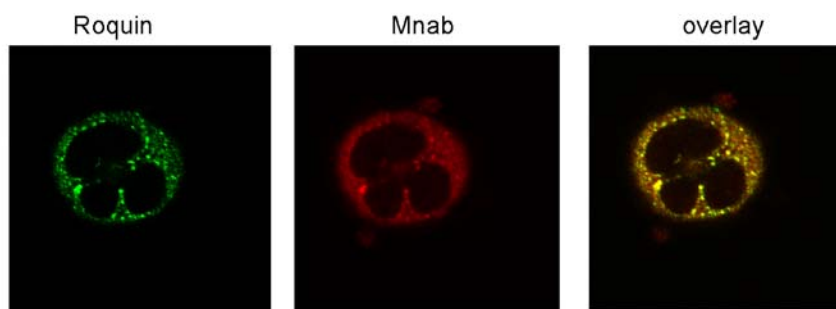

Figure 8-15: <u>Roquin and MNAB co-localize.</u> Immunofluorescence in A549 cells infected with adenovirus encoding GFP-Roquin and antibody stained MNAB as indicated.

Roquin has previously been described to co-localize with TIA-1 in stress granules [2]. The proposed localization was tested and confirmed after induction of stress by treatment with arsenite (Figure 8-16). Arsenite treatment is well known to induce a stress response in cells.
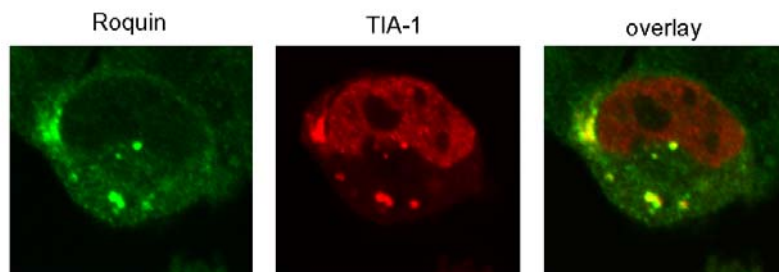

Figure 8-16: <u>TIA-1 and Roquin co-localize after stress-induction by arsenite.</u> HEK293A cells were transfected with FuGene HD and vectors encoding Roquin and YFP-tagged TIA-1, treated with 0.5 mM arsenite for 1 hour and stained for Roquin with the monoclonal antibody Q4-4 (section 6.1).

However, this co-localization was not observed in cells that were not exposed to stress (data not shown). To find out whether Roquin-mediated downregulation of ICOS acts through TIA-1-dependent induction of stress granules, Roquin function was tested in the absence of TIA-1. MEF cells deficient for TIA-1 have been shown to be impaired in stress granule assembly as determined by TIAR, G3BP and eIF3 staining [123]. TIA-1-deficient and control MEF cells (Figure 8-17 a) were sequentially transduced with retroviruses encoding ICOS and Roquin expression constructs and tested for Roquin-mediated ICOS repression. The data show no effect of TIA-1 deficiency on Roquin-mediated ICOS repression (Figure 8-17 b).
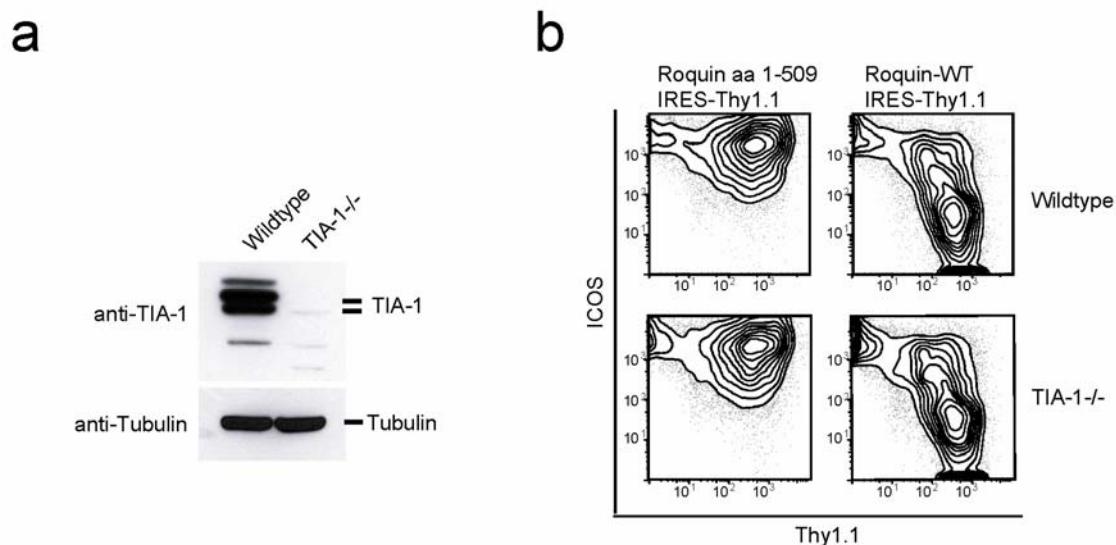

Figure 8-17: <u>Roquin activity is independent of a TIA-1-mediated stress response.</u> (a) Western Blot analysis of TIA-1 wildtype and knockout cells for TIA-1 and Tubulin protein levels. (b) Wildtype and TIA-1 -/- mouse embryonic fibroblasts were retrovirally transduced with human ICOS coding sequence containing its 3'UTR. Superinfection was subsequently performed using bicistronic retroviral vectors expressing Roquin aa 1-509 (inactive mutant) or Roquin-WT and Thy1.1 from an IRES sequence. Flow cytometric analysis shows antibody-stained ICOS and Thy1.1 expression.

These results suggest that, at least in the absence of cellular stress, Roquin-mediated ICOS repression does not depend on TIA-1 function, but rather involves localization of Roquin to P bodies. To test which domain in the Roquin protein determines the localization to P bodies, amino- and carboxy-terminal deletion-mutants of Roquin were generated (Figure 6-2) and tested for localization (Figure 8-18, page 69). The Roquin-specific punctate pattern in the cytoplasm was observed for all but one mutant. Mutants lacking the carboxy-terminal coiled-

coil domain (Roquin aa 1-951), the amino-terminal RING finger and ROQ domains (Roquin aa 55-1130 and Roquin aa 338-1130) or the RING finger, ROQ and zinc finger domains (Roquin aa 441-1130) all maintained the characteristic expression pattern of Roquin (Figure 8-18). Interestingly, the carboxy-terminal deletion-mutant Roquin aa 1-509 exhibited aberrant diffuse cytoplasmic as well as low-level nuclear localization (Figure 8-18). These findings imply that the carboxy-terminal region of Roquin is sufficient to co-localize Roquin with P body-markers and may confer repressive activity towards ICOS.
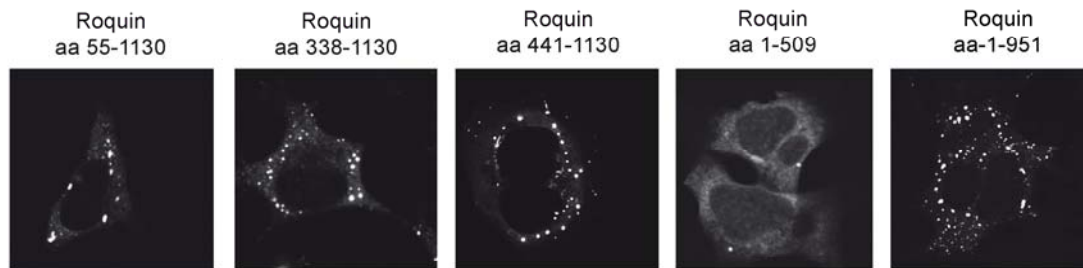

Figure 8-18: <u>**The carboxy-terminus of Roquin determines the characteristic localization pattern of Roquin.**</u> **The localization of the indicated GFP-tagged wildtype and mutant Roquin proteins in HEK293A cells is shown. Explanatory notes: Roquin aa 55-1130 is lacking the RING finger domain, Roquin aa 338-1130 is lacking the RING finger and ROQ domain, Roquin aa 441-1130 is lacking the RING finger, the ROQ and Zinc finger domain, Roquin aa 1-509 is lacking the carboxy-terminal regions, including the proline-rich region, Roquin aa 1-951 is lacking the coiled-coil domain.**

To confirm that localization to P bodies is essential for Roquin function, the carboxy-terminal deletion-mutants of Roquin were tested for their efficiency to downregulate ICOS (Figure 8-19). As expected, the Roquin aa 1-509 mutant is completely inactive (Figure 8-19). Importantly, this mutation (Roquin aa 1-509) did not lead to lower expression levels (Figure 8-4, page 56) and therefore was used as a negative control in the experiments seen in Figure 8-6, page 58, Figure 8-7, page 59, Figure 8-17, page 68, Figure 8-27, page 78, and Figure 8-29, page 81. The Roquin mutant lacking the coiled-coil domain (Roquin aa 1-951) has a slightly reduced activity (Figure 8-19, page 70). This reduction could be intrinsic to the mutant protein, but may also be due to a weaker expression, which the Roquin aa 1-951 mutant shows upon transfection in HEK293A cells (Figure 8-4, page 56). Together, these

findings imply that the carboxy-terminal region of Roquin is essential for ICOS downregulation and sufficient to co-localize Roquin with P body markers.
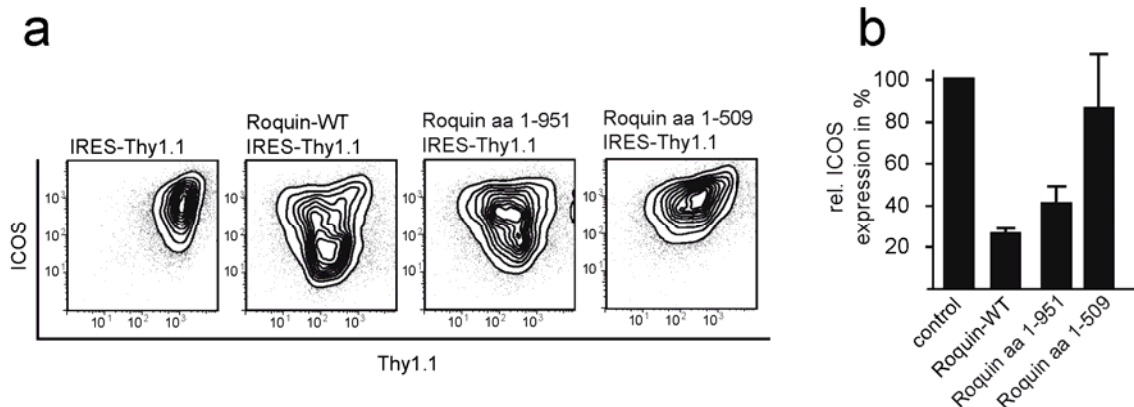

Figure 8-19: <u>**The carboxy-terminus is required for Roquin-mediated ICOS repression.**</u> **(a-b) MEF cells were sequentially transduced with retroviruses encoding ICOS and the indicated Roquin proteins that co-expressed Thy1.1 from an IRES sequence. Flow cytometric analysis showing antibody-stained surface expression of ICOS and Thy1.1 in contour plots (a) and a bar diagram of the average MFI of ICOS (from three independent experiments) normalized to ICOS levels in empty vector (IRES-Thy1.1)-transduced cells (b). Explanatory notes: Roquin aa 1-509 is lacking the carboxy-terminal regions, including the proline-rich region, Roquin aa 1-951 is lacking the coiled-coil domain.**

8.2.4 Roquin requires the P body components Rck and Lsm1 for posttranscriptional gene silencing of ICOS

To test whether Roquin-mediated repression of ICOS depends on P body function, an adenoviral knockdown against the two P body components *Rck* and *Lsm1* (section 5.3.2) was established. The knockdown of *Roquin* itself (shRc3h1) was used as a positive control. One shRNA sequence out of four was identified to efficiently reduce Roquin or Rck target proteins or *Lsm1* target mRNA, as determined by Western blot or quantitative PCR, respectively (Figure 8-20, page 71). MEF cells were transduced with retroviruses that encoded ICOS and Roquin IRES-Thy1.1 and superinfected with adenoviruses that encoded shRNAs directed against *Roquin*, *Rck* or *Lsm1*. Cells that were infected with an shRNA against *Roquin* (Rc3h1) strongly decreased the levels of the Thy1.1 marker protein that was co-expressed with Roquin from an IRES sequence (Figure 8-21 a, third plot from the left, page 72). A similar strong decrease was observed for the Roquin protein itsel (Figure 8-20, page 71). Therefore, not only Roquin protein levels were visually affected, but also the marker protein that was co-expressed from the bicistronic mRNA. At the same time ICOS surface

expression increased to levels that even exceeded the expression on cells that were not transduced with Roquin retroviruses (Figure 8-21 a, compare third and first contour plot from the left, page 72). The data imply that ICOS levels are repressed by exogenous as well as endogenous Roquin. This is consistent with detectable endogenous Roquin expression in MEF cells (Figure 8-27 c, page 78). Although introduction of an shRNA directed against *Lsm1* had only a moderate effect on Lsm1 mRNA levels (Figure 8-20 b, page 71), the knockdown led to partially increased ICOS levels in Roquin expressing cells (Figure 8-21 a, c, page 72). Importantly, a knockdown of *Rck* very effectively increased ICOS levels in Roquin expressing cells (Figure 8-21 b, d, page 72). These levels increased to even higher levels than in cells that were not Roquin transduced, similar to the effect observed upon *Roquin* knockdown. However, in this case the increase of ICOS occurred in the absence of changes in Thy1.1 expression. This finding indicates that the knockdown of *Rck* neutralized the function of endogenous as well as exogenous Roquin proteins without affecting expression of the mRNA encoding Roquin and IRES-Thy1.1 (Figure 8-21 b, page 72).
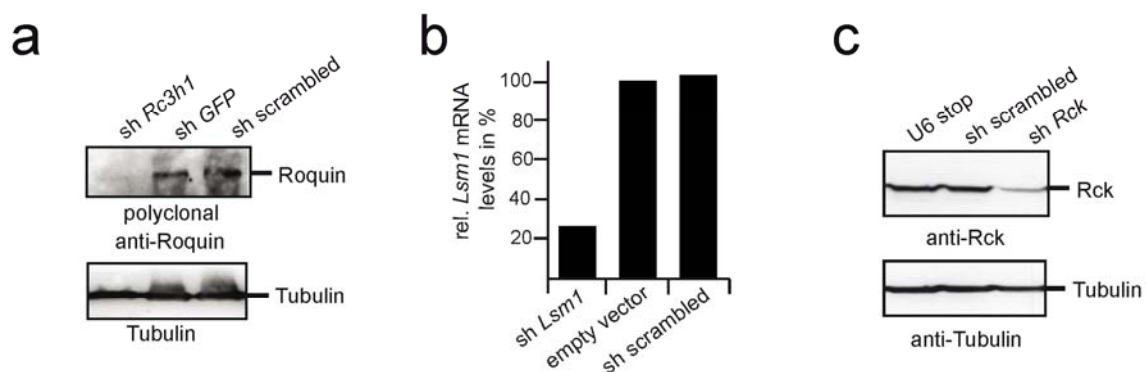

Figure 8-20: Evaluation of adenoviral knockdown of Roquin, Lsm1 and Rck. Protein or RNA extracts from cells expressing adenoviral shRNA hairpin constructs against *Rc3h1*, *Lsm1* or *Rck* were evaluated by Western blots against Roquin (a) and Rck (c) or by quantitative PCR for *Lsm1* (b). Please note that the cells used in (a, b) correspond to the transduced MEF cells shown in Figure 8-21, whereas Rck knockdown (c) was evaluated in A549 cells.
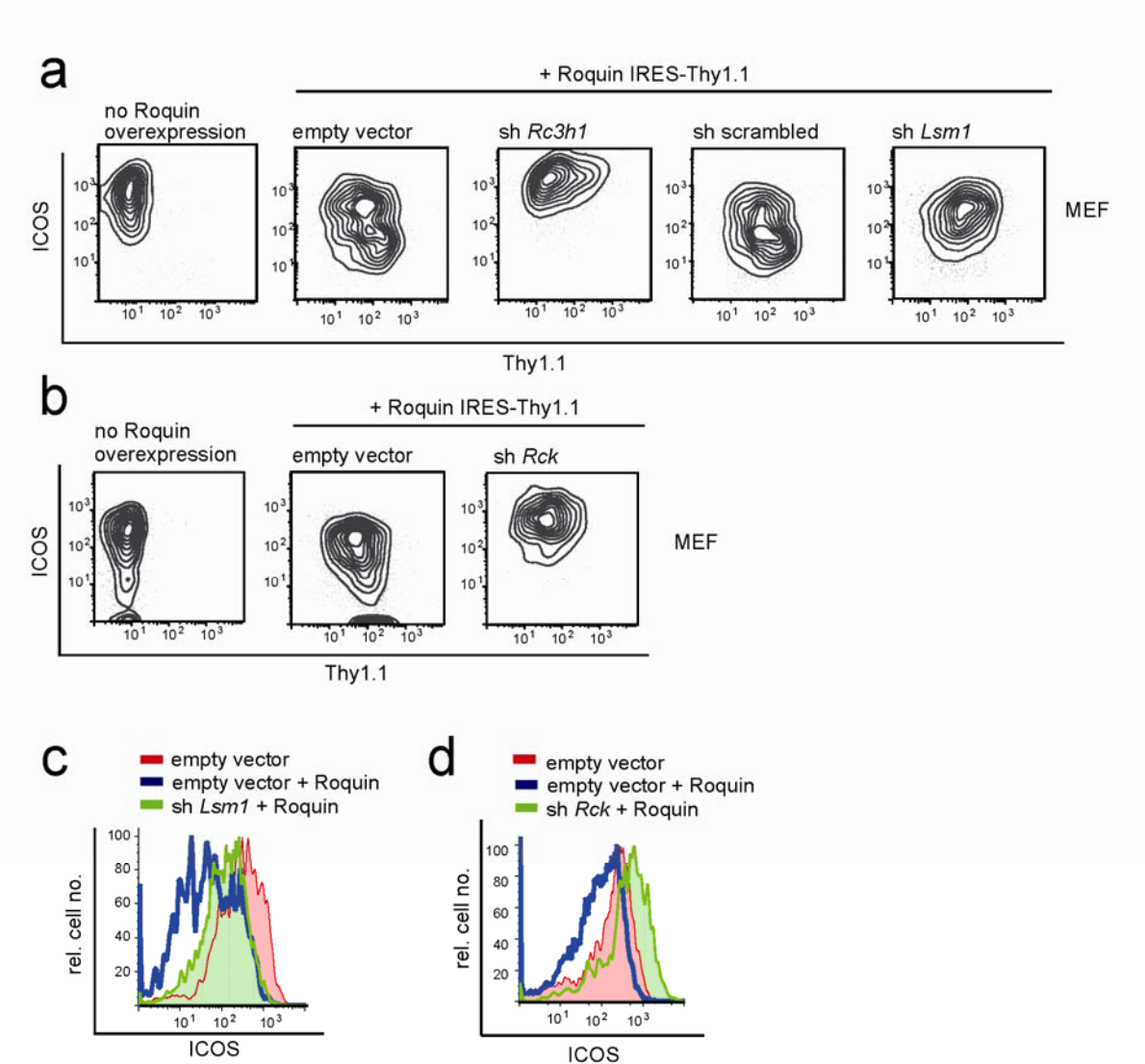
Figure 8-21: <u>Knockdown of *Roquin, Lsm1* or *Rck* increases ICOS expression.</u> (a-d) MEF cells were sequentially transduced with retroviruses to co-express ICOS and Roquin and were superinfected with adenoviruses encoding shRNAs against the indicated target mRNAs. Flow cytometric analysis shows ICOS and Thy1.1 levels in contour plots (a, b) or relative ICOS expression in histograms (c, d) three days after superinfection.

In summary, the data presented in this chapter demonstrate that Roquin-mediated ICOS repression on the one hand requires carboxy-terminal sequences that translocate Roquin to P bodies (section 8.2.3). On the other hand repression strongly depends on functional interaction with the P body components Rck and Lsm1.

8.2.5   The amino-terminus of Roquin binds to *ICOS* mRNA

A possible mechanism by which Roquin could posttranscriptionally repress *ICOS* mRNA would be binding of Roquin to *ICOS* mRNA and its translocation into P bodies. To test this hypothesis, an interaction of Roquin with *ICOS* mRNA was tested in two different approaches. First, RNA-IPs were performed under highly stringent conditions and with protein extracts prepared after crosslinking of intact cells with formaldehyde treatment and subsequent sonication (section 7.3.6). For that, HEK293 cells were transfected with constructs expressing GFP-Roquin and *ICOS* mRNA containing its 3'UTR. Subsequently, RNA-IPs were performed using anti-GFP antibodies. PCR reactions with specific primers for ICOS were performed on reversely transcribed RNA prepared from immunoprecipitates. The results revealed that *ICOS* mRNA was strongly bound by Roquin (Figure 8-22 upper panel, lane 1). This interaction was increased over background levels of *ICOS* mRNA as judged by a negative control measuring unspecific *ICOS* mRNA-GFP protein interactions (Figure 8-22, upper panel, compare lanes 2 and 1). As an additional negative control, the abundantly expressed 5S rRNA from the RNA-IPs was PCR-amplified as described above. No unspecific interaction of Roquin-GFP and 5S rRNA was detected (Figure 8-22, lower panel, lanes 1 and 2). This further indicated that the detected interaction between Roquin-GFP and *ICOS* mRNA was specific.
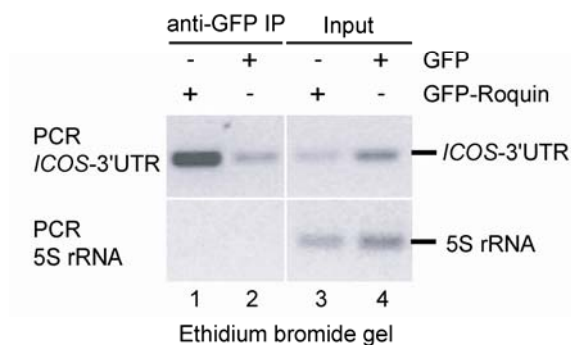

Figure 8-22: <u>Roquin interacts with *ICOS* mRNA.</u> RNA-IPs were performed with anti-GFP antibodies on extracts from crosslinked and sonicated HEK293T cells that were co-transfected with expression vectors for *ICOS* and GFP tagged-Roquin or GFP alone. RNA in the precipitates were reversly transcribed and PCR-amplified with primers specific for the 3'UTR of human *ICOS* or primers specific for 5S rRNA and analyzed on ethidium bromide stained agarose gels.

In a second approach we wanted to test whether endogenous Roquin interacts with endogenous *ICOS* mRNA. Extracts were prepared from primary Th1 cells and immunoprecipitations or mock precipitations, this time without crosslinking, were performed with antibodies against Roquin. Roquin protein was found to be efficiently enriched after immunoprecipitation (Figure 8-23 a). In parallel immunoprecipitation experiments, the associated RNA was extracted and *ICOS* mRNA amounts were determined after reverse transcription and quantitative PCR. The physical association of endogenous Roquin with endogenous *ICOS* mRNA in T cells was confirmed in three independent experiments (Figure 8-23 b).
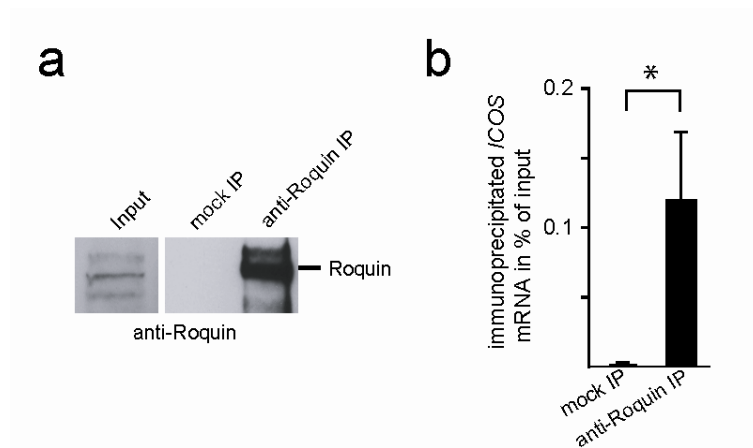

Figure 8-23: <u>Roquin binds to endogenous *ICOS* mRNA in T cells.</u> (a-b) Co-immunoprecipitation of endogenous *ICOS* mRNA with endogenous Roquin protein from Th1 cell protein extracts applying anti-Roquin antibodies. (a) Immunoprecipitated Roquin protein was detected by Western blot. (b) The average co-immunoprecipitated endogenous mouse *ICOS* mRNA was determined by quantitative PCR and was normalized to input levels from three independent experiments. Statistical significance was determined by Student's T-test with a p value of 0.02.

To analyze the involvement of individual Roquin domains in *ICOS* mRNA binding, GFP-fused deletion-mutants of Roquin were co-transfected with an human ICOS expression construct into HEK293T cells (Figure 8-24 a, page 75). Clearly, the interaction between Roquin and *ICOS* mRNA did not depend on the carboxy- but rather on the amino-terminus of Roquin. In fact, the interaction of Roquin and *ICOS* mRNA was even increased for the inactive deletion-mutant Roquin aa 1-509, compared to Roquin wildtype (Figure 8-24 a, page 75). However, this effect was most likely due to increased efficiency of immunoprecipitation for this mutant, compared to the other Roquin mutants (data not shown). The fact that this mutant cannot localize to P bodies (section 8.2.3) indicates that the detected RNA-interactions result rather from interactions in the cytoplasm than from interactions in P bodies. Deletion

of the amino-terminal RING finger alone (Roquin aa 55-1130) had a small negative effect on *ICOS* mRNA interaction (Figure 8-24). However, *ICOS* mRNA interaction was completely abolished for the mutant lacking the RING finger and ROQ domain (Roquin aa 338-1130) or the mutant lacking the RING finger, ROQ and zinc finger domain (Roquin aa 441-1130) (Figure 8-24).
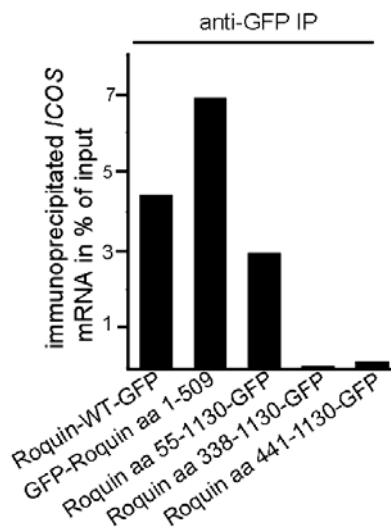

Figure 8-24: The amino-terminal ROQ domain is critical for RNA-binding. RNA immuno-precipitation with anti-GFP antibodies using protein extracts from HEK293T cells that were co-transfected with GFP tagged- wildtype or deletion-mutants of Roquin together with *ICOS*. The bar diagram displays the fraction of co-immunoprecipitated *ICOS* mRNA compared to input levels. Explanatory notes: Roquin aa 1-509 is lacking the carboxy-terminal region including the proline-rich region, Roquin aa 55-1130 is lacking the RING finger domain, Roquin aa 338-1130 is lacking the RING finger and ROQ domain, Roquin aa 441-1130 is lacking the RING finger, the ROQ and Zinc finger domain.

To investigate if RNA-binding is essential for Roquin repressive activity, the amino-terminal mutants were analyzed for their capacity to downregulate ICOS. MEF cells were sequentially transduced with retroviral vectors coding for ICOS and Roquin wildtype or mutants. In these experiments Roquin-mediated repression of ICOS was abolished for the mutant lacking the ROQ domain (Roquin aa 338-1130) and also for the mutant lacking the ROQ and zinc finger domain (Roquin aa 441-1130) (Figure 8-25, page 76). This result clearly shows that RNA-binding by the ROQ domain is essential for Roquin activity. To investigate a possible involvement of the CCCH-type zinc finger, two conserved cysteines C419 and C428 were replaced with arginines. Individual mutations of conserved cysteines in TTP have been demonstrated to interfere with RNA binding [70]. Combined mutations of the first and second cysteines in the zinc finger of Roquin did not decrease ICOS expression of this mutant (Figure 8-25, page 76), but revealed a moderate negative effect on its activity. This was most apparent in cells with high levels of Thy1.1 expression (Figure 8-25, page 76). These findings suggest that zinc finger and RING finger (section 8.2.1) domain may cooperate

physically or functionally with the ROQ domain. However, only the ROQ domain is essential for binding to *ICOS* mRNA.
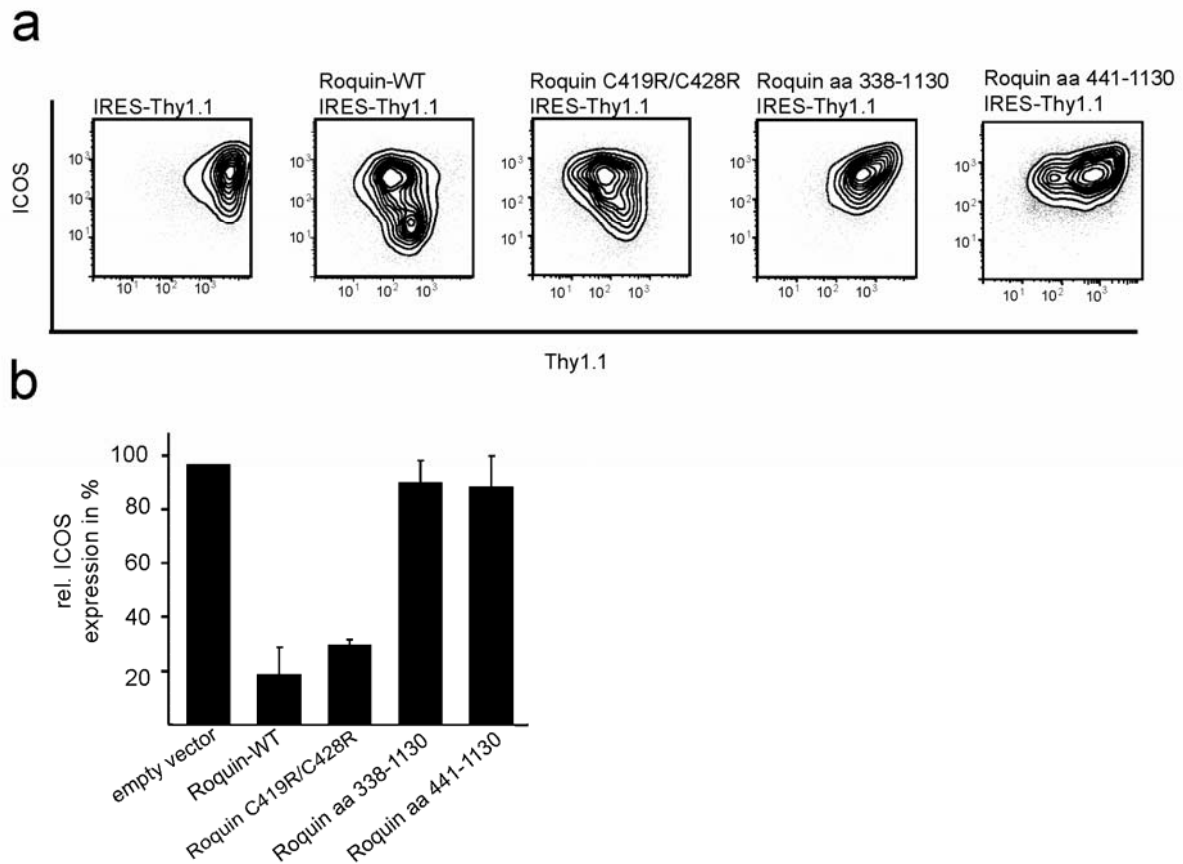

Figure 8-25: <u>The ROQ domain is essential for Roquin-mediated ICOS repression.</u> **(a-b) MEF cells were sequentially transduced with ICOS and the indicated wildtype or mutant Roquin encoding retroviral vectors. Flow cytometric analysis showing antibody-stained ICOS and Thy1.1 surface expression levels in contour plots (a) or the average ICOS MFI, from three independent experiments, normalized to control transduced cells (b). Explanatory notes: Roquin C419R/C428R is mutated at two conserved cysteines within the Zinc finger domain, Roquin aa 338-1130 is lacking the RING finger and ROQ domain, Roquin aa 441-1130 is lacking the RING finger, the ROQ and Zinc finger domain.**

In summary, it was demonstrated that the amino-terminus and carboxy-terminus of Roquin provide essential functions for efficient posttranscriptional ICOS repression by binding to *ICOS* mRNA and by localization to P bodies, respectively.

8.2.6 Roquin activity is Argonaute independent

P bodies are not only enriched in enzymes of the general mRNA decay machinery but also in components of the miRNA-pathway, e.g. Argonaute proteins (section 5.3.1). Argonaute proteins bind to microRNAs and represent the core enzyme of the miRISC. No inhibitory miRNA effect can be imposed on mRNAs without Argonaute (Ago) proteins or miRISC formation. The miRISC requires, similar to Roquin, the P body components Rck and, in some cases, also Lsm1 (section 5.3.1) for translational repression (section 8.2.4). It was previously suggested that Roquin-dependent ICOS repression is mediated by miRNAs [1]. How Roquin cooperates with the miRNA pathway was not clarified. Therefore, we tested contribution of miRISC components for Roquin-mediated ICOS repression. Among the mammalian Argonaute 1-4 family members Ago2 is unique, because it is the only Ago protein with endonucleolytic activity [124]. We obtained Ago2 knockout MEF cells to analyze Roquin-mediated ICOS repression in the absence of Ago2. First, it was tested whether reconstitution with human Flag-tagged Ago2 (hAgo2) restored shRNA-dependent knockdown of target mRNAs. In this process Ago2 cleaves mRNAs that contain perfectly matching sequences complementary to the sh/siRNA used. After retroviral introduction of human Flag-tagged Ago2, the cells re-acquired the ability to efficiently support shRNA dependent knockdown of ectopically expressed mouse CD4. The same shRNA against *CD4* had no effect on CD4 expression in Ago2-deficient cells (Figure 8-26).
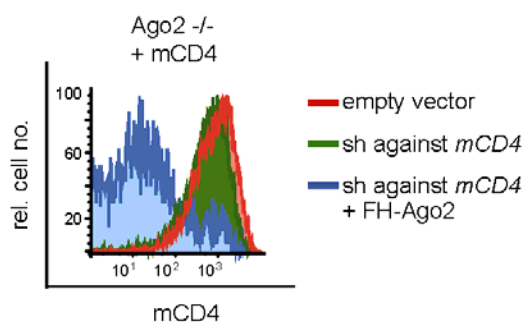

Figure 8-26: <u>Ago2-/- MEFs can re-establish siRISC activity after Ago2 overexpression.</u> Ago2 -/- MEF cells were sequentially transduced with mouse CD4 or control retroviruses and superinfected with retroviruses encoding an shRNA against *mCD4* or superinfected with the shRNA in combination with Flag-HA tagged-Ago2. Cells were analyzed by flow cytometry to show an overlay histogram of relative CD4 expression in the transduced cells.

Roquin activity was determined in Ago2 knockout MEF cells or knockout cells, in which human Flag-tagged Ago2 was re-expressed. The absence of Ago2 did not compromise

Roquin-dependent downregulation of ICOS. ICOS levels strongly decreased upon co-expression of Roquin wildtype (Figure 8-27 a, upper panel, right contour plot, page 78) as compared to expression of the inactive mutant of Roquin (Figure 8-27 a, upper panel, left contour plot). Surprisingly, re-expression of functional human Ago2 strongly interfered with Roquin-dependent downregulation of ICOS (Figure 8-27 a, lower panel, right contour plot).
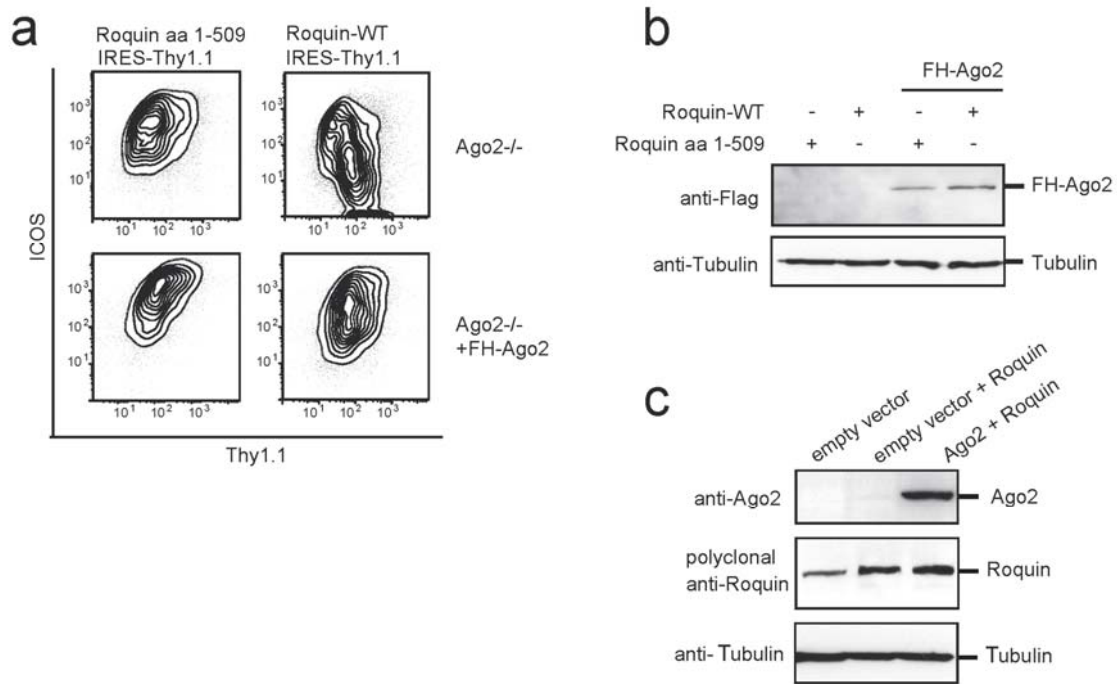

Figure 8-27: <u>Ago2 overexpression interferes with Roquin activity.</u> (a-b) Ago2-/- MEF cells were transduced with retroviruses to co-express ICOS together with wildtype or mutant Roquin from IRES-Thy1.1 vectors alone or in combination with human Flag-tagged Ago2. (a) Flow cytometric analysis showing ICOS and Thy1.1. (b) Western blot analysis for Flag-tagged Ago2 levels based on the cells shown in (a). (c) Western blots of MEF cells, which were retrovirally transduced, as indicated, to overexpress Flag-tagged Ago2 and Roquin and were analyzed for Ago2, Roquin and Tubulin expression.

To rule out that Ago2 overexpression affected Roquin expression, both proteins were analyzed in retrovirally co-transduced MEF cells (Figure 8-27 c). Ago2 overexpression did not change Roquin protein levels (Figure 8-27 c). These findings accentuate that Roquin-dependent silencing of ICOS does not require the endonucleolytic activity of Ago2, but operates in a closely connected pathway, which is inhibited by experimentally increased Ago2 expression levels. Ago2 functionally overlaps with Ago1, 3 and 4 in miRNA-dependent

translational inhibition. Therefore Roquin-induced downregulation of ICOS was tested in embryonic stem (ES) cells containing homozygous deletions of *Ago1, 3* and *4* genes (ES cell line B9) [125]. In addition, the ES cell line E7, which is deficient for endogenous mouse *Ago1-4* gene products, was analyzed. Since complete absence of all Ago proteins results in apoptosis, these cells can only be expanded in culture as they express low levels of a human Ago2 transgene from a loxP-flanked locus. In these cells human Ago2 can be deleted by activation of an estrogen receptor fused Cre recombinase, induced by tamoxifen (4'OH-T) treatment. After tamoxifen treatment these cells are completely devoid of *Ago1-4* gene products, but remain viable for up to 4 days before they start to undergo apoptosis [125]. Co-infection of Roquin IRES-GFP or GFP with a ICOS 3'UTR luciferase reporter construct (section 6.3) revealed that Roquin was still able to repress the ICOS 3'UTR in cells without mouse *Ago1, 3 and 4* (ES cell line B9) and in cells that lack mouse *Ago1-4* but contain low amounts of hAgo2 (ES cell line E7).

Importantly, E7 cells after 4'OH-T treatment showed an arrest in cell growth but were not impaired for Roquin-dependent ICOS repression (Figure 8-28 a, page 80). The same results were obtained in these cells when Roquin activity on ICOS levels was analyzed by flow cytometry (Figure 8-28 b, page 80). Measuring surface ICOS levels in cells that co-express GFP or Roquin IRES-GFP, a 4 to 10-fold repression of ICOS levels by FACS was detected (Figure 8-28 b, page 80) compared to a 6 to 9-fold repression of the ICOS reporter detected in luciferase assays (Figure 8-28 c, page 80). Independent of the way of assessment, Roquin-mediated ICOS repression was comparable strong in Ago knockout ES cells as observed in wildtype MEF cells and did not decrease after Tamoxifen treatment of E7 cells.

These experiments demonstrate that Roquin-mediated ICOS repression does not require the presence of Ago1-4 proteins and is likely independent of miRNAs. However, the role of miRNAs for Roquin activity will be addressed in detail in the following chapter.
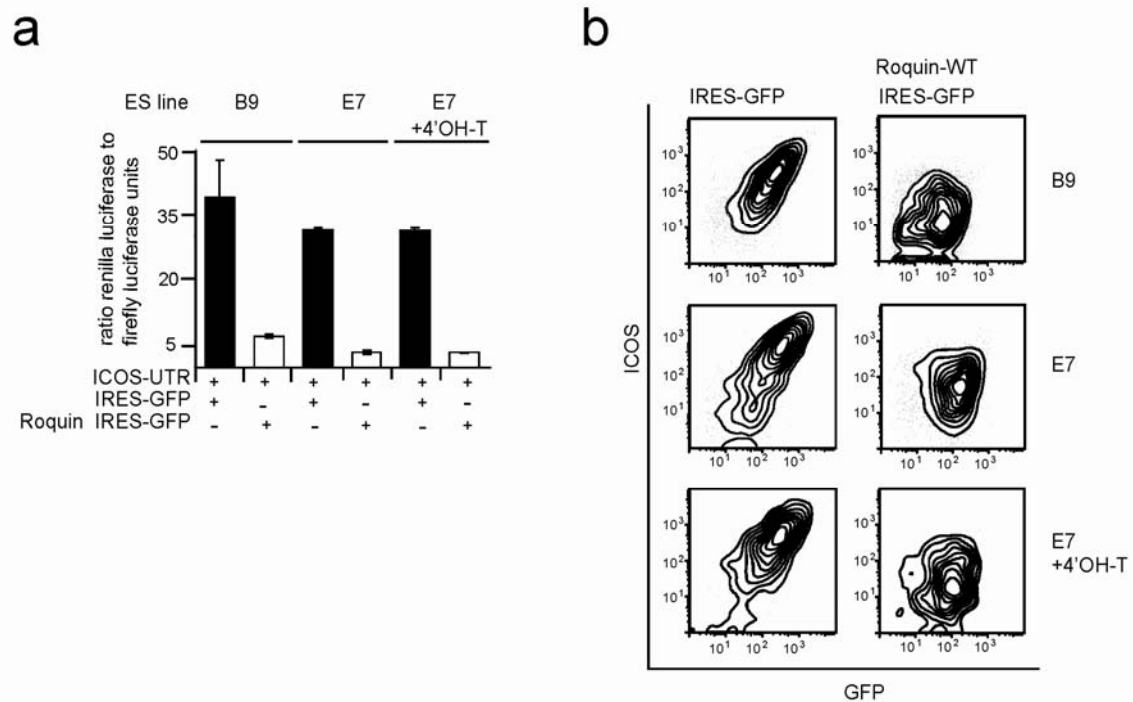
Figure 8-28: <u>Ago 1, 2, 3 and 4 proteins are not required for Roquin-mediated ICOS repression.</u> **The ES cell lines B9 and E7, or E7 treated with 4-hydroxy-tamoxifen (4'OH-T), were infected with adenoviruses that allow expression of GFP or Roquin IRES-GFP and were simultaneously co-infected with a second adenovirus that enables independent expression of renilla and firefly luciferases. The renilla luciferase open reading frame was fused to the 3'UTR of ICOS. (a) The average ratio from three independent experiments of renilla and firefly luciferase light units is shown. (b) Flow cytometric analysis showing ICOS and GFP levels of the indicated ES cell lines that were co-transduced with ICOS and Roquin-IRES-GFP or GFP encoding retroviruses.**

8.2.7 Roquin activity does not require miRNAs

Although miRNA function in the absence of Ago1-4 proteins has not been reported, a second genetic approach was carried out to rule out a requirement for miRNAs in Roquin-mediated ICOS repression. To obtain cells deficient in RNAi, Dicer-deficient MEF clones were generated (section 8.1.3). Wildtype and Dicer-deficient cells were subsequently transduced with ICOS and Roquin, or with its inactive mutant (Roquin aa 1-509). Of note, expression tests for several miRNAs by quantitative PCR revealed that miRNA levels were undetectable or more than hundredfold reduced in Dicer-deficient MEFs (Figure 8-29 a, page 81). A fraction of the same cells that were used for miRNA quantification was analyzed by flow cytometry. Roquin efficiently downregulated ICOS protein in wildtype, as well as in Dicer-

deficient cells, compared to the inactive Roquin mutant (Figure 8-29 b). To determine a possible partial contribution of miRNAs to Roquin-dependent downregulation of ICOS, ICOS levels were quantified in cells with low, intermediate or high surface expression of Thy1.1, the marker that was co-expressed with Roquin proteins from an IRES. Roquin repressed ICOS levels in Dicer wildtype and knockout cells without attenuation and in a similar dose response (Figure 8-29 c). It was previously reported that Roquin expression not only affects ICOS protein, but also mRNA levels [1]. The experiments presented here clearly demonstrate that Roquin induced a similar decay of *ICOS* mRNA in wildtype and Dicer-deficient cells (Figure 8-29 d).
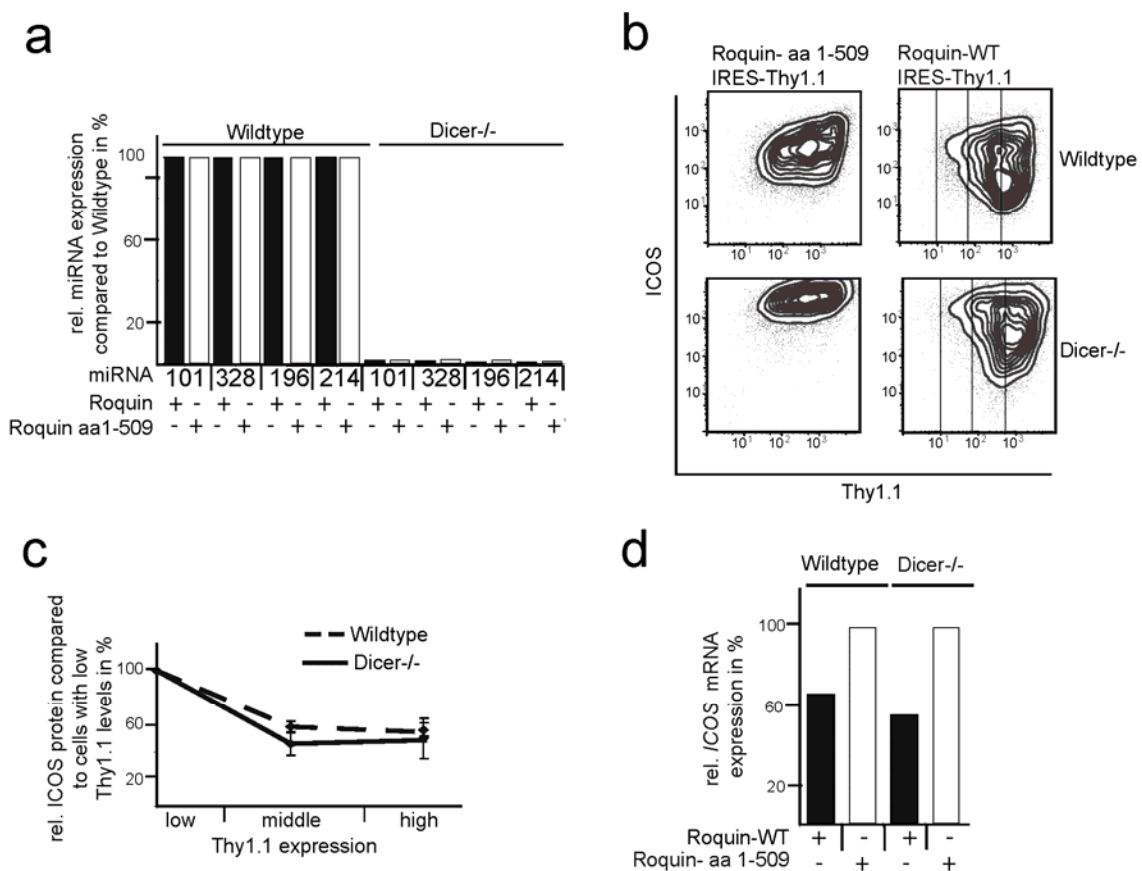

Figure 8-29: <u>Roquin activity remains unaltered in the absence of miRNAs.</u> (a-d) Dicer-/- and wildtype MEF clones were sequentially transduced with retroviruses to co-express ICOS and the indicated Roquin proteins. (a) Quantification of miRNA levels in Dicer-/- MEF cells normalized to wildtype levels. (b) Flow cytometric analysis of antibody-stained Thy1.1 and ICOS surface levels in wildtype and Dicer-/- MEF cells. (c) The average ICOS MFI is shown for middle and high Thy1.1 expressing cells, normalized to low Thy1.1 expressing cells, from three independent experiments. (D) Quantification of *ICOS* mRNA levels. All results shown in this figure are based on the same wildtype and Dicer-/- MEF cells.

To ensure that the generated Dicer-deficient cells are impaired in miRISC function the translational repression by miR-196a of the *Hoxc8* 3'UTR, a well-established target of this miRNA [126], was measured by using a dual luciferase assay. The *Hoxc8* 3'UTR was strongly repressed by co-expression of a construct encoding pre-miR-196a in wildtype, but not in Dicer-deficient cells. However, the same cells were still able to support Roquin-mediated repression through the 3'UTR of ICOS as determined by dual luciferase measurement (Figure 8-30).
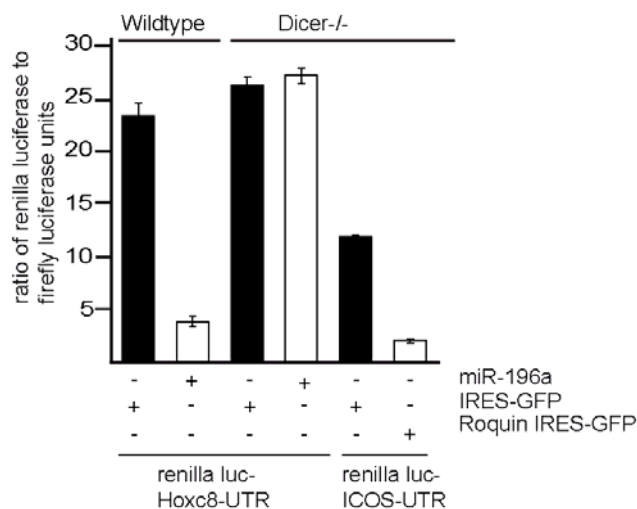

Figure 8-30: <u>Dicer deficient cells are impaired in miRNA function.</u> Wildtype and Dicer-/- MEF cells were co-transduced with GFP or miR-196 IRES-GFP and Hoxc8 3'UTR luciferase reporter adenoviruses or with GFP or Roquin IRES-GFP and ICOS 3'UTR luciferase reporter adenoviruses. The ratio of measured renilla and luciferase light units is shown.

Together, these data completely rule out a requirement for miRNAs in Roquin-mediated ICOS repression as suggested earlier. However, similar to the recent publication [1], a region in the 3'UTR of ICOS mRNA that contains the possible miR-101 recognition motif was found to contribute to Roquin-dependent ICOS repression (Figure 8-31). In fact, Roquin-mediated repression was substantially impaired, when ICOS was expressed from a construct that contained a 3'-truncated 3'UTR (ICOS bp 1-2211), which lacked the putative miR-101 binding site (Figure 8-31). Nevertheless, this truncated 3'UTR still responded to a significant extent to Roquin-induced ICOS repression (Figure 8-31), indicating a more complex regulation.
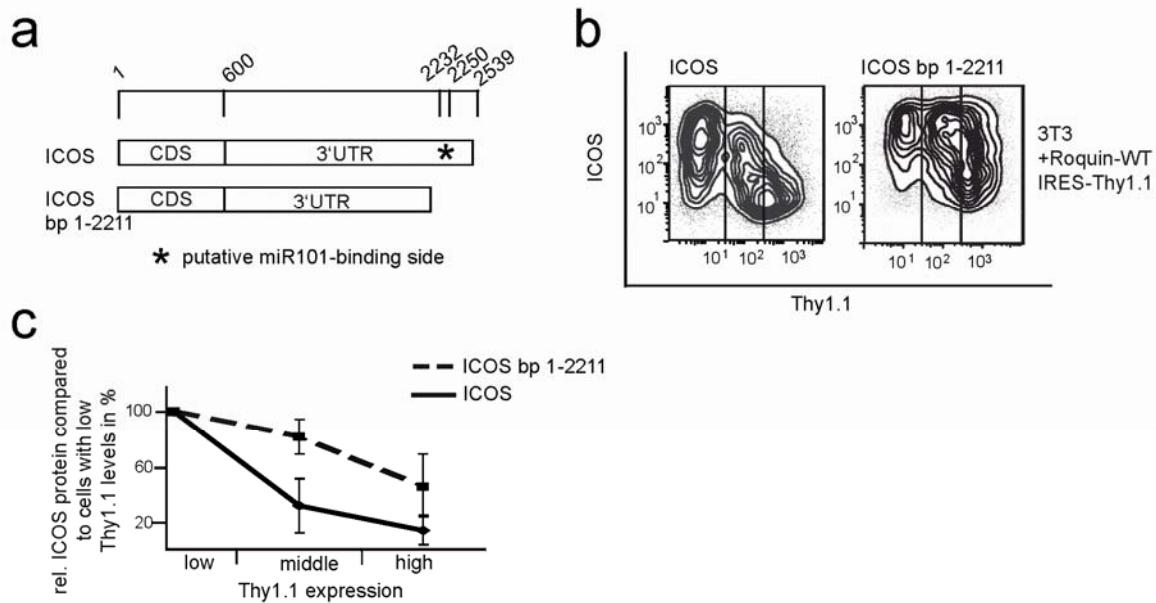
Figure 8-31: <u>A region in the 3'UTR of *ICOS* mRNA, containing the putative miR-101 binding site, is important for translational repression by Roquin.</u> (a-c) NIH3T3 cells were transduced with retroviruses encoding the full length ICOS or partial ICOS (bp 1-2211) cDNAs as depicted in (a) and superinfected with Roquin IRES-Thy1.1 retroviruses. (b) Flow cytometric analyses showing ICOS and Thy1.1 levels. (c) The average ICOS MFI is shown for middle and high Thy1.1 expressing cells, normalized to low Thy1.1 expressing cells, from three independent experiments.

8.2.8 Induced miRISC formation inhibits Roquin activity

To test whether expression of Ago2 inhibits Roquin activity due to increased Ago2 protein levels or due to an increase in miRISC formation, the previously observed effect of Ago2 overexpression was tested in wildtype and Dicer knockout cells. Overexpression of Ago2 can only induce increased miRISC formation in Dicer wildtype cells. Retroviral transduction led to a dramatic overexpression of Ago2, which was comparable in wildtype and Dicer-deficient cells (Figure 8-32 a, page 84). Furthermore it slightly changed the cellular levels of several mature miRNAs in wildtype, but not in Dicer knockout cells (Figure 8-32 c, page 84). Importantly, overexpression of Ago2 only counteracted Roquin-induced ICOS repression in wildtype (Figure 8-32 b, upper panel, compare left and right contour plots, page 84), but not in Dicer-deficient cells (Figure 8-32 b, lower panel, compare left and right contour plot, page 84).
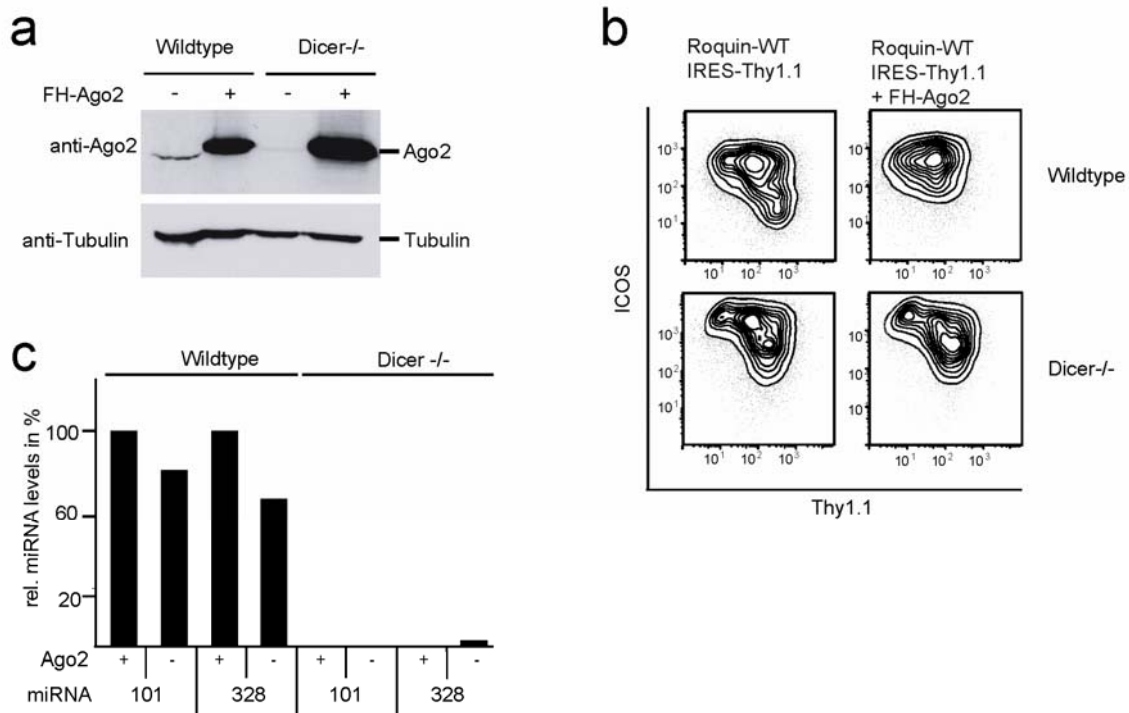
Figure 8-32: <u>Induced miRISC formation interferes with Roquin activity.</u> **Wildtype and Dicer-/- MEF cells were sequentially transduced with ICOS and Roquin together with Flaf-HA tagged Ago2. Cells were analyzed for Ago2 levels by Western blot (a), for miRNA levels by RT-PCR (c) or for Roquin-mediated ICOS repression by measuring antibody-stained ICOS and Thy1.1 surface expression by flow cytometry (b).**

Subsequently, two conserved phenylalanines of Ago2 were mutated, which have been reported to be essential for the interaction with GW182 (section 5.3.3) as well as for miRNA loading [104]. These phenylalanines were changed to valines (F470V/F505V). In contrast to wildtype Ago2, the F470V/F505V Ago2 mutant was unable to de-repress Roquin-mediated ICOS repression (Figure 8-33, page 85). The findings demonstrate that Ago2 interferes with Roquin's function, but only in the context of intact miRNA biogenesis pathway and when miRNAs can be loaded onto RISC complexes. Only when miRNAs are bound by the RISC complex, a functional interaction of Ago2 and GW182 occurs, which is essential for translational inhibition by miRNAs [127].
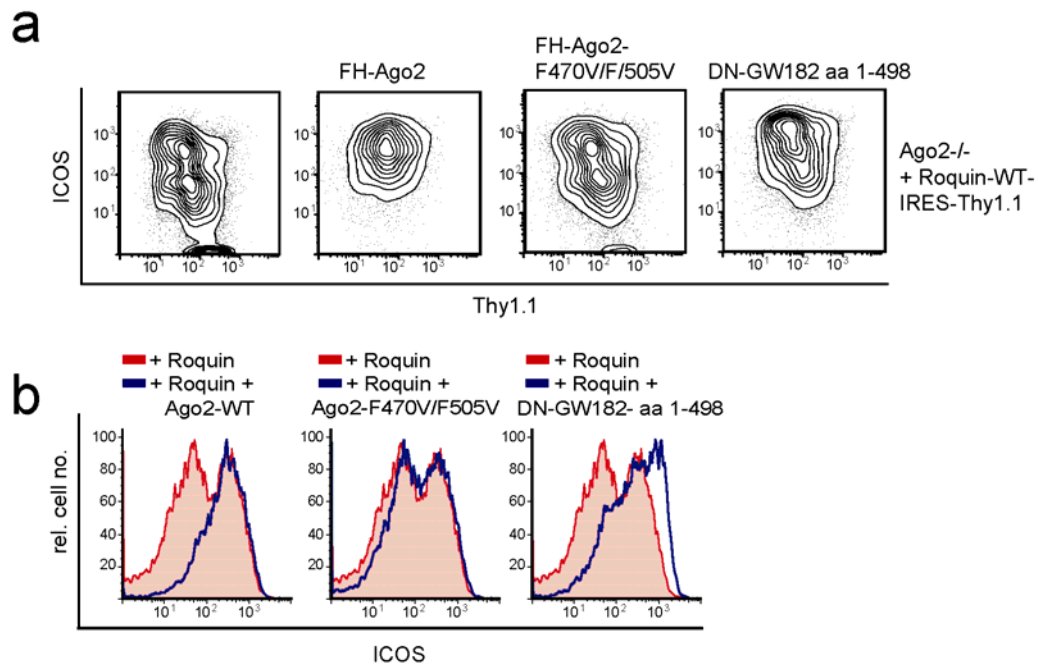
Figure 8-33: <u>**Inhibiting of GW182 function interferes with Roquin activity.**</u> **Ago2-/- MEF cells were sequentially transduced with ICOS and Roquin encoding retroviruses and superinfected with wildtype or mutant Ago2 (F470V/F505V) or dominant-negative (DN) GW182 (1-498). Flow cytometry was used to analyze ICOS and Thy1.1 expression (a) or to compare relative ICOS levels (b).**

The amino-terminus of GW182 has been shown to bind to Argonaute proteins and a carboxy-terminal truncated GW182 can function as a dominant-negative protein for the siRNA and miRNA pathway, as well as for P body formation [102, 128, 129]. Interestingly, overexpression of the dominant-negative GW182 protein (1-498) also interfered strongly with Roquin's activity and resulted in even higher ICOS levels than observed in cells in which Roquin activity was blocked by Ago2 overexpression (Figure 8-33). These results indicate that inhibition of GW182 function not only interferes with Argonaute and miRISC function, but also impairs Roquin-mediated ICOS repression. Interestingly an interaction of Roquin with Ago2 was observed (Figure 8-34, page 86). For that, HEK293T cells were transfected with constructs encoding GFP-tagged Roquin and Flag-tagged Ago2. Immunoprecipitations for GFP were afterwards treated with RNase A (section 7.4.1). Flag-tagged Ago2 co-immunoprecipitated with GFP-Roquin efficiently and in a manner that was insensitive to RNase treatment, suggesting a direct protein-protein interaction. It is tempting to speculate that the observed inhibition of Roquin activity by Ago2 overexpression is due to an interaction of the miRISC with Roquin, involving a possible mutual negative regulation.
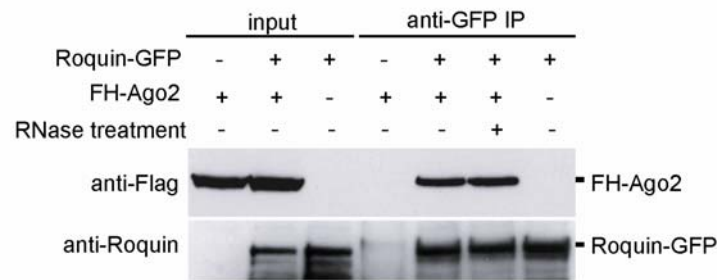
Figure 8-34: <u>Ago2 and Roquin interact in an RNA-independent manner.</u> HEK293T cells were transfected using the calcium phosphate method with constructs encoding GFP-tagged Roquin and human Flag-tagged Ago2 as indicated. Cells were lyzed and 5% of the cell lysates were loaded as input controls. Anti-GFP- immunoprecipitations were performed as described in section 7.4.1, treated with RNase A as indicated, washed and eluted from beads by boiling in SDS loading buffer.

8.2.9 Summarizing results: Parallel pathways of Roquin- or miRNA-mediated posttranscriptional gene silencing

The data presented are consistent with the following model: Roquin and miRISC posttranscriptional gene silencing are two parallel pathways that share downstream factors.

miRNAs are bound by Argonaute proteins, which are part of the miRISC complex. The loaded RISC complex can then bind to the target mRNA by complementary binding of the miRNA to recognition motifs within the 3'UTR of the target mRNA (section 5.3.3). Translocation of the target mRNA into P bodies can occur, but is not required for inhibition of translation. Nevertheless, P body components, such as GW182 and Rck, are necessary for translational inhibition by miRNAs. Lsm1, for example, is required for translation repression of approximately 5% of miRNA-targets (section 5.3.3).

The amino-terminus of Roquin is required for RNA binding and can be functionally replaced by conserved sequences from Roquin's paralog MNAB (section 8.2.2). The carboxy-terminus mediates P body localization and has specialized in Roquin for efficient repression of ICOS (section 8.2.3). Roquin does neither require miRNAs nor Argonaute proteins for translational inhibition of ICOS (sections 8.2.6 and 8.2.7) but depends on the P body components Rck, GW182 and Lsm1 (section 8.2.4 and 8.2.8). Enhanced miRISC function thereby may inhibit Roquin activity (section 8.2.8) through competition of Roquin and the miRISC for common factors like Rck, GW182 and Lsm1 (section 8.2.4), possibly by direct inhibition and interaction with Argonaute 2.
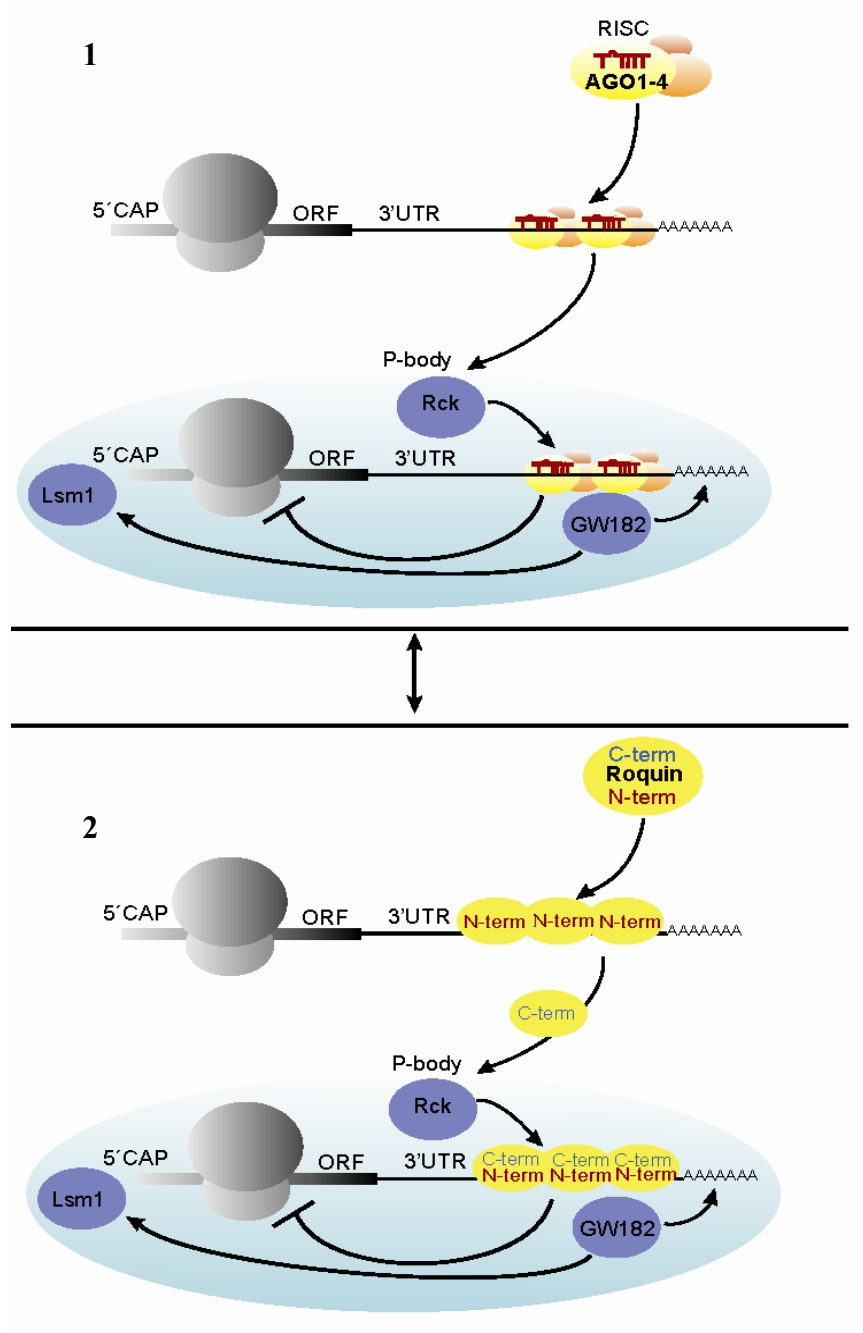
Figure 8-35 : <u>Schematic representation of translation repression by (1) miRNAs and by (2) Roquin.</u> (1) miRNAs and proteins of the miRNA pathway are specialized *trans*-acting factors (section 5.3.1). Argonaute proteins can bind with the help of miRNAs to mRNAs, which causes translational repression and mRNA instability. P body components, such as Lsm1, Rck and GW182, have been demonstrated to play a role in miRNA-dependent translational repression. (2) Roquin can also bind to mRNA via its amino-terminal ROQ domain. The carboxy-terminal regions within Roquin specify its localization to P bodies. Certain P body components, such as Rck, GW182 and Lsm1 are required for full activity of Roquin. Roquin-mediated repression does not require miRNAs and Argonaute proteins, but is inhibited through experimentally induced miRISC formation.

9 Discussion

9.1 *Molecular mechanism of Roquin-mediated ICOS repression*

This thesis demonstrates the molecular mechanism of Roquin-mediated ICOS repression and reveals Roquin as a *trans*-acting factor for ICOS expression. The key experiments and results that are presented in here and lead to this model, will be discussed in this section. Some important follow-up experiments will be proposed.

9.1.1 Roquin binds to *ICOS mRNA*

Testing the hypothesis that Roquin could bind *ICOS* mRNA, we find that mRNA binding is actually one critical part of the molecular mechanism by which Roquin represses ICOS. The fact that Roquin protein and *ICOS* mRNA can be crosslinked in intact cells suggests that Roquin is in direct physical contact with RNA (Figure 8-22). Additionally, endogenous mouse *ICOS* mRNA can be detected in immunoprecipitations of endogenous Roquin from T cell extracts (Figure 8-23). Binding to RNA has been described for CCCH-type zinc finger proteins, such as TTP and Zc3h12a (section 5.3.1). However, this thesis demonstrates that Roquin binds primarily via its ROQ domain to *ICOS* mRNA (Figure 8-24). This conclusion arose from our GFP-immunoprecipitations with GFP-tagged deletion-mutants of Roquin, which produced reliable results. It remained a technical challenge to estimate the exact contribution of the other amino-terminal domains to RNA binding, because point-mutated Roquin constructs were cloned without a GFP-tag, and immunoprecipitations with an antibody against Roquin were weaker and therefore more variable. Nevertheless, we propose that Roquin binds to RNA through a protein surface that is composed of the ROQ domain and additional domains such as the zinc finger or even RING finger, because point-mutations in these domains impaired ICOS repression (Figure 8-10 and Figure 8-25). Such a novel mode of interaction with RNA is supported by an earlier report showing that individual mutation of two cysteines in the zinc finger of the paralog MNAB did not abolish, but rather reduced binding of MNAB to DNA [114]. Further support for a composite interaction of the ROQ and zinc finger domains with RNA comes from data demonstrating that the TTP protein cannot bind to RNA when only one of its two tandem CCCH-type zinc fingers is intact [70].

Similarly, it was reported that Zc3h12a requires a composition of its CCCH-type zinc finger and its amino-terminal adjacent so-called PIN domain to promote degradation of RNA [115]. Currently, we cannot exclude the possibilty that Roquin is a general RNA-binding protein without recognizing a specific *cis*-element in *ICOS* mRNA (section 9.1.2), because we can also see that house keeping genes, such as Hprt1, are also bound by Roquin in immunoprecipitation experiments. However, *ICOS* mRNA was always significantly more enriched in these experiments (data not shown).

Still, our data suggest that the Roquin M199R mutation, which is located within the ROQ domain and causes autoimmunity in *san/san* mice [2], might decrease the ability of Roquin to bind to mouse *ICOS* mRNA. We can indeed confirm that the M199R mutation decreases the ability of Roquin to downregulate ICOS protein in T cells (Figure 8-12), as reported earlier [1]. However, we could not yet demonstrate that the M199R mutant has a decreased ability to bind to *ICOS* mRNA, which would be a very attractive way to explain the autoimmune phenotype of *san/san* mice.

9.1.2   Roquin represses ICOS through its 3'UTR

Trans-acting factors recognize sequence motifs or secondary structures in the mRNAs they regulate (section 5.3.1). Our data together with previously published results show that Roquin's function is dependent on the 3'UTR of ICOS and is independent of the remainder of the mRNA (section 8.2.1). First, we confirmed that Roquin represses ICOS through the 3'UTR and that Roquin overexpression promotes *ICOS* mRNA decay (Figure 8-6), as proposed earlier [1]. Second, we demonstrated that Roquin overexpression led to downregulation of the reporter genes GFP, human CD4 and renilla luciferase in the context of the ICOS 3'UTR (Figure 8-7 and Figure 8-8). The fact that the repression of Roquin was weaker for constructs that contained the GFP or human CD4 coding region than for the construct that contained the ICOS coding region, could indicate that regions within the coding region of ICOS are actually supportive for the repression of ICOS. However, we believe that the differences are most likely due to differences in translation rates or protein stability. In addition, we can report that Roquin does not repress ICOS via inhibition of 5'CAP-dependent translation (Figure 8-9). This could indicate that mRNA decay is the major mechanism of repression or that translation is inhibited in a different way. Although decapping activators can promote mRNA decay, deadenylation is the first step in the decay of many mRNAs (section 5.3.1). Experiments confirming that Roquin downregulates ICOS by promoting

deadenylation of the mRNA are still missing. Therefore, Roquin could still promote ICOS translational repression and mRNA decay in a different way. For instance, we did not experimentally exclude the possibility that Roquin is an RNase that bears intrinsic RNA degrading activity. However, this seems unlikely, since Roquin actually requires additional factors for the repression of ICOS (section 8.2.4).

It has not been addressed in the scope of this thesis which cis-element in the 3'UTR of ICOS mRNA Roquin recognizes. It was proposed that Roquin directly or indirectly recognizes a miRNA-101 binding site within the 3'UTR of ICOS [1]. Therefore, we tested Roquin activity in Dicer- and Ago1-4-deficient cells by co-expressing Roquin with full-length ICOS. The results from these experiments rule out a necessity for miRNAs in Roquin-mediated translational repression of ICOS (section 8.2.6 and 8.2.7). Vinuesa and colleagues proposed an involvement of miRNAs based on experiments in which they already had a strong decline in the efficiency of Roquin-mediated repression for a reporter gene in the context of a minimal response element [1]. Actually, we can confirm that deletion of a region that contained the minimal response element caused a substantial, yet incomplete, impairment of Roquin-mediated ICOS downregulation (Figure 8-31). This minimal response element, identified by Vinuesa and colleagues, does not contain any known cis-elements. For example, three AUUUA pentamers, which could be classified as AREs (section 5.3.1), are located at other positions within the 3'UTR of ICOS. It is not clear whether these can act as additional cis-elements for Roquin-mediated ICOS silencing or whether Roquin even recognizes a novel cis-element within the ICOS 3'UTR. We assume that ICOS repression is not controlled by one single cis-element, but rather by a combination of cis-elements within the 3'UTR, which could be recognized by Roquin and so-far unknown Roquin interaction partners. This hypothesis receives is supported by the deletion-mutagenesis of the ICOS 3'UTR which, in our hands, indicated to a contribution of different regions of the 3'UTR of ICOS to Roquin-mediated repression (Figure 8-31). Most likely, ICOS mRNA is regulated in a complex way and is incorporated into messenger ribonucleoproteins, which are committed to translational repression or RNA degradation. Therefore, it cannot be excluded that a shared component of miRISC- and Roquin-mediated posttranscriptional gene silencing could yield in a positive cooperation, but only in the context of the minimal response element. We believe that Roquin-mediated ICOS repression cannot be analyzed as previously described by Vinuesa and colleagues using a reporter gene fused to a minimal response element. The question, which *cis*-element is recognized by Roquin, should be addressed systematically through point-mutagenesis in the context of full-length *ICOS* mRNA.

9.1.3 Roquin requires the P body components Rck and Lsm1 for translational repression of ICOS

Many proteins involved in mRNA decay are functionally linked by the use of common factors and physically linked by co-localization to cytoplasmic foci, so-called P bodies (section 5.3.2). We found that this is also true for Roquin by demonstrating that Roquin functionally requires the helicase Rck and decapping activator Lsm1 (Figure 8-21) and localizes to P bodies (section 8.2.3). This section will discuss the experiments which were accomplished in that context.

First, we tested and confirmed the proposed localization of Roquin to stress granules [2] (Figure 8-16). Similarly to Roquin, other trans-acting factors can also localize to stress granules [76]. Stress granules form by the aggregation of TIA-1 proteins that leads to translational inhibition of a distinct set of mRNAs (section 5.3.2). In this respect it should be noted, that the functional requirement for a TIA-1-mediated stress response for many trans-acting factors that localize to stress granules has not been analyzed in prior publications. However, MEF cells deficient for TIA-1 have been shown to be impaired in stress granule assembly [123]. Therefore, we tested Roquin-mediated ICOS repression in TIA-1 knockout MEF cells in section 8.2.3 and excluded a functional requirement of TIA-1-mediated stress response for Roquin activity. The findings indicated that a cellular stress response may not be required for Roquin-mediated ICOS-regulation. Therefore, we analyzed Roquin localization in the absence of cellular stress and found that Roquin co-localizes with Rck and Ago2 (Figure 8-14), two proteins described to localize to P bodies (section 5.3.2). Studies of deletion-mutants of Roquin identified the carboxy-terminal regions to be essential for the Roquin-specific localization pattern (Figure 8-18) and to be essential for Roquin-mediated ICOS repression (Figure 8-19). This indicates that the P body localization is crucial for Roquin activity. P bodies are cytoplasmic regions, which are enriched in translationally inactive mRNAs and proteins that are essential for translational repression (section 8.2.3). The carboxy-terminus of Roquin might facilitate the formation of aggregates of Roquin together with proteins that localize to P bodies. Glutamine stretches can act as polar zippers in prion proteins [130]. An increased content of glutamine and asparagine (Q/N) residues is present in 20 different P body components, as detected in frames of 80 amino acids [131]. It is possible that these Q/N-rich regions, which typically occur adjacent to proline-rich regions, will influence protein/protein interactions between proteins that consist of Q/N-rich regions. Intriguingly, the carboxy-terminus of Roquin contains frames of 80 amino acids that are

moderately enriched in Q/N residues. These frames are located adjacent to the proline-rich region and reach a maximum content of 17 Q/N residues in mouse Roquin, with 7.68 as the predicted average. This observation raised the question, whether Roquin is functionally dependent on P body components. Therefore, a knockdown directed against the two P body components Lsm1 and Rck was established (Figure 8-20). Roquin-mediated ICOS repression was impaired in cells with reduced levels of Rck and Lsm1 (Figure 8-21). Knockdown of Rck caused a complete block of Roquin-dependent ICOS repression. However, knockdown of Lsm1, inhibited only partially Roquin activity. As we do not have access to an antibody that recognizes Lsm1, we cannot exclude that the different functional impact of Lsm1 and Rck knockdown can reflect a weaker knockdown of the Lsm1 compared to the Rck protein. On the other hand, these findings could also indicate that Lsm1 has only a partial contribution in Roquin-mediated ICOS repression. The Lsm1-7 protein complex is involved in mRNA decay by decapping, in which it recognizes oligo-adenylated mRNAs that appear after de-adenylation of poly-adenylated mRNAs [63, 106]. Rck has also a critical role in mRNA decay, but it is also required for mRNA protein complex remodeling for entry into translation repression, storage or decay (section 5.3.1). The strong impairment of Roquin-dependent ICOS downregulation in the knockdown of Rck may therefore indicate that Roquin, in addition to promoting ICOS mRNA decay, also causes translational repression. Rck and Lsm1 knockdowns has been shown previously to inhibit P body formation [106]. Whether the knockdown of Lsm1 and Rck in these experiments also caused inhibition of P body formation or changed Roquin localization, has not been tested here. Therefore, it is not clear yet if Roquin-dependent repression requires intact P bodies or just requires components that also localize to P bodies. Additionally, it would be interesting to test whether overexpression of Roquin itself leads to the formation of P bodies.

9.1.4 Roquin acts parallel to the miRNA pathway

Although it was suggested that miRNAs are involved in Roquin-mediated ICOS repression [1], we did not find evidence for an involvement of the miRISC (section 8.2.6 and 8.2.7). In contrast, experimental induction of miRISC formation was a strong inhibitor for Roquin-mediated ICOS repression (section 8.2.8). Ago2 overexpression has been demonstrated to promote miRNA processing [132] and to cause increased functioning of cellular RNAi pathways [133]. Intriguingly, overexpression of Ago2 had a negative effect on Roquin function (Figure 8-27). This effect was not observed in Dicer-deficient cells that are impaired

in miRNA biogenesis and therefore miRISC formation (Figure 8-32). The observed inhibition of Ago2 overexpression on Roquin activity could be due to the following three reasons: First, Roquin and Ago2 compete for the substrate, the ICOS mRNA, but Ago2 can only bind to the target mRNA, when miRNAs are bound [104]. Actually, Vinuesa and colleagues demonstrated that overexpressed miRNAs can trigger decay of endogenous ICOS mRNA [1]. Therefore, it remains possible that ICOS levels are not only controlled by Roquin but also by the miRNA pathway. However, the pathways do not cooperate as we demonstrate in section 8.2.6 and 8.2.7. Second, Roquin and Ago2 could compete for functional interaction with common downstream factors, such as the P body factor Rck, which is required for Roquin- (Figure 8-21) as well as miRNA-dependent translational inhibition [106]. Third, Roquin and Ago2 could compete for the direct interaction partner of Ago2, which is GW182. This scenario receives support from the observation that Roquin activity was also impaired through introduction of a dominant-negative version of GW182 (Figure 8-33), and from the fact that Ago2 can only bind to GW182 in the context of bound miRNAs [104], which could also explain why Ago2 overexpression has no effect on Roquin activity in Dicer-deficient cells. In this case, the binding site of Roquin on the protein surface of GW182 should be in close proximity to the binding site for Ago2, since the dominant-negative version of GW182 contains only the amino-terminal region of GW182 that binds Argonaute proteins. An interaction of Roquin with this region of GW182 has not been confirmed yet due to technical difficulties of GW182 detection in immunoblots. Unexpectedly, an interaction of Roquin with Ago2 was revealed in our immunoprecipitation experiments (Figure 8-34). Although the reason for the interaction between Roquin and Ago2 remains unclear, the interaction of both proteins indicates that they are functionally connected, a link that may rather involve negative regulation, as presented in this thesis (section 8.2.9). It is tempting to speculate that the negative regulation could also be mutual. For example, Ago2 could represent a target of Roquin-mediated ubiquitination. The negative regulation of miRISC formation on Roquin-mediated ICOS repression has so far only been observed in an experimentally-induced situation. It appears likely that miRISC activity is subject to physiologic regulation which so far has not been described. Nevertheless, our findings provide a first example of regulated Roquin activity.

9.2   Placing this work into context

9.2.1   Differences to previous publications

Previously, it has been suggested that miRNAs are involved in the repression of ARE-containing mRNAs through the *trans*-acting factor TTP, as well as in the molecular mechanism by which Roquin silences ICOS [112]. However, it has not been clarified in these reports how and at which stage TTP or Roquin cooperate with the miRNA pathway. It is possible that many translational repression pathways overlap [111], but often they have just been poorly separated from another in publications. We report a genetic "dissection" of Roquin function from the miRNA pathway and demonstrate that Roquin, instead of using miRNAs to select its target mRNA, binds itself to RNA and is a novel trans-acting factor. We can even report a negative influence of miRISC formation on Roquin activity (section 8.2.8). We are convinced that the previously described dependence of Roquin on miRNAs for the recognition of the ICOS mRNA arose from the use of a minimal response element. This short 47bp element was expressed in the context of a reporter and, as we suspect, exhibited aberrant regulation. Therefore, we aimed to re-investigate the *cis*-elements for Roquin-mediated repression combining initial deletion analysis with point-mutagenesis of the full length ICOS 3'UTR. We did not yet extent our investigation to the proposed cooperation of TTP with the miRNA pathway, which should be easily accomplished now using the established experimental set-up.

Another difference to a previous report [2] is our finding that Roquin represses ICOS TIA-1-independently (Figure 8-17). TIA-1 knockout cells have been shown to be impaired in stress granule formation [123] and Vinuesa and colleagues suggested a model in which Roquin regulated *ICOS* mRNA via co-localization of Roquin and ICOS RNA in stress granules leading to miRNA-induced export of ICOS mRNA into P bodies [1]. We cannot exclude the possibility that Roquin acts in an undiscovered stress pathway that is independent of TIA-1. However, we consider this unlikely since we show that Roquin-dependent ICOS repression depends on factors important for P body formation and function (section 8.2.4). We think that the localization of Roquin to stress granules that we confirmed could be due to the relocalization of an interaction partner of Roquin that, upon stress, translocates into stress granules and may be necessary for the regulation of other targets. Actually, many other *trans*-acting factors, including TTP, have been shown to localize to stress granules (section 5.3.2), but the requirement for TIA-1 by these *trans*-acting factors has not been analyzed to date.

Nevertheless, our data do not exclude a stress-responsive regulation of ICOS through Roquin, which might occur during the so-called integrated stress response. This response appears to be TIA-1-mediated and inhibits interleukin-4 translation but not transcription during the first antigen-encounter of a naïve CD4 T cell and is relieved upon restimulation of the effector T cells [88].

Taken together the differences to previous publications mostly affect the concept of the molecular mechanism of Roquin-mediated ICOS repression. This concept is currently forming and therefore requires continuous adjustments before a full understanding has been obtained.

9.2.2 Implications for MNAB

Mouse MNAB and mouse Roquin are two highly homologues proteins with an amino acid identity of 72 % in the amino-terminal domains (Figure 6-3), indicating that these proteins could exert similar functions. Only one previous report about human MNAB can be found in the literature, describing MNAB as membrane-associated nucleic acid binding protein [114]. We were curious, whether MNAB, similar to Roquin, can also repress ICOS in T cells. The data presented here show that ICOS levels remain largely unaffected by overexpression of MNAB in CD4 T cells (Figure 8-12 a). However, we discovered that a chimera consisting of the carboxy-terminus of Roquin and the amino-terminus of MNAB is able to downregulate ICOS (Figure 8-13). This indicates that MNAB might also function as a translational repressor for other mRNAs, with a range of targets that is probably not restricted to *ICOS* mRNA. We show that the amino-terminus of Roquin can bind to *ICOS* mRNA, the part that is highly homologues to MNAB. In support of this notion, MNAB has been reported to bind to DNA *in vitro* [114]. Therefore, we would expect that MNAB also binds to *ICOS* mRNA. It would be very interesting now to identify mRNA targets of MNAB and to confirm that MNAB can repress their translation. MNAB and Roquin share only amino acid 34 % identity in the carboxy-terminal regions and our experiments confirm that Roquin's carboxy-terminus has evolved for efficient ICOS repression. Localization studies demonstrate that the carboxy-terminus determines Roquin localization to P bodies (Figure 8-18). We were curious whether MNAB can also localize to P bodies or whether this is unique for Roquin. MNAB was described to localize to cytoplasmic spots, but it was suggested that these are ER-associated [114]. Here, we report co-localization of MNAB and Roquin, indicating that MNAB localizes to P bodies, too (Figure 8-15). However, MNAB seems to be more diffusely

distributed in the cytoplasm. Whether this difference, which still has to be studied more intensively, can explain why Roquin is more efficient in ICOS repression, is unclear at this point. Roquin could also have higher activity due to other reasons, for example by binding to different interacting partners. The co-localization of MNAB and Roquin could also indicate that these highly homologues proteins interact with each other. Interestingly, they show similar mRNA expression in several lymphoid organs (Figure 8-11 b), but with higher protein expression of MNAB, at least in thymi (Figure 8-11 a). It would be interesting to test whether Roquin and MNAB interact and whether both proteins cooperate.

In summary, the here presented localization of MNAB and its possible RNA-binding activity strongly imply that MNAB could also be a *trans*-acting factor, which might be more efficient in a similar pathway of repression in other cell types or by acting on different targets than *ICOS* mRNA.

9.2.3   Importance of the results for autoimmune diseases

In this study, experimental proof is presented that excludes the requirement or even the contribution of miRNAs in Roquin-mediated ICOS repression. We have reached these conclusions due to experiments that analyzed Roquin-mediated repression of full-length *ICOS* mRNA and on the basis of genetic evidence.

Roquin function is critical in follicular helper T (T_{FH}) cells to prevent T cell help to self-reactive B cells and to suppress the production of autoantibodies. In fact, a single point-mutation in Roquin has been shown to cause systemic lupus erythematosus-like disease in homozygous mice. An earlier publication by Yu and colleagues [1] implicated that autoantibody production in lupus-like disease was under the control of miRNAs and suggested that Roquin has to cooperate with the miRISC in T_{FH} cells to silence ICOS. These conclusions promote the idea that miRNA-targeting of ICOS should allow for new future therapies [1]. Consequently, our demonstration that Roquin is a *trans*-acting factor that binds to *ICOS* mRNA without the contribution of miRNAs will be enlightening for ongoing applied research and may help to adjust strategies of therapeutic intervention in systemic lupus erythematosus.

9.3   *Outlook and future directions*

9.3.1   Identification of the Roquin-bound *cis*-element

Our data demonstrate that *ICOS* mRNA binding by Roquin is essential for its repression by Roquin. Although we identified domains within Roquin that bind to *ICOS* mRNA (section 8.2.5), we could not identify the bound element within the *ICOS* mRNA. In principal, it should be possible to uncover the *cis*-element that is recognized by Roquin through a systematic deletion-mutagenesis of the 3'UTR of ICOS coupled with functional and RNA-binding assays. Because we speculate that Roquin might recognizes more than one *cis*-element within the *ICOS* 3'UTR (section 9.1.2) and that ICOS is more likely regulated in a complex way, it may be more promising to first identify additional targets of Roquin in a whole-genome approach (section 9.3.3). Bioinformatic comparison of target 3'UTR may then reveal common *cis*-acting elements, which can thereafter be experimentally confirmed (section 9.3.3).

9.3.2   Role of the RING finger domain in Roquin and MNAB.

The evolutionary conservation of the RING finger domain in MNAB and Roquin suggests that these proteins could regulate target protein levels via E3 ubiquitin ligase activity (section 5.3). To address the role of the RING finger in Roquin we deleted the whole domain or point-mutated critical cysteines in the RING finger, and tested the importance of the RING finger for Roquin-mediated ICOS repression. For both mutants a reduced activity to downregulate ICOS was observed, as compared to Roquin wildtype (Figure 8-10). These results indicate that the RING finger helps to reach the full extent of translational inhibition of ICOS, but is not essential. Other E3 ubiquitin ligases, like Cbl-b, Itch and Grail, which are also involved in the control of immune reactivity against self-antigens, critically depend on their intact RING fingers or HECT domains [26]. In this respect, Roquin appears to differ from these proteins that are thought to entirely depend on their E3 ligase activity ubiquitinylating proteins to target them for degradation [25, 120, 121]. However, it has not been resolved in the framework of this thesis whether the partial contribution of the RING finger of Roquin results from E3 ligase activity or other possible functions of the RING finger. The fact that Roquin did not show autoubiquitination *in vivo* ubiquitination assays [134] (data not shown) indicates that the RING finger of Roquin might not exert E3 ubiquitin ligase activity, or

cannot be detected by autoubiquitination in cells. However, it is also possible that the RING finger is involved in an unanticipated molecular function. There are previous reports documenting molecular functions for RING domains other than E3 ubiquitin ligase activity. For instance, RING domains have been described to fulfill a function in the assembly of macromolecular structures [135, 136]. This function seems unlikely to apply to the RING domain of Roquin. Although Roquin appears to be part of macromolecular structures in P bodies, as seen by confocal microscopy (Figure 8-14) we showed that deletion of the RING finger domain did not change the Roquin-specific punctate pattern (Figure 8-18). Another report stated that the RING domain of PML can repress 5'CAP-dependent translation by direct inhibition of the translation initiation factor eIF4E [137]. This function also seems unlikely to hold true for the RING finger domain of Roquin, since we can show that at least one function of Roquin, namely Roquin-mediated ICOS repression, is independent of 5'CAP-dependent translation (Figure 8-9). Finally, the observed small negative effect of RING finger deletion on Roquin binding to *ICOS* mRNA could be interpreted such that the RING is one of the domains that contribute to a composite surface of the RING finger, ROQ domain and zinc finger that together bind to RNA.

9.3.3 Which other mRNA targets are regulated by Roquin?

Differential gene regulation has been determined for CD4 T cells derived from *san/san* and wildtype mice [2]. However, this and later publications [19, 23] demonstrate that expression of the M199R mutant of Roquin in *san/san* mice predominantly changed the activation status of CD4 T cells towards activation and furthermore shifted the percentage of helper T cell subsets by favoring the T_{FH} cell phenotype. It was just recently discovered in three publications that the transcription factor Bcl-6 is important for T_{FH} cells. It was shown that Bcl-6 is necessary and sufficient for *in vivo* differentiation of T_{FH} cells [138], is required for programming T_{FH} cell generation [139] and directs follicular T helper cell lineage commitment [140]. Furthermore, *Bcl-6* mRNA has a relative long 3'UTR (1600 bp for transcript variant 2 in human). Therefore, *Bcl-6* mRNA is a promising candidate for Roquin regulation. However, whether *Bcl-6* mRNA or other deregulated mRNAs in san/san mice are direct targets of Roquin regulation will have to be verified experimentally. Vinuesa and colleagues reported that *neuropilin 1* mRNA was downregulated upon Roquin overexpression [1] and that *IL-2* mRNA expression is higher in *san/san* CD28 -/- mice than in Roquin wildtype CD28-/- mice. This indicates that *IL-2* mRNA might also be a target of Roquin.

We can report additionally that overexpression of Roquin in T cells negatively effects IL-2 and CD40L protein expression after restimulation (data not shown). We did not test mRNA levels in these experiments and cannot exclude that these are indirect downstream effects of Roquin-mediated repression of ICOS or T cell differentiation. A global approach to analyze mRNAs in cells with short-term ectopic over-expression of Roquin in activated follicular helper T cells should be performed in order to measure differential expression of direct mRNA targets.

9.3.4   Which other proteins cooperate in Roquin mediated-translational repression?

Since many *trans*-acting factors exert their function via interaction with the general mRNA decay machinery (section 0), we have to assume that Roquin, in addition to Rck and Lsm1, also requires other factors involved in mRNA decay for the repression of ICOS. Another *trans*-acting factor that exerts gene-specific regulation and that has been well studied, is TTP. TTP requires Lsm1 for its activity, similar to Roquin. In addition, TTP has been shown to interact with CCR4 (a component of the CCR4-Not deadenylation complex), with DCP2 (a component of the DCP1:DCP2 decapping complex) and the 5'-3' exonuclease XrnI [75]. Therefore, it is very likely that also Roquin requires factors that can promote either deadenylation or decapping of mRNAs and thereby assist in ICOS repression. It would therefore be of great interest to identify Roquin associated factors that participate in translational repression and thus also play a role in the prevention of autoimmunity.

9.3.5   How is Roquin activity regulated?

We find that induced miRISC formation interferes with Roquin-mediated ICOS repression (section 8.2.8). ICOS levels have to be tightly regulated in order to prevent reactivity against self (section 5.2). It is therefore interesting to study the mechanisms by which miRISC formation interferes with Roquin activity. Although miRISC formation appears to be a constitutive process, globally decreased levels of mature miRNAs have been reported in the development of cancer [141]. In addition, Roquin activity could be altered by modification of Roquin itself. This could be achieved for example through phosphorylation of Roquin. In support of this hypothesis, Roquin has been identified in a large-scale phosphorylation analysis of mouse liver [142]. The analysis identified Roquin-peptides phosphorylated at the

amino acid positions 1107 and 1110 in the protein. Phosphorylation of Roquin could therefore be one way to either activate or inactivate the protein. Phosphorylation could alter a binding site for interacting proteins or lead to induced degradation or prevent destruction of Roquin and thereby affect ICOS levels.

10 Conclusion

The interest in Roquin was sparked amongst immunologists and molecular biologists after it had been suggested that Roquin cooperates with miRNAs to regulate ICOS [1]. This regulation is essential for the prevention of autoimmune diseases [2]. This thesis uncovers that Roquin does not cooperate with the miRNA pathway to repress ICOS. Instead, we propose a model in which Roquin-mediated repression is parallel to posttranscriptional gene silencing by miRNAs. Our evidence includes the new findings that induced miRISC formation inhibits Roquin activity and that Roquin and Ago2 interact with each other. Furthermore, we demonstrate that Roquin binds *ICOS* mRNA, localizes to P bodies and requires P body factors for its function. These characteristics are in common with miRNAs during posttranscriptional gene silencing.

We discover that the newly defined ROQ domain of Roquin is a novel RNA-binding domain, by showing that it is essential for *ICOS* mRNA binding.

The Roquin protein was only recently discovered and research concerning its molecular mechanism is still in its infancy. Revealing the mechanism by which Roquin represses ICOS makes a contribution to our understanding of posttranscriptional gene regulation and may enable future identification of target structures for therapeutic intervention in autoimmune diseases.

11 Contributions and acknowledgments

Monoclonal antibodies against mouse Roquin and MNAB, as described in section 6.1, were produced in collaboration with Elisabeth Kremmer's group.

Carola Vinuesa, Steven Hefeneider and Gunter Meister kindly provided vectors for PCR amplification of Roquin, ICOS, MNAB and Argonaute 2 (section 6.3).

Greg Hannon kindly provided MEFs cells deficient in Ago2, and Nancy Kedersha and Paul Anderson provided MEFs cells deficient in TIA-1. ES cells deficient in mouse Ago 1, 3, 4 or Ago1-4 were obtained in collaboration from Xiaozhong Wang.

Ernesto Merino inserted the knockdown sequence for mouse CD4 into a modified pSuper-retroviral vector.

Dicer fl/fl mice were obtained from Greg Hannon and CD4 Cre mice, for breeding in, were acquired from Ursula Strobl.

12 Literature

1. Yu, D., et al., *Roquin represses autoimmunity by limiting inducible T-cell co-stimulator messenger RNA*. Nature, 2007. **450**(7167): p. 299-303.
2. Vinuesa, C.G., et al., *A RING-type ubiquitin ligase family member required to repress follicular helper T cells and autoimmunity*. Nature, 2005. **435**(7041): p. 452-8.
3. Walker, E.J., et al., *CTLA4/ICOS gene variants and haplotypes are associated with rheumatoid arthritis and primary biliary cirrhosis in the Canadian population*. Arthritis Rheum, 2009. **60**(4): p. 931-7.
4. Takahashi, N., et al., *Impaired CD4 and CD8 effector function and decreased memory T cell populations in ICOS-deficient patients*. J Immunol, 2009. **182**(9): p. 5515-27.
5. Ihara, K., et al., *Association studies of CTLA-4, CD28, and ICOS gene polymorphisms with type 1 diabetes in the Japanese population*. Immunogenetics, 2001. **53**(6): p. 447-54.
6. Vinuesa, C.G. and M.C. Cook, *Genetic analysis of systemic autoimmunity*. Novartis Found Symp, 2007. **281**: p. 103-20; discussion 120-8, 208-9.
7. Janeway, C.A., Travers, P., Walport, M., Shlomchik, M., *IMMUNOBIOLOGY, the immune system in health and disease*. Garland Science Publishing. Vol. 6th edition. 2005.
8. Jacobson, D.L., et al., *Epidemiology and estimated population burden of selected autoimmune diseases in the United States*. Clin Immunol Immunopathol, 1997. **84**(3): p. 223-43.
9. Goodnow, C.C., et al., *Cellular and genetic mechanisms of self tolerance and autoimmunity*. Nature, 2005. **435**(7042): p. 590-7.
10. Greenwald, R.J., G.J. Freeman, and A.H. Sharpe, *The B7 family revisited*. Annu Rev Immunol, 2005. **23**: p. 515-48.
11. Vinuesa, C.G., et al., *Follicular B helper T cells in antibody responses and autoimmunity*. Nat Rev Immunol, 2005. **5**(11): p. 853-65.
12. Nemazee, D. and K.A. Hogquist, *Antigen receptor selection by editing or downregulation of V(D)J recombination*. Curr Opin Immunol, 2003. **15**(2): p. 182-9.
13. Kim, E.Y., et al., *Regulation of autoimmune arthritis by the pro-inflammatory cytokine interferon-gamma*. Clin Immunol, 2008. **127**(1): p. 98-106.
14. Kim, I.J., et al., *Microarray gene expression profiling for predicting complete response to preoperative chemoradiotherapy in patients with advanced rectal cancer*. Dis Colon Rectum, 2007. **50**(9): p. 1342-53.
15. Mosser, D.M. and X. Zhang, *Interleukin-10: new perspectives on an old cytokine*. Immunol Rev, 2008. **226**: p. 205-18.
16. Healy, J.I. and C.C. Goodnow, *Positive versus negative signaling by lymphocyte antigen receptors*. Annu Rev Immunol, 1998. **16**: p. 645-70.
17. Schwartz, R.H., et al., *T-cell clonal anergy*. Cold Spring Harb Symp Quant Biol, 1989. **54 Pt 2**: p. 605-10.
18. Grossman, Z. and W.E. Paul, *Self-tolerance: context dependent tuning of T cell antigen recognition*. Semin Immunol, 2000. **12**(3): p. 197-203; discussion 257-344.
19. Linterman, M.A., et al., *Roquin differentiates the specialized functions of duplicated T cell costimulatory receptor genes CD28 and ICOS*. Immunity, 2009. **30**(2): p. 228-41.
20. Zurier, R.B., *Systemic lupus erythematosus*. Hosp Pract, 1979. **14**(8): p. 45-54.
21. Arbuckle, M.R., et al., *Development of anti-dsDNA autoantibodies prior to clinical diagnosis of systemic lupus erythematosus*. Scand J Immunol, 2001. **54**(1-2): p. 211-9.

22. Arbuckle, M.R., et al., *Development of autoantibodies before the clinical onset of systemic lupus erythematosus.* N Engl J Med, 2003. **349**(16): p. 1526-33.

23. Linterman, M.A., et al., *Follicular helper T cells are required for systemic autoimmunity.* J Exp Med, 2009. **206**(3): p. 561-76.

24. Ardley, H.C. and P.A. Robinson, *E3 ubiquitin ligases.* Essays Biochem, 2005. **41**: p. 15-30.

25. Heissmeyer, V., et al., *Calcineurin imposes T cell unresponsiveness through targeted proteolysis of signaling proteins.* Nat Immunol, 2004. **5**(3): p. 255-65.

26. Heissmeyer, V. and A. Rao, *E3 ligases in T cell anergy--turning immune responses into tolerance.* Sci STKE, 2004. **2004**(241): p. pe29.

27. Guhaniyogi, J. and G. Brewer, *Regulation of mRNA stability in mammalian cells.* Gene, 2001. **265**(1-2): p. 11-23.

28. Carter, B.Z. and J.S. Malter, *Regulation of mRNA stability and its relevance to disease.* Lab Invest, 1991. **65**(6): p. 610-21.

29. Hollams, E.M., et al., *MRNA stability and the control of gene expression: implications for human disease.* Neurochem Res, 2002. **27**(10): p. 957-80.

30. Fraser, M.M., et al., *CaSm-mediated cellular transformation is associated with altered gene expression and messenger RNA stability.* Cancer Res, 2005. **65**(14): p. 6228-36.

31. Schiavi, S.C., J.G. Belasco, and M.E. Greenberg, *Regulation of proto-oncogene mRNA stability.* Biochim Biophys Acta, 1992. **1114**(2-3): p. 95-106.

32. Wilusz, C.J. and J. Wilusz, *Bringing the role of mRNA decay in the control of gene expression into focus.* Trends Genet, 2004. **20**(10): p. 491-7.

33. Fasken, M.B. and A.H. Corbett, *Process or perish: quality control in mRNA biogenesis.* Nat Struct Mol Biol, 2005. **12**(6): p. 482-8.

34. Valencia-Sanchez, M.A., et al., *Control of translation and mRNA degradation by miRNAs and siRNAs.* Genes Dev, 2006. **20**(5): p. 515-24.

35. Alberts, B., Johnson, A., Lewis, J., Raff, M., Roberts, K., Walter, P., *Molecular Biology of THE CELL.* Vol. 5th edition. 2008.

36. Muhlemann, O., *Recognition of nonsense mRNA: towards a unified model.* Biochem Soc Trans, 2008. **36**(Pt 3): p. 497-501.

37. Seko, Y., et al., *The role of cytokine mRNA stability in the pathogenesis of autoimmune disease.* Autoimmun Rev, 2006. **5**(5): p. 299-305.

38. Raghavan, A., et al., *Genome-wide analysis of mRNA decay in resting and activated primary human T lymphocytes.* Nucleic Acids Res, 2002. **30**(24): p. 5529-38.

39. Bernstein, P., S.W. Peltz, and J. Ross, *The poly(A)-poly(A)-binding protein complex is a major determinant of mRNA stability in vitro.* Mol Cell Biol, 1989. **9**(2): p. 659-70.

40. Bernstein, P. and J. Ross, *Poly(A), poly(A) binding protein and the regulation of mRNA stability.* Trends Biochem Sci, 1989. **14**(9): p. 373-7.

41. Brewer, G. and J. Ross, *Poly(A) shortening and degradation of the 3' A+U-rich sequences of human c-myc mRNA in a cell-free system.* Mol Cell Biol, 1988. **8**(4): p. 1697-708.

42. Fort, P., et al., *Regulation of c-fos gene expression in hamster fibroblasts: initiation and elongation of transcription and mRNA degradation.* Nucleic Acids Res, 1987. **15**(14): p. 5657-67.

43. Lieberman, A.P., P.M. Pitha, and M.L. Shin, *Poly(A) removal is the kinase-regulated step in tumor necrosis factor mRNA decay.* J Biol Chem, 1992. **267**(4): p. 2123-6.

44. Coller, J. and R. Parker, *General translational repression by activators of mRNA decapping.* Cell, 2005. **122**(6): p. 875-86.

45. Eulalio, A., I. Behm-Ansmant, and E. Izaurralde, *P bodies: at the crossroads of post-transcriptional pathways.* Nat Rev Mol Cell Biol, 2007. **8**(1): p. 9-22.

46. Ross, J., *mRNA stability in mammalian cells.* Microbiol Rev, 1995. **59**(3): p. 423-50.

47. Marzluff, W.F. and N.B. Pandey, *Multiple regulatory steps control histone mRNA concentrations.* Trends Biochem Sci, 1988. **13**(2): p. 49-52.

48. Schumperli, D., *Multilevel regulation of replication-dependent histone genes.* Trends Genet, 1988. **4**(7): p. 187-91.

49. Alberta, J.A., K. Rundell, and C.D. Stiles, *Identification of an activity that interacts with the 3'-untranslated region of c-myc mRNA and the role of its target sequence in mediating rapid mRNA degradation.* J Biol Chem, 1994. **269**(6): p. 4532-8.

50. Chen, C.Y. and A.B. Shyu, *Selective degradation of early-response-gene mRNAs: functional analyses of sequence features of the AU-rich elements.* Mol Cell Biol, 1994. **14**(12): p. 8471-82.

51. Kabnick, K.S. and D.E. Housman, *Determinants that contribute to cytoplasmic stability of human c-fos and beta-globin mRNAs are located at several sites in each mRNA.* Mol Cell Biol, 1988. **8**(8): p. 3244-50.

52. Lee, W.M., C. Lin, and T. Curran, *Activation of the transforming potential of the human fos proto-oncogene requires message stabilization and results in increased amounts of partially modified fos protein.* Mol Cell Biol, 1988. **8**(12): p. 5521-7.

53. Caput, D., et al., *Identification of a common nucleotide sequence in the 3'-untranslated region of mRNA molecules specifying inflammatory mediators.* Proc Natl Acad Sci U S A, 1986. **83**(6): p. 1670-4.

54. Stoecklin, G., et al., *Genome-wide analysis identifies interleukin-10 mRNA as target of tristetraprolin.* J Biol Chem, 2008. **283**(17): p. 11689-99.

55. Stoecklin, G., S. Hahn, and C. Moroni, *Functional hierarchy of AUUUA motifs in mediating rapid interleukin-3 mRNA decay.* J Biol Chem, 1994. **269**(46): p. 28591-7.

56. Shaw, G. and R. Kamen, *A conserved AU sequence from the 3' untranslated region of GM-CSF mRNA mediates selective mRNA degradation.* Cell, 1986. **46**(5): p. 659-67.

57. Sonenberg, N., *eIF4E, the mRNA cap-binding protein: from basic discovery to translational research.* Biochem Cell Biol, 2008. **86**(2): p. 178-83.

58. Chen, C.Y., Y. You, and A.B. Shyu, *Two cellular proteins bind specifically to a purine-rich sequence necessary for the destabilization function of a c-fos protein-coding region determinant of mRNA instability.* Mol Cell Biol, 1992. **12**(12): p. 5748-57.

59. Houseley, J. and D. Tollervey, *The many pathways of RNA degradation.* Cell, 2009. **136**(4): p. 763-76.

60. Weston, A. and J. Sommerville, *Xp54 and related (DDX6-like) RNA helicases: roles in messenger RNP assembly, translation regulation and RNA degradation.* Nucleic Acids Res, 2006. **34**(10): p. 3082-94.

61. Coller, J.M., et al., *The DEAD box helicase, Dhh1p, functions in mRNA decapping and interacts with both the decapping and deadenylase complexes.* RNA, 2001. **7**(12): p. 1717-27.

62. Tritschler, F., et al., *Structural basis for the mutually exclusive anchoring of P body components EDC3 and Tral to the DEAD box protein DDX6/Me31B.* Mol Cell, 2009. **33**(5): p. 661-8.

63. Tharun, S., *Lsm1-7-Pat1 complex: A link between 3' and 5'-ends in mRNA decay?* RNA Biol, 2009. **6**(3).

64. Simon, E., S. Camier, and B. Seraphin, *New insights into the control of mRNA decapping.* Trends Biochem Sci, 2006. **31**(5): p. 241-3.

65. Denis, C.L. and J. Chen, *The CCR4-NOT complex plays diverse roles in mRNA metabolism.* Prog Nucleic Acid Res Mol Biol, 2003. **73**: p. 221-50.

66. Brown, R.S., *Zinc finger proteins: getting a grip on RNA.* Curr Opin Struct Biol, 2005. **15**(1): p. 94-8.

67. Hall, T.M., *Multiple modes of RNA recognition by zinc finger proteins.* Curr Opin Struct Biol, 2005. **15**(3): p. 367-73.

68. Brennan, C.M. and J.A. Steitz, *HuR and mRNA stability.* Cell Mol Life Sci, 2001. **58**(2): p. 266-77.

69. Blackshear, P.J., *Tristetraprolin and other CCCH tandem zinc-finger proteins in the regulation of mRNA turnover.* Biochem Soc Trans, 2002. **30**(Pt 6): p. 945-52.

70. Lai, W.S., et al., *Evidence that tristetraprolin binds to AU-rich elements and promotes the deadenylation and destabilization of tumor necrosis factor alpha mRNA.* Mol Cell Biol, 1999. **19**(6): p. 4311-23.

71. Carballo, E., W.S. Lai, and P.J. Blackshear, *Evidence that tristetraprolin is a physiological regulator of granulocyte-macrophage colony-stimulating factor messenger RNA deadenylation and stability.* Blood, 2000. **95**(6): p. 1891-9.

72. Lai, W.S., et al., *Interactions of CCCH zinc finger proteins with mRNA. Binding of tristetraprolin-related zinc finger proteins to Au-rich elements and destabilization of mRNA.* J Biol Chem, 2000. **275**(23): p. 17827-37.

73. Lai, W.S. and P.J. Blackshear, *Interactions of CCCH zinc finger proteins with mRNA: tristetraprolin-mediated AU-rich element-dependent mRNA degradation can occur in the absence of a poly(A) tail.* J Biol Chem, 2001. **276**(25): p. 23144-54.

74. Carballo, E., W.S. Lai, and P.J. Blackshear, *Feedback inhibition of macrophage tumor necrosis factor-alpha production by tristetraprolin.* Science, 1998. **281**(5379): p. 1001-5.

75. Sandler, H. and G. Stoecklin, *Control of mRNA decay by phosphorylation of tristetraprolin.* Biochem Soc Trans, 2008. **36**(Pt 3): p. 491-6.

76. Kedersha, N., et al., *Stress granules and processing bodies are dynamically linked sites of mRNP remodeling.* J Cell Biol, 2005. **169**(6): p. 871-84.

77. Bashkirov, V.I., et al., *A mouse cytoplasmic exoribonuclease (mXRN1p) with preference for G4 tetraplex substrates.* J Cell Biol, 1997. **136**(4): p. 761-73.

78. Eystathioy, T., et al., *A phosphorylated cytoplasmic autoantigen, GW182, associates with a unique population of human mRNAs within novel cytoplasmic speckles.* Mol Biol Cell, 2002. **13**(4): p. 1338-51.

79. Eystathioy, T., et al., *The GW182 protein colocalizes with mRNA degradation associated proteins hDcp1 and hLSm4 in cytoplasmic GW bodies.* RNA, 2003. **9**(10): p. 1171-3.

80. Floor, S.N., B.N. Jones, and J.D. Gross, *Control of mRNA decapping by Dcp2: An open and shut case?* RNA Biol, 2008. **5**(4): p. 189-92.

81. Maillet, L., et al., *The essential function of Not1 lies within the Ccr4-Not complex.* J Mol Biol, 2000. **303**(2): p. 131-43.

82. Cougot, N., S. Babajko, and B. Seraphin, *Cytoplasmic foci are sites of mRNA decay in human cells.* J Cell Biol, 2004. **165**(1): p. 31-40.

83. Teixeira, D., et al., *Processing bodies require RNA for assembly and contain nontranslating mRNAs.* RNA, 2005. **11**(4): p. 371-82.

84. Sheth, U. and R. Parker, *Decapping and decay of messenger RNA occur in cytoplasmic processing bodies.* Science, 2003. **300**(5620): p. 805-8.

85. Andrei, M.A., et al., *A role for eIF4E and eIF4E-transporter in targeting mRNPs to mammalian processing bodies.* RNA, 2005. **11**(5): p. 717-27.

86. Stoecklin, G., et al., *MK2-induced tristetraprolin:14-3-3 complexes prevent stress granule association and ARE-mRNA decay.* EMBO J, 2004. **23**(6): p. 1313-24.

87. Anderson, P. and N. Kedersha, *Visibly stressed: the role of eIF2, TIA-1, and stress granules in protein translation.* Cell Stress Chaperones, 2002. **7**(2): p. 213-21.

88. Scheu, S., et al., *Activation of the integrated stress response during T helper cell differentiation.* Nat Immunol, 2006. **7**(6): p. 644-51.

89. Anderson, P. and N. Kedersha, *RNA granules: post-transcriptional and epigenetic modulators of gene expression.* Nat Rev Mol Cell Biol, 2009. **10**(6): p. 430-6.

90. Leung, A.K. and P.A. Sharp, *Function and localization of microRNAs in mammalian cells.* Cold Spring Harb Symp Quant Biol, 2006. **71**: p. 29-38.

91. Weinmann, L., et al., *Importin 8 is a gene silencing factor that targets argonaute proteins to distinct mRNAs.* Cell, 2009. **136**(3): p. 496-507.

92. Sen, G.L. and H.M. Blau, *Argonaute 2/RISC resides in sites of mammalian mRNA decay known as cytoplasmic bodies.* Nat Cell Biol, 2005. **7**(6): p. 633-6.

93. Lee, R.C., R.L. Feinbaum, and V. Ambros, *The C. elegans heterochronic gene lin-4 encodes small RNAs with antisense complementarity to lin-14.* Cell, 1993. **75**(5): p. 843-54.

94. Hoefig, K.P. and V. Heissmeyer, *MicroRNAs grow up in the immune system.* Curr Opin Immunol, 2008. **20**(3): p. 281-7.

95. Xiao, C., et al., *Lymphoproliferative disease and autoimmunity in mice with increased miR-17-92 expression in lymphocytes.* Nat Immunol, 2008. **9**(4): p. 405-14.

96. Costinean, S., et al., *Pre-B cell proliferation and lymphoblastic leukemia/high-grade lymphoma in E(mu)-miR155 transgenic mice.* Proc Natl Acad Sci U S A, 2006. **103**(18): p. 7024-9.

97. Kluiver, J., et al., *BIC and miR-155 are highly expressed in Hodgkin, primary mediastinal and diffuse large B cell lymphomas.* J Pathol, 2005. **207**(2): p. 243-9.

98. Bagga, S., et al., *Regulation by let-7 and lin-4 miRNAs results in target mRNA degradation.* Cell, 2005. **122**(4): p. 553-63.

99. Eulalio, A., E. Huntzinger, and E. Izaurralde, *Getting to the root of miRNA-mediated gene silencing.* Cell, 2008. **132**(1): p. 9-14.

100. Giraldez, A.J., et al., *Zebrafish MiR-430 promotes deadenylation and clearance of maternal mRNAs.* Science, 2006. **312**(5770): p. 75-9.

101. Lim, L.P., et al., *Microarray analysis shows that some microRNAs downregulate large numbers of target mRNAs.* Nature, 2005. **433**(7027): p. 769-73.

102. Jakymiw, A., et al., *Disruption of GW bodies impairs mammalian RNA interference.* Nat Cell Biol, 2005. **7**(12): p. 1267-74.

103. Liu, J., et al., *A role for the P-body component GW182 in microRNA function.* Nat Cell Biol, 2005. **7**(12): p. 1261-6.

104. Eulalio, A., E. Huntzinger, and E. Izaurralde, *GW182 interaction with Argonaute is essential for miRNA-mediated translational repression and mRNA decay.* Nat Struct Mol Biol, 2008. **15**(4): p. 346-53.

105. Lian, S.L., et al., *The C-terminal half of human Ago2 binds to multiple GW-rich regions of GW182 and requires GW182 to mediate silencing.* RNA, 2009. **15**(5): p. 804-13.

106. Chu, C.Y. and T.M. Rana, *Translation repression in human cells by microRNA-induced gene silencing requires RCK/p54.* PLoS Biol, 2006. **4**(7): p. e210.

107. Eulalio, A., et al., *Target-specific requirements for enhancers of decapping in miRNA-mediated gene silencing.* Genes Dev, 2007. **21**(20): p. 2558-70.

108. Behm-Ansmant, I., et al., *mRNA degradation by miRNAs and GW182 requires both CCR4:NOT deadenylase and DCP1:DCP2 decapping complexes.* Genes Dev, 2006. **20**(14): p. 1885-98.

109.   Eulalio, A., et al., *Deadenylation is a widespread effect of miRNA regulation.* RNA, 2009. **15**(1): p. 21-32.

110.   Rehwinkel, J., et al., *A crucial role for GW182 and the DCP1:DCP2 decapping complex in miRNA-mediated gene silencing.* RNA, 2005. **11**(11): p. 1640-7.

111.   Tourriere, H., K. Chebli, and J. Tazi, *mRNA degradation machines in eukaryotic cells.* Biochimie, 2002. **84**(8): p. 821-37.

112.   Jing, Q., et al., *Involvement of microRNA in AU-rich element-mediated mRNA instability.* Cell, 2005. **120**(5): p. 623-34.

113.   Li, W., et al., *RLE-1, an E3 ubiquitin ligase, regulates C. elegans aging by catalyzing DAF-16 polyubiquitination.* Dev Cell, 2007. **12**(2): p. 235-46.

114.   Siess, D.C., et al., *A human gene coding for a membrane-associated nucleic acid-binding protein.* J Biol Chem, 2000. **275**(43): p. 33655-62.

115.   Matsushita, K., et al., *Zc3h12a is an RNase essential for controlling immune responses by regulating mRNA decay.* Nature, 2009. **458**(7242): p. 1185-90.

116.   Wan, Y.Y., et al., *Transgenic expression of the coxsackie/adenovirus receptor enables adenoviral-mediated gene delivery in naive T cells.* Proc Natl Acad Sci U S A, 2000. **97**(25): p. 13784-9.

117.   Ansel, K.M., et al., *Mouse Eri1 interacts with the ribosome and catalyzes 5.8S rRNA processing.* Nat Struct Mol Biol, 2008. **15**(5): p. 523-30.

118.   Ota, S., et al., *The RING finger domain of Cbl is essential for negative regulation of the Syk tyrosine kinase.* J Biol Chem, 2000. **275**(1): p. 414-22.

119.   Rao, N., I. Dodge, and H. Band, *The Cbl family of ubiquitin ligases: critical negative regulators of tyrosine kinase signaling in the immune system.* J Leukoc Biol, 2002. **71**(5): p. 753-63.

120.   Anandasabapathy, N., et al., *GRAIL: an E3 ubiquitin ligase that inhibits cytokine gene transcription is expressed in anergic CD4+ T cells.* Immunity, 2003. **18**(4): p. 535-47.

121.   Jeon, M.S., et al., *Essential role of the E3 ubiquitin ligase Cbl-b in T cell anergy induction.* Immunity, 2004. **21**(2): p. 167-77.

122.   Serman, A., et al., *GW body disassembly triggered by siRNAs independently of their silencing activity.* Nucleic Acids Res, 2007. **35**(14): p. 4715-27.

123.   Gilks, N., et al., *Stress granule assembly is mediated by prion-like aggregation of TIA-1.* Mol Biol Cell, 2004. **15**(12): p. 5383-98.

124.   Liu, J., et al., *Argonaute2 is the catalytic engine of mammalian RNAi.* Science, 2004. **305**(5689): p. 1437-41.

125.   Su, H., et al., *Essential and overlapping functions for mammalian Argonautes in microRNA silencing.* Genes Dev, 2009. **23**(3): p. 304-17.

126.   Yekta, S., I.H. Shih, and D.P. Bartel, *MicroRNA-directed cleavage of HOXB8 mRNA.* Science, 2004. **304**(5670): p. 594-6.

127.   Ding, L. and M. Han, *GW182 family proteins are crucial for microRNA-mediated gene silencing.* Trends Cell Biol, 2007. **17**(8): p. 411-6.

128.   Eulalio, A., F. Tritschler, and E. Izaurralde, *The GW182 protein family in animal cells: New insights into domains required for miRNA-mediated gene silencing.* RNA, 2009.

129.   Eulalio, A., et al., *A C-terminal silencing domain in GW182 is essential for miRNA function.* RNA, 2009. **15**(6): p. 1067-77.

130.   Michelitsch, M.D. and J.S. Weissman, *A census of glutamine/asparagine-rich regions: implications for their conserved function and the prediction of novel prions.* Proc Natl Acad Sci U S A, 2000. **97**(22): p. 11910-5.

131.   Reijns, M.A., et al., *A role for Q/N-rich aggregation-prone regions in P-body localization.* J Cell Sci, 2008. **121**(Pt 15): p. 2463-72.

132.   Diederichs, S. and D.A. Haber, *Dual role for argonautes in microRNA processing and posttranscriptional regulation of microRNA expression.* Cell, 2007. **131**(6): p. 1097-108.

133.   Diederichs, S., et al., *Coexpression of Argonaute-2 enhances RNA interference toward perfect match binding sites.* Proc Natl Acad Sci U S A, 2008. **105**(27): p. 9284-9.

134.   Espinosa, A., et al., *The Sjogren's syndrome-associated autoantigen Ro52 is an E3 ligase that regulates proliferation and cell death.* J Immunol, 2006. **176**(10): p. 6277-85.

135.   Kentsis, A., R.E. Gordon, and K.L. Borden, *Self-assembly properties of a model RING domain.* Proc Natl Acad Sci U S A, 2002. **99**(2): p. 667-72.

136.   Kentsis, A., R.E. Gordon, and K.L. Borden, *Control of biochemical reactions through supramolecular RING domain self-assembly.* Proc Natl Acad Sci U S A, 2002. **99**(24): p. 15404-9.

137.   Cohen, N., et al., *PML RING suppresses oncogenic transformation by reducing the affinity of eIF4E for mRNA.* EMBO J, 2001. **20**(16): p. 4547-59.

138.   Johnston, R.J., et al., *Bcl6 and blimp-1 are reciprocal and antagonistic regulators of T follicular helper cell differentiation.* Science, 2009. **325**(5943): p. 1006-10.

139.   Nurieva, R.I., et al., *Bcl6 mediates the development of T follicular helper cells.* Science, 2009. **325**(5943): p. 1001-5.

140.   Yu, D., et al., *The Transcriptional Repressor Bcl-6 Directs T Follicular Helper Cell Lineage Commitment.* Immunity, 2009.

141.   Lu, J., et al., *MicroRNA expression profiles classify human cancers.* Nature, 2005. **435**(7043): p. 834-8.

142.   Villen, J., et al., *Large-scale phosphorylation analysis of mouse liver.* Proc Natl Acad Sci U S A, 2007. **104**(5): p. 1488-93.

13 Lebenslauf

Ausbildung

Seit März 2006	Ph.D. Studentin HelmholtzZentrum münchen, München, Deutschland Abteilung: molekulare Immunologie, Arbeitsgruppe: Heissmeyer Feld: molekulare Grundlagen zur Prävention von Autoimmunerkrankungen, Arbeitstechniken: bakterielle und humane Genetik, Proteinchemie, RNA-Arbeit, Zellkultur und Mausmodelle
April 2005-Februar 2006	Diplomandin Max-Planck-Institut für Biochemie, München, Deutschland Abteilung: Stukturbiologie (Prof. Baumeister), Arbeitsgruppe: Witt Feld: Grundlagen zum Faltungsprozess großer Proteine (20S Proteasom) Arbeitstechniken: bakterielle Genetik und Proteinchemie Titel der Diplomarbeit: "The assembly pathway of the 20S Proteasome of Rhodococcus erythropolis"
2000-2005	Studentin Universität zu Köln, Köln, Deutschland Fachsemester: 8 Abschlussprüfungen in Zoologie, Chemie und Biochmie, Gesamtnote: 1.0
1999-2000	Auszubildende Grünenthal GmbH, Aachen, Deutschland Pharmazeutische Laborarbeiten `in vivo`-Tests
1990 – 1999	Gymnasiastin Nelly-Sachs-Gymnasium, Neuss, Deutschland Leistungskurse: Biologie und Mathematik Nebenfächer: Deutsch, Geschichte
1986-1990	Grundschülerin Grundschule Grefrath, Neuss, Deutschland